Philipp Freislederer

Product design based on event-related potentials during rapid serial visual presentation

Master's Thesis

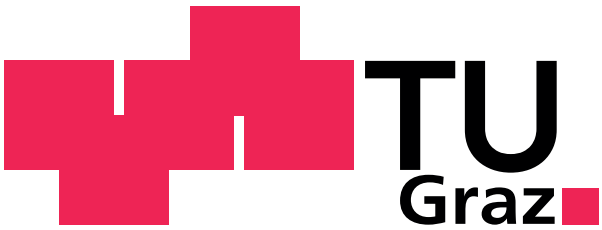

Institut für Semantische Datenanalyse/Knowledge Discovery
Graz University of Technology
Krenngasse 37/IV, A - 8010 Graz
Head: Assoc.Prof. Dipl.-Ing. Dr.techn. Gernot Müller-Putz

Supervisor: Assoc.Prof. Dipl.-Ing. Dr.techn. Gernot Müller-Putz

Evaluator: Assoc.Prof. Dipl.-Ing. Dr.techn. Gernot Müller-Putz

Graz, May 2012

EIDESSTATTLICHE ERKLÄRUNG

Ich erkläre an Eides statt, dass ich die vorliegende Arbeit selbstständig verfasst, andere als die angegebenen Quellen/Hilfsmittel nicht benutzt, und die den benutzten Quellen wörtlich und inhaltlich entnommenen Stellen als solche kenntlich gemacht habe.

Graz, am ....

(Unterschrift)

STATUTORY DECLARATION

I declare that I have authored this thesis independently, that I have not used other than the declared sources / resources, and that I have explicitly marked all material which has been quoted either literally or by content from the used sources.

....

date (signature)

Acknowledgements

First, I would like to thank Gernot Müller-Putz for supervising this thesis, his guidance, sympathy, and most of all for his patience during the development of this project.

Also, I wish to thank the staff and the other students of the Laboratory of Brain-Computer Interfaces, especially Alex, Vera, Günther, Martin, Christian, Josef, Petar, Christoph, Selina, Hanna, Sebastian, and of course Raphaela. Without the help and support from these people, this thesis could not have been accomplished.

This work was partially supported by the Faculty of Electrical and Information Engineering, Graz University of Technology.

Special thanks are due to my parents, who have always supported me generously throughout my whole life and especially during the time of my studies.

And finally, words can't describe my thankfulness towards my partner, Nastassja. Without her continuous support and love, nothing is possible.

Abstract

The human visual system is a powerful tool for the recognition and discrimination of objects. Several studies have been conducted in order to determine the speed of visual processing during rapid serial visual presentation (RSVP). If placed in front of a monitor and focused on it, the human eye and visual cortex can thoroughly distinguish between rapidly flashing target and distractor images. This phenomena has been already used to design computer vision systems for rapid image search and reactions to these images can be recorded with modern electroencephalography (EEG) methods. It has also been examined that emotional target pictures show a greater detectability because of more distinct event-related potentials (ERPs) when presented during RSVP. The question arises, whether the human visual system can also be used for product design by distinguishing between objects of someone's personal favor, if they are presented during RSVP.
A preliminary study with 5 subjects has been conducted in order to examine possible distinct ERPs, wherein presumably "likeable" objects (causing favor of the subject) and "not-likable" objects (inflicting negative emotions) will be displayed using RSVP. The classification accuracy between positive, neutral, and negative images was calculated in between 55.62 % and 70.91 % using stepwise linear discriminant analysis (SWLDA). Subsequently, a series of different objects (car and chair images) was be presented to a number of subjects ($n = 10$) and their reactions were recorded using EEG. Afterwards, these subjects participated in a self-assessement test, where they were asked to rate the objects they have seen during the RSVP according to their attracitveness, comfortability, and innovativeness. Also, to validate the paradigm and the processing routine, a so-called "oddball paradigm" has been conducted, in which the subjects were asked to focus on one of the images (target).
It was possible to detect this target image in all of the subjects through a one-vs-all classification between all conditions ($n = 80$) with classification accuracies between 82.48 % and 98.55 %. There was no significant correlation between the self-assesed attractiveness/comfortability/innovativeness of the images and the resulting classification accuracies for each condition.
Further work on this topic is needed in order to create a "product-design BCI" based on ERPs during RSVP.

Keywords: Brain-Computer Interface, Rapid Serial Visual Presentation, Event-related Potentials, Product Design, Stepwise Linear Discriminat Analysis

Zusammenfassung

Das menschliche visuelle System besitzt die Fähigkeit, Objekte aussergewöhnlich gut zu erkennen und verschiedene Objekte voneinander zu unterscheiden. Verschiedene Studien wurden bereits durchgeführt, um die Eigenschaft der visuellen Signalverarbeitung auf ihre Schnelligkeit hin mittels Rapid Serial Visual Presentation (RSVP) zu untersuchen. Wenn Probanden vor einem Monitor platziert und darauf fokussiert werden, so kann dass menschliche Auge in Verbindung mit dem visuellen Kortex aufblitzende Ziel- und Ablenkungsbilder unterscheiden obwohl diese bewusst selten wahrgenommen werden. Dieses Phänomen wurde bereits genutzt, um ein Computer-Vision-System für die schnelle Suche in einer Serie von Bildern zu entwickeln. Die Reaktionen auf Bilder, welche mittels RSVP präsentiert werden, können mittels modernen Elektroenzephalographie (EEG)-Methoden aufgezeichnet werden. Ausserdem zeigte sich bereits, dass emotionelle Bilder während solchen Präsentationen deutlicher erkannt werden als neutrale Bilder, was sich in deutlichen ereignis-korrelierte Potentiale (EKPs) im EEG darstellt.
Nun tritt die Frage auf, ob sich das menschliche Visualsystem während einer RSVP auch für eine Art des Produktdesigns nutzen lässt, indem es zwischen Objekten oder Bildern, welche positiv auf eine Person wirken und solchen, welche einen eher negativen Einfluss auf die Gefühlslage haben, unterscheiden kann.
Eine Vorstudie mit 5 Probanden wurde durchgeführt um festzustellen, ob mögliche klar unterscheidbare EKPs bei einer RSVP von Bildern mit unterschiedlichem emotionalem Inhalt erkannt werden. Mit einer Klassifikationsgenauigkeit zwischen 55.62 % und 70.91 % wurden positive, negative und neutrale Bilder mittels schrittweiser linearer Diskriminazanalyse (SWLDA) voneinander diskriminiert. Anschließend wurde eine Reihe von verschiedenen Objekten (Autos und Stühle) 10 Probanden präsentiert und deren Reaktion darauf aufgezeichnet. Alle Probanden nahmen an einem Fragebogen teil, um herauszufinden, inwiefern die Objekte attraktiv, komfortabel oder innovativ auf jeden einzelnen Probanden wirken. Um das Messparadigma zu validieren, wurde danach ein sogenanntes "Oddball-Paradigma" ausgeführt, in dem sich die Probanden auf eines der gezeigten Bilder konzentrieren sollten, um eine P300-Antwort zu erhalten. Dies wurde dazu benutzt, die Signalverarbeitungsroutine und das vorangegangene Paradigma zu überprüfen.
Im Oddball-Paradigma wurde das Zielbild, auf welches sich die Probanden konzentrierten bei allen korrekt mittels einer "Einer gegen den Rest"-Klassifikation zwischen allen Konditionen ($n = 80$) mit einer Klassifikationsgenauigkeit zwischen 82.48 % und 98.55 % identifiziert. Es zeigte sich weder eine statistisch signifikante Korrelation zwischen der subjektiven Attraktivität, dem Komfort oder der Innovativität der Bilder und den Klassifikationsergebnissen bei einem Klassifikationsversuch zwischen allen Konditionen.
Um ein "Produktdesign-BCI" zu entwickeln, welches auf EKPs während einer RSVP basiert, benötigt es daher noch einen großen weiteren Aufwand.

Stichwörter: Brain-Computer Interface, Rapid Serial Visual Presentation, Ereigniskorrelierte Potentiale, Produktdesign, Schrittweise linearer Diskriminazanalyse

Contents

List of Tables

List of Figures

1. Introduction

1.1. Neuromarketing

Neuromarketing combines economics, psychology, and neuroscience into one single research field and makes it possible to apply scientific findings in all of these three fields on a new marketing concept. This method of generating novel marketing concepts has been created by the group of Zaltman at Harvard University in the 1990s. He used Damasio's explanation [8] about the consciousness of mind, that 95 % of the decision-making of consumers is made unconsciously [58]. The use of neuromarketing can help to make a better approach to customers, investigate the impact of brands, communication, and products on the the consumer, and to gain insights about how advertisement has to be built up, in order to satisfy the customers' wishes and needs and also to create new desires and needs [46].

1.2. Brain-Computer Interface

With a Brain-Computer Interface (BCI) it is possible, to establish a direct connection between the human brain and a computer [57]. A connection like this can help for example high tetraplegics to regain control of some of their body functions to a certain extent [42, 57] or can be used for communication [2, 36, 57]. Figure 1 depicts the standard BCI scheme, which is applicable to all of the modern BCIs.

At first, brain signals, either gained through electroencephalography (EEG), electrocorticography (ECoG), near-infrared spectroscopy (NIRS), magnetoencephalography (MEG) or through other resources, which can be either invasive or non-invasive, have to be recorded. Various preprocessing steps such as spatial and/or temporal filtering and detrending of the signal are applied, before certain features can be extracted [57]. These features (either in the time or in the frequency domain [57]) are then used for a classification attempt. The outcome is passed on to an interface, which can control any application the BCI has been designed for. In any BCI, feedback is given to the user. For a high tetraplegic, the application could be the control of one of his or her hand using functional electrical stimulation (FES) [42] or moving a wheelchair [35]. Another use would be spelling devices for communciation [2, 42].

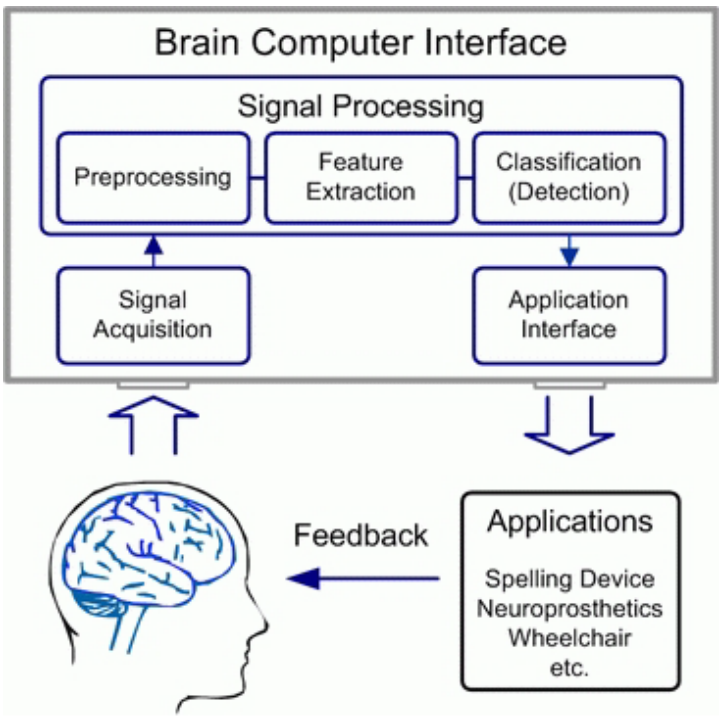

Figure 1: Scheme of a BCI. After acquiring the brain signals and converting them into digital values, three signal processing steps have to be conducted: Preprocessing, feature extraction, and classification. The gathered information is used to control an interface, which also gives feedback to the BCI user. This images was adapted from Graimann (2002) [21].

Signal Aquisition

There are two different possibilities of acquiring the EEG signals: invasive and non-invasive techniques. Both of them require either a recording of the neuroelectrical or the metabolic activity from the scalp or the surface of the brain. More information can be found in [57].

- **Invasive**
  One of the invasive methods of recording is called electrocorticography (ECoG). Here, electrodes are directly placed on the dura or on the cortical surface of the brain. This technique has a high spatial resolution, but, of course, requires surgery [12]. Also, multi unit activity signals can be used for the control of a BCI. These signals are measured using multielectrode arrays implanted in the cortex exactly on the region of interest [57]. Again, a high spatial resolution and signal quality is provided, but up to now, intracortical electodes of good quality suitable for a stable long-term use in humans are rare [57].

- **Non-Invasive**
  Non-invasive techniques have lower spatial resolutions than invasive, but are easier to apply. EEG, MEG, NIRS, and fMRI measure the neuronal activity of the brain outside of the body, for example on the scalp. While EEG measures the neuro-electrical activity directly, MEG, NIRS, and fMRI guide to the neuronal activity indirectly, i.e. by measuring the magnetic or metabolic changes, respectively.

  – *Electroencephalography (EEG)*
    EEG is a commonly used method for BCIs, as it is cheap, non-invasive, mobile, and has a high temporal resolution (ms). The disadvantages of EEG are the low spatial resolution (cm), as one electrode recordes the massed activity of a huge number of neurons, a high sensivity to noise and the fact that only cortical activity can be measured. Here, differences in the electrical potential of the brain are measured on the surface of the head.

  – *Magnetoencephalography (MEG)*
    As active neurons produce magnetic fields, these can also be measured using MEG. The spatial resolution is quite high ($\sim 5\,\text{mm}$) and also, the temporal resolution is as good as in EEG-measurements (ms). A huge disadvantage is the high cost of MEG-systems and that these are also bound to a laboratory. The small magnetic fields (about $10-50\cdot10^{-15}\,\text{T}$) are recorded using SQUIDs (Superconducting Quantum Interference Device).

  – *Near-infrared spectroscopy (NIRS)*
    Near-infrared spectroscopy uses the optical properties of hemoglobin in the brain, where changes can be measured using absorption or dispertion of light. As a neuronal activation is correlated with changes in the regional cerebral blood flow (rCBF), the regional cerebral blood voulme (rCBV) and the cerebral metabolic rate of oxygen (CMRO2), these can be measured with NIRS. The spatial resolution of NIRS varies in the range of cm and mm with rather low temporal resolution (s). NIRS systems can be rather inexpensive and portable.

  – *Functional magnetic resonance imaging (fMRI)*
    Functional magnetic resonance imaging uses the so-called blood oxygen level dependent (BOLD) contrast, in which oxygen-rich blood has different magnetic properties than blood with low oxygen levels. This is due to the paramagnetic properties of deoxyhemoglobin (hemoglobin without the bound oxygen). As an activation of a certain brain region causes an increased consumption of energy and oxygen in this region, the rCBF and the rCBV increase. As more oxygenated hemoglobin is used for the activation of a brain region, there is a shift in the equilibrium between oxy- and desoxyhemoglobin, which can be measured according to it's corresponding magnetic shift. With a high spatial (mm) and a low temporal resolution (s), this technique is also very expensive.

Brain Signals

Various signals from the human brain can be used for on a EEG-based BCI. There are two main types to be distinguished from each other:

- Event-Related-Potentials (ERP)
  ERPs are defined as the brain's neuroelectrical activity that is triggered through particular events or stimuli. This activity is phase- and time locked to this certain event/stimulus and can be analyzed for example through time averaging, or through analysis of the frequency domain [39]. By taking the mean over the dataset of ERPs, the signal-to-noise ratio (SNR) can be increased by increasing the number of averages. Equation 1 shows this relationship:

$$SNR(dB) = 20 \cdot \log \frac{\sqrt{N} \cdot U_S}{U_R} \tag{1}$$

  Here, U_S denotes a signal voltage and U_R a noise voltage, whereas N is the number of averages. The units of the SNR are decibel (dB).

  - **Evoked Potentials (EP)**
    Evoked potentials are a sensory subset of ERPs. They are classified by the type of external stimulus: Visually evoked potentials (VEP), auditory evoked potentials (AEP), olfactory evoked potentials (OEP), and somatosensory evoked potentials (SEP). One of the first BCIs using the VEP was developed by Vidal in the 1970s [55, 56].
  - **Steady-state evoked Potentials (SSEP)**
    These brain signals, which can also be elicited visually, auditory, and somatosensory result from repetitive stimulation with a certain frequency. Corresponding fundamental frequencies and also higher harmonics and subharmonics are detectable in the EEG signal. Steady-state visual evoked potentials (SSVEP) have been used in [34], where a light flickers at a certain frequency and by focusing on this stimulus, this frequency can be found in the corresponding EEG. Also, steady-state somatosensory evoked potentials have been used for the control of a BCI. More information on this topic can be found in [38].
  - **Slow Cortical Potentials (SCP)**
    SCPs have been used for BCIs as soon as in around 1980 [15]. These signals are slow shifts of the EEG with a duration ranging from 300 ms up to several seconds [39].
  - **P300**
    The P300 has been described by Donald in 1971 [10]. If focused on a certain type of rare event, a positive peak at about 300 ms after this event is evoked. The P300 can be elicited using a so-called "oddball paradigm". Multiple BCIs make use of that certain component, for example Donchin et al. [11].

- Dynamics of Brain Oscillations
  The spontaneous EEG changes during a mental task, i.e. motor imagery, can be explored in form of an event-related desynchronization (ERD) or event-related synchronization (ERS), which both are no longer phase-locked to the event, which induces these signals. Processing techniques of higher order have to be applied in order to make use of ERDS. More information on this topic can be found in [41].
  - **Event-related Desynchronization (ERD)**
    A relative decrease of amplitude or power in the frequency bands according to a reference period is called ERD. This is due to a low number of neurons working in a synchronous state because they are activated.
  - **Event-related Synchronization (ERS)**
    ERS is the relative increase in amplitude or power within certain frequency bands. In contrary to ERD, most neurons are in in synchronous state because of low information processing.

Experimental Strategies

Three mental strategies can be used for a BCI: Birbaumer et al. used operant conditioning for the control of SCP [2]. Mental imagery, for example motor imagery, was successfully used in several applications as the imagination of a motor task results in the activation of distinct cortical areas. These features can be used to operate a BCI efficiently [42].
The third mode of operation is the focus on an external stimulus or more stimuli. Donchin et al. [11] used this strategy for a P300-based BCI and Middendorf et al. [34] designed a SSVEP-based BCI.

Mode of Operation

A BCI can either work synchronous or asynchronous. Asynchronos BCIs process the user input or the user's reactions continuously, while synchronous BCIs need certain time slots and a corresponding trigger to process the information.

Passive BCI

An extension of the BCIs used for patients is the passive BCI for cognitive monitoring. Here, information on the cognitive state of the BCI user is collected and it is used to command a computer and for communication through it. So, a passive BCI "derives its outputs from brain activity arising without the purpose of voluntary control[...]." [59].

Signal Processing

There are several ways of processing the digitalized signals. At first, artefacts have to be reduced or rejected, for example manually by inspection of the raw data. Other methods of preprocessing include spatial and temporal filtering, downsampling, and averaging of the data. The other two main aspects of signal processing are the extraction of certain distinct features and classification. Various methods of feature extraction can be implemented in a BCI, for example spatial filtering, voltage amplitude measurements, or spectral analysis [57]. With these methods, the distance between certain patterns can be explored and these features are then used for classification: A classifier is needed to evaluate, whether the feature belongs to one or the other of two classes which are later on used for control (of course, more classes than two can be combined in a BCI, see [42]). Exemplary classification methods nowadays are linear discriminant analysis (LDA), support vector machines (SVM), or neural networks.

1.3. The Human Visual System and Visual Perception

The Human Visual System
The visual system in humans consists of the eye, the visual nerve, and the visual cortex, which all together build up the visual pathway.

- The Eye
  The main components of the human eye are the cornea and the lens in the front and the retina on the backside of the eye. Cornea and lens together create a sharp image, which is displayed on the retina. The incident light stimulates the receptor cells on the retina and these signals are transduced through the optical nerve. Two types of photoreceptors exist on the retina: rods, responsible for scotopic vision (vision at low light levels) and cones, which provide the eye's color sensitivity [3, 20]. A schematic drawing of the human eye can be seen in Figure 2.

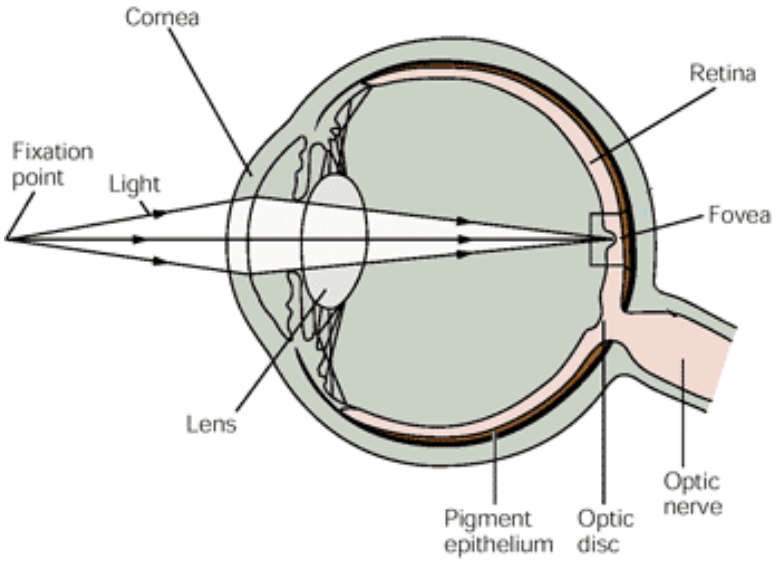

Figure 2: Schematic drawing of the human eye. Light enters the cornea and is focused by the lens onto the retina, in this particular case on the fovea, where the image is perceived in it's least distorted form. This image was adapted from Kandel et al. [28].

- The Optical Pathway
  The photoreceptor cells of the retina project to bipolar cells and these synapse directly on retinal ganglion cells. The action potential from these cells is guided through their axons, which form the optic nerve (N. opticus), to the optic chiasm

(Chiasma opticum), where the fibres from the nasal visual fields cross. Afterwards, most axons terminate in the Thalamus (more precisely in the Lateral geniculate nucleus, Corpus geniculatum laterale) and axons of the genicular neurons terminate in the primary visual cortex [3].

- The Visual Cortex
  The primary visual or striate cortex, also called visual area 1 (V1) is located caudally in the occipital lobe of the brain, meaning it is anatomically positioned in the Brodman area 17 (BA17). It organizes simple inputs of the retina into visual images. From here, the ventral cortical pathway leads to visual area 2 (V2, BA18), which is responsible for illusory and actual contours and to V4 (BA19), which responds to forms [28]. Figure 3 shows two possible information pathways for information processing.

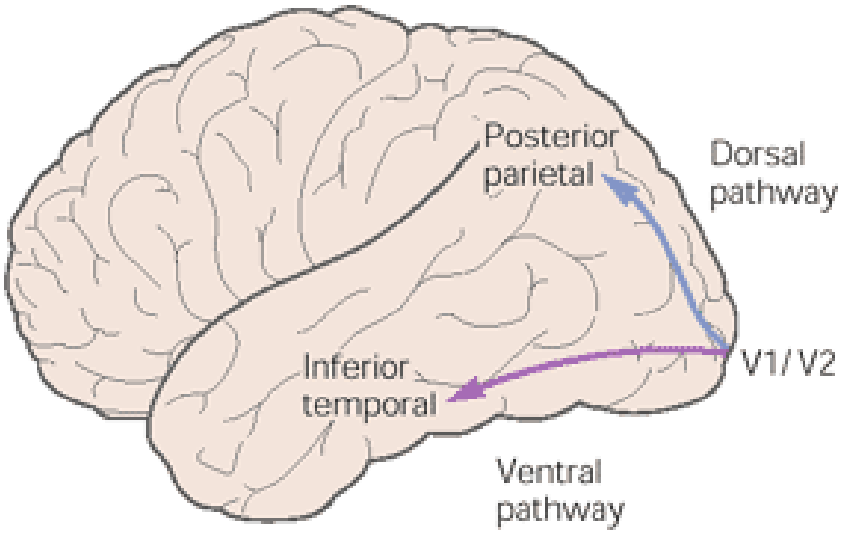

Figure 3: Scheme of visual processing in the human brain. This image was adapted from Kandel et al. [28]. The visual pathways are shown on a side view of the brain. The information is processed in the primary visual cortex (V1). From there on, the information is directed to other areas (V2,V4) in the inferior temporal direction and also on a doral pathway, where location matching is made [28].

Visual Perception
After light enters the eye, is converted into an electrical signal, and sent through the optical nerve for further processing steps, visual perception continues. Motion, depth and form have been processed by the visual cortex. Now, object perception is carried out. When the brain processes visual information, a strong activity in in the inferior temporal cortex (IT) and in other regions can be detected. Sheinberg and Logothetis reported, that the inferior temporal cortex and the visual areas of the cortex of superior temporal sulcus represent a stage of processing, where the brain's internal views rather than a retinal stimulus dominate [53].
Antoher study of perception tried to locate the fusiform face area (FFA) in humans and found out, that this area is involved in face detection and identification [22].
Is attention also a factor which is essential to perception? Of course, attention is important for the perception of objects, but it has been found out that attention is in fact a crucial factor to perception. Further information on this topic can be found in [20].

The pathway of visual perception and the corresponding time each region takes for processing can be seen in Figure 4. In this figure, the signal pathway of a visual stimulus, which is transduced into a muscular command is shown. Thorpe et al. concluded, that for a highly demanding visual task, processing of the information can be accomplished in under 150ms [54].

Visual perception is therefore one of the most crucial factors when it comes to the investigation of the reactions to certain visual stimuli.

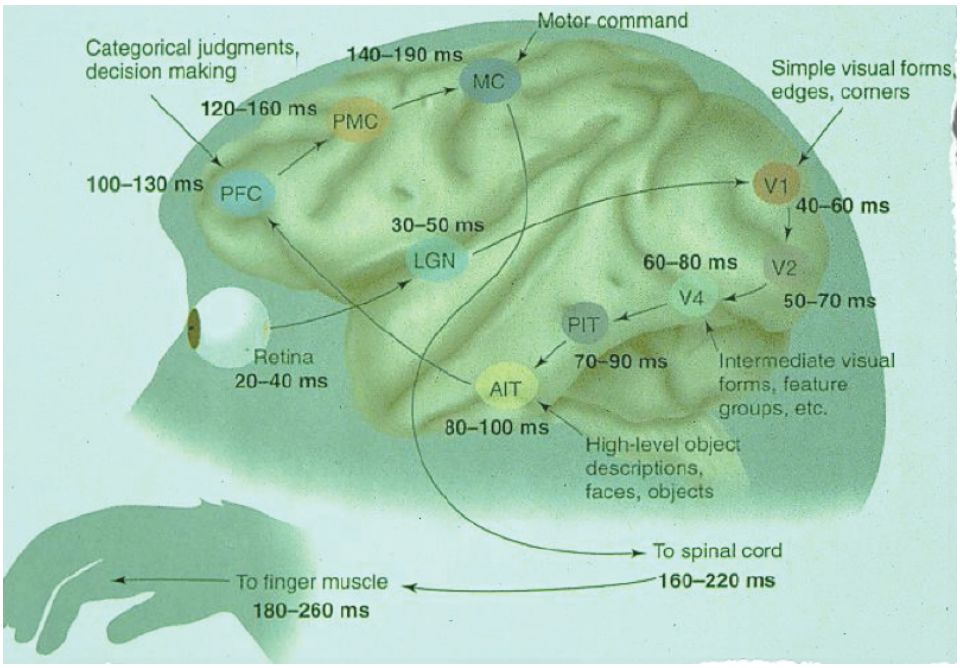

Figure 4: Visual Perception in the human brain as shown examplary for the execution of a motor task. This image was adapted from [3]. Light passes through the retina and is transduced to the visual area 1 (V1) via the lateral geniculate nucleus (LGN). From there, the signal is passed on to visual area 2 (V2) and visual area 4 (V4), where i.e. intermediate forms are processed. The anterior inferotemporal cortex (AIT) is than reached, at which the description of high-level objects occurs. This information is processed in the prefrontal cortex (PFC), transduced into the primary motor cortex (PMC) and the motor cortex (MC), from where it is passed on to the spinal cord and the corresponding muscle [3].

1.4. Rapid Serial Visual Presentation

The rapid sequential presentation of visual stimuli and the research of what information can be acquired from such a presentation started with the research of Potter and Levy in 1969 [44] and of Forster in 1970 [18]. Forster also termed this technique as RSVP (rapid serial visual presentation). His interests were mainly in the processes of sentence comprehension and he showed that RSVP does not degrade the stimulus material, for example a series of letters or words. Potter and Levy postulated the term conceptual short-term memory (STM) during their research with the comprehension and memory of photographs of scenes, while they are presented rapidly [44]. Intraub reported in 1980 that the visuospatial properties of a picture can be processed and remembered for at least 1 second after the stimulus, unless another stimulus, which is to be remembered occurs in this time [25]. In 1981, Intraub extended her research and found out that pictures, when presented during a RSVP, can be understood momentarily, but are quickly forgotten afterwards [26].
Nowadays, RSVP is commonly used to speed up the reading rates of people. In EEG-related research, presentations at high speeds have been already used to determine the speed of visual processing [54] and also to investigate a phenomenon called the attentional blink [45, 52]. The attentional blink describes the difficulty of reporting the second target stimulus in a dual target detection task, if this stimulus occurs right after a first one. This phenomenon is also sometimes called “attentional blindness”.
Image detection is one applicable use for RSVP [6]. Also, various attempts have been made to use the visual system for speeding up the pattern recognition of software [43, 19]. Gerson et al. [19] created a system which uses a BCI-based system to couple the image processing software of a computer with the image processing capabilities of the human brain for rapid image search. With this so-called "Cortically coupled Computer Vision for Rapid Image Search" [19], a real-time EEG-based BCI system has been created, where a target image in a sequence of non-target images can be detected using the human visual system as an interface and therefore, the triage of a large number of images in a series is accelerated. Bigdely-Shamlo et al. also proposed a BCI system based on RSVP, which aides to search through large sets of images and might be useful for the search for specific features in a large high-resolution image [1]. These are all various ways of detecting one or multiple target images in a series of target and non-target images.
What has also been thoroughly studied, is the reaction to emotionally arousing images. An overview of most of the recent work is given in [40]. Affective pictures show greater detectability because of more distinct ERPs, compared to neutral pictures when presented in a RSVP [17]. The brain quickly discriminates between stimuli of different emotional content even at high presentation rates [27]. Carretié et al. found out, that the amplitude of ERPs depends on the emotional content of the stimuli [5].

Figure 5 shows a schematic drawing of a RSVP as it is used in the preliminary study.

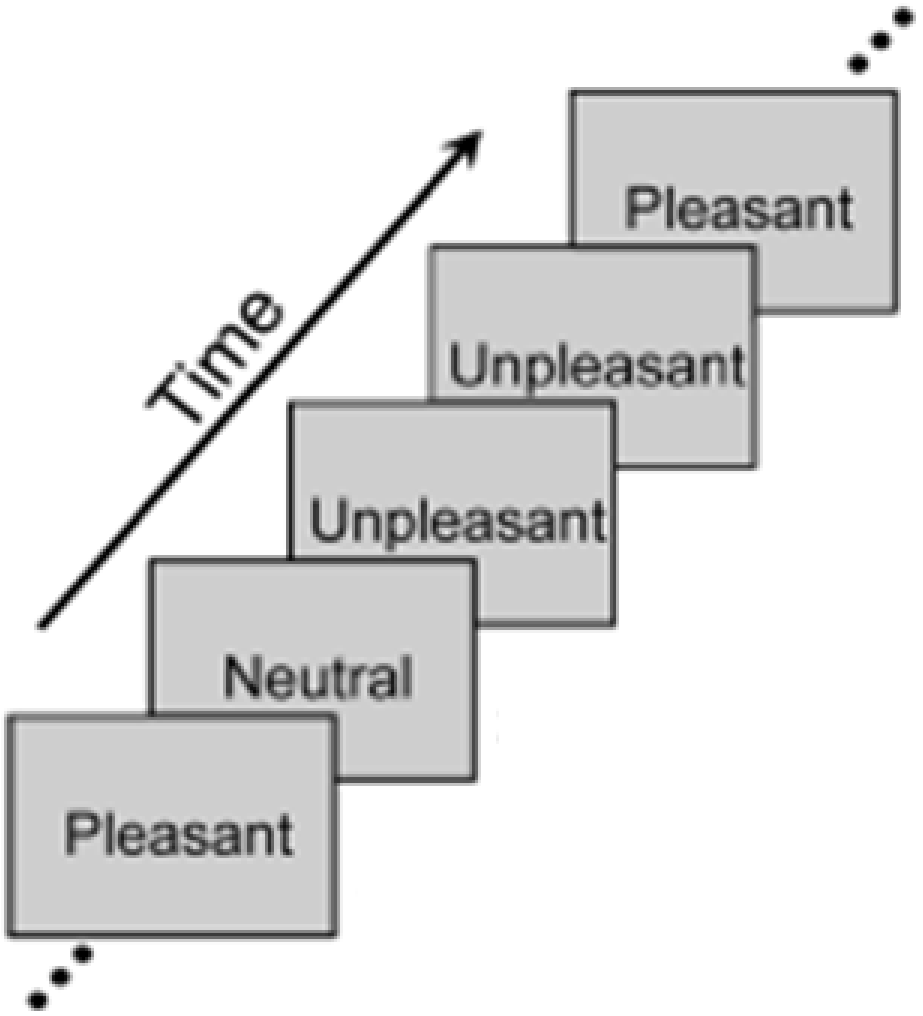

Figure 5: Scheme of a Rapid serial visual presentation(RSVP). The images are presented serially after each other with or without a interstimuls interval (ISI). This image was adapted from [17].

1.5. Motivation

As emotional target images show a greater detectability during RSVP, the question arises, if pictures with lower obvious emotional content, such as scenes or images of the everyday life also show differences in the ERP reactions to them. Can BCI-technology in combination with a RSVP also be used in other fields of neuroscience like neuromarketing, i.e. for a certain type of product design process, which might be faster, more accurate, and also more congruent with the customer's personal favor?

Previously, the components of a BCI system and the prior use of RSVP have been defined. As the literature uses ERPs for distinguishing between certain images, these potentials will also be used in this thesis and as certain triggers will be needed to conduct the experiments, a synchronous system will be used. The motivation of this work is the evaluation of the possibility of BCI-technology, which discriminates between objects of someones personal favor and thus can be used for a certain type of product design.

1.6. Goal

The goal of this thesis is not to create a BCI system, but rather to combine the findings of Carretié et al. [5] and Junghöfer et al [27] with pictures of lower emotional content and therefore pave the way for a product design BCI system.
At first, an attempt of replicating the results of Junghöfer et al [27] will be made and this data will be used to generate a offline classification routine. This serves as a preliminary study. Afterwards, certain types of stimuli (images of objects, as seen in advertisement or in everyday life) will be chosen for a main study and an attempt to discriminate the reactions to these stimuli from each other will be made.
Is the classification between attractive and unattractive images possible, the result might be the beginning of a passive BCI system applicable for a broad mass of users, especially in the areas of neuromarketing and marketing itself.

2. Materials and Methods

In this chapter, all methods used in the experiments and the signal analysis, including the used hardware and software, are described.

2.1. Principle

In order to examine the reactions to certain images on the human brain, a rapid serial visual presentation (RSVP) including pictures of emotional content will be displayed to a number of subjects while recording their neuroelectrical responses using EEG. Afterwards, images with a lower emotional content will be displayed to another group of subjects. The recorded EEG data will then be preprocessed (filtering, downsampling, and artefact removal) and a classification routine using SWLDA (stepwise linear discriminant analysis) will be performed so as to determine, which images inflict positive or negative reactions of each individual subject.
Figure 6 shows a schematic drawing of the principle of the experiment.

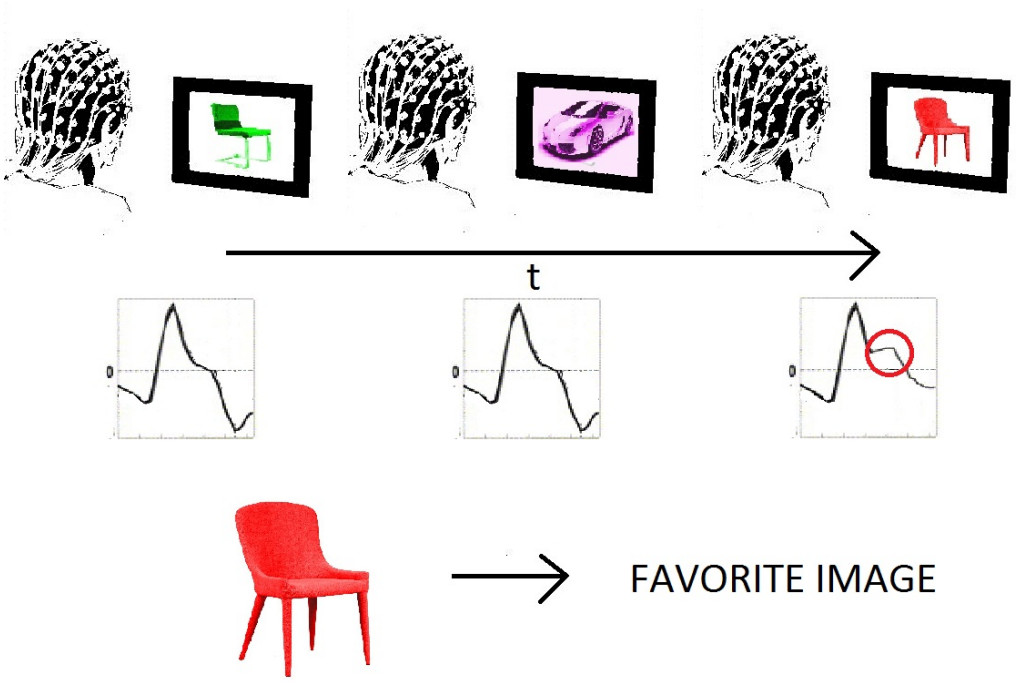

Figure 6: Scheme of the principle of the study: A person watches images of certain objects during RSVP and his reactions are recorded using EEG. If there is a difference between one of the images and all the others, this image is selected based on distinct event related potentials (ERP).

2.2. Hardware

Electrode Cap
The incorporated electrode cap (EASYCAP GmbH, Herrsching-Breitbrunn, Germany[1]) is based in the international 10-20 system, which positions the EEG electrodes on a fixed layout on the human skull (see Figure 7). This results in an standardized intra-subject relationship between the location of the applied electrodes and the corresponding areas of the cerebral cortex.

Electrodes
In order to acquire the EEG signals, 32 Ag/AgCl electrodes, manufactured by EASYCAP GmbH, were applied to the scalp and another 3 electrodes were applied on the forehead in order to collect the EOG signals. Abrasive electrolyte paste was used to keep the impedance of the electrodes below 5 kΩ. This paste decreases the impedance by roughing up the skin and thus enhancing the conductivity. To check, whether electrode impedances are below 5 kΩ, a portable electrode impedance measurement system (g.Zcheck, Guger Technologies OEG, Graz, Austria[2]) and impedance check software (which uses the impedance values measured by the amplifier) were used.

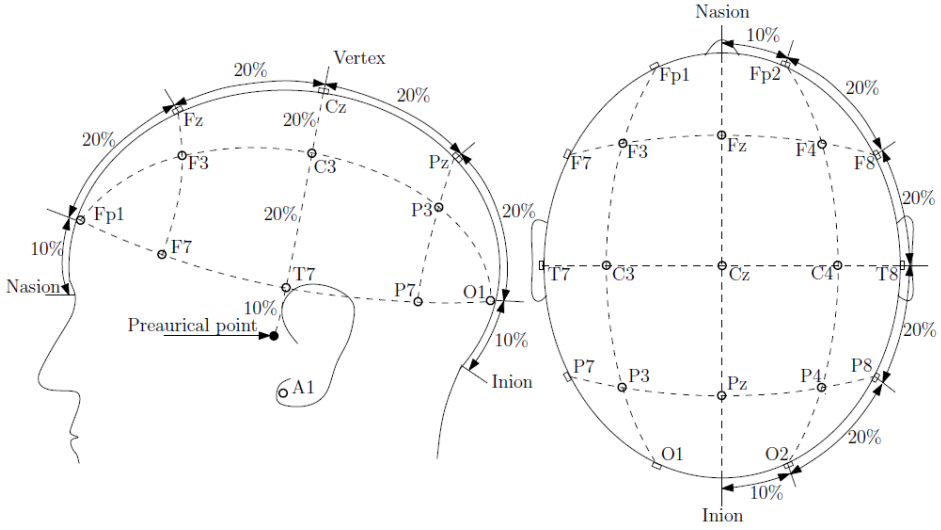

Figure 7: International 10-20 electrode system

[1] www.easycap.de
[2] www.gtec.at

Biosignal Amplifier
As 32 Channels of EEG and 3 Channels of EOG were to be recorded, 3 g.USBamp biosignal amplifiers with 16 channels each (Guger Technologies OG, Graz, Austria[3]) with a sampling rate of 38.4 kHz per channel were used. These amplifiers already have several preprocessing and digital filtering methods built in, for example low-pass and high-pass filtering and a notch filter at $f_{notch} = 50\,\text{Hz}$ for the purpose of cancellation of the power line interferences. All data was acquired with a sampling rate of $f_s = 512\,\text{Hz}$.

PCs
Two standard PCs were used for the experiments: One to acquire the EEG and EOG signals and another one to display the paradigms.

2.3. Software

All recordings, preprocessing steps and the complete data analysis was accomplished in MATLAB®/ SIMULINK® (MathWorks, Natick, Massachusetts, U.S.A.[4]) using features from the BioSig toolbox and the rtsBCI package[5] [47, 48]. The experimental paradigms were presented via E-PRIME® 2.0 (Psychology Software Tools, Inc., Sharpsburg, PA, U.S.A[6]).
The measurement data is saved by MATLAB® in the "General Data Format" (.gdf-File) [49].

[3] www.gtec.at
[4] www.mathworks.com
[5] both available at biosig.sourceforge.net
[6] www.pstnet.com

2.4. Experimental Paradigms

In the following section, the two different paradigms for the prestudy and the main study are described. The electrode setup for both studies can be seen in Figure 8. It was chosen in this certain way, because earlier studies located the best electrode positions during an RSVP experiment from these standard positions [24].

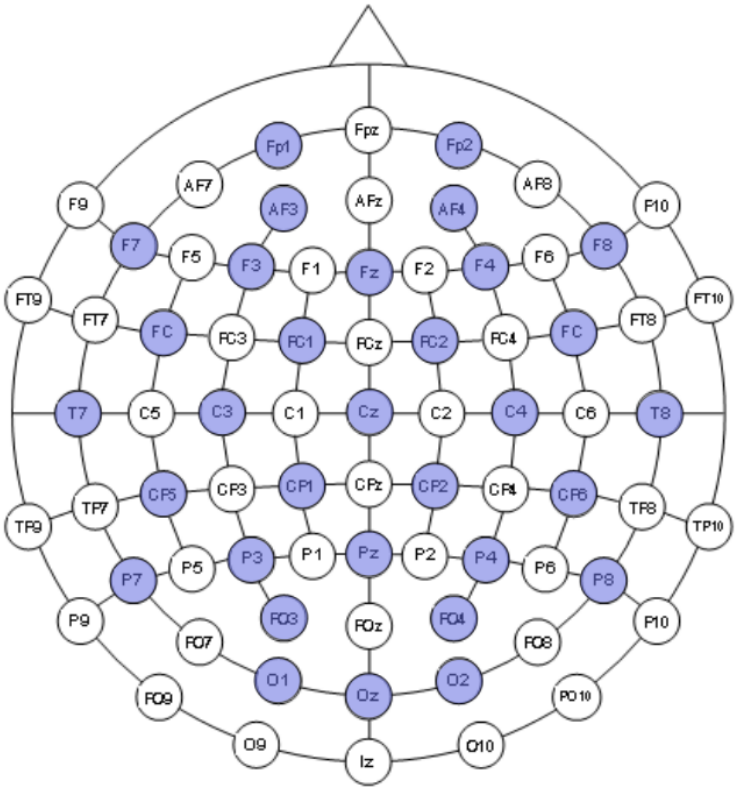

Figure 8: Electrode positions (blue) in the incorporated electrode cap.

2.4.1. Preliminary Study

Paradigm

For the preliminary study, a set of 300 pictures[7] from the International Affective Picture System (IAPS, [32]), all varying in their hedonic valence, were chosen. In this standardized collection, the pictures are categorized by three different hedonic values: pleasure, arousal and dominance. For the selection of images, only the values for pleasure and arousal were taken, as dominance was not included as a variable in previous studies ([17]). In the IAPS, pictures are rated on a SAM-scale (Self-Assessment Manikin), ranging from 1-9. The ratings in this picture set are scored such that 9 represents a high rating on each dimension (i.e., high pleasure, high arousal), and 1 represents a low rating on each dimension (i.e., low pleasure, low arousal) ([32]).

In total, 300 pictures were split into three categories: positive (high pleasure, high arousal), neutral (medium pleasure, medium arousal), and negative pictures (low pleasure, high arousal). The mean and standard deviation values for each category are shown in table 1. All images had the size of 1024x768 pixels.

Table 1: Valence and arousal values for the selected prestudy images. All values are mean ± standard deviation.)

	Valence	Arousal
Positive Images	7.013 ± 0.490	6.119 ± 0.585
Neutral Images	5.133 ± 0.368	3.115 ± 0.377
Negative Images	2.062 ± 0.420	6.452 ± 0.453

[7]The IAPS and technical manuals are available upon request at the NIMH Center for the Study of Emotion and Attention, University of Florida, Gainesville, FL. IAPS catalog numbers for the pictures used in this study are: pleasant: 1650, 1710, 2216, 2389, 4220, 4250, 4290, 4311, 4490, 4505, 4520, 4525, 4542 ,4597, 4598, 4599, 4604, 4607, 4608, 4609, 4611, 4612, 4614, 4616, 4626, 4628, 4640, 4641, 4643, 4645, 4650, 4651, 4652, 4656, 4658, 4659, 4660, 4664, 4668, 4670, 4676, 4677, 4680, 4681, 4687, 4689, 4690, 4694, 4695, 4698, 4800, 4810, 5460, 5470, 5621, 5623, 5626, 5700, 5833, 5910, 7270, 7405, 7451, 7650, 7660, 8001, 8030, 8031, 8034, 8040, 8080, 8116, 8158, 8161, 8163, 8170, 8178, 8179, 8180, 8185, 8186, 8190, 8193, 8200, 8206, 8210, 8300, 8341, 8380, 8400, 8420, 8470, 8490, 8492, 8496, 8499, 8500, 8501, 8502, 9156; neutral: 2002, 2104, 2190, 2200, 2210, 2215, 2305, 2357, 2377, 2381, 2382, 2383, 2384, 2393, 2396, 2397, 2411, 2435, 2480, 2485, 2506, 2512, 2513, 2514, 2516, 2518, 2570, 2580, 2593, 2870, 2890, 2980, 5390, 5471, 5500, 5510, 5520, 5530, 5731, 5740, 7000, 7001, 7002, 7003, 7009, 7012, 7014, 7016, 7017, 7025, 7026, 7030, 7031, 7032, 7034, 7035, 7036, 7037, 7038, 7039, 7040, 7041, 7042, 7043, 7045, 7050, 7052, 7053, 7055, 7056, 7057, 7059, 7060, 7061, 7062, 7090, 7100, 7110, 7130 ,7140 ,7150 ,7160, 7161, 7170, 7179, 7180, 7185, 7192, 7235, 7255, 7300, 7512, 7513, 7546, 7547, 7700, 7705, 7710, 8311, 8312; unpleasant: 2352.2, 2683, 2703, 2717, 2730, 2811, 3000, 3000, 3001, 3005.1, 3010, 3010, 3015, 3016, 3030, 3051, 3053, 3059, 3062, 3063, 3064, 3068, 3069, 3071, 3080, 3100, 3102, 3103, 3110, 3120, 3130, 3131, 3140, 3150, 3168, 3191, 3195, 3213, 3261, 3266, 3400, 3500, 3530, 3550.1, 6021, 6022, 6200, 6210, 6213, 6230, 6231, 6260, 6263, 6313, 6315, 6350, 6360, 6415, 6510, 6520, 6540, 6550, 6560, 6563, 6570, 6830, 6834, 8230, 8485, 9006, 9040, 9050, 9075, 9163, 9183 ,9185, 9187, 9250, 9252, 9254, 9300, 9321, 9325, 9405, 9410, 9412, 9413, 9414, 9420, 9425, 9433, 9570, 9571, 9600, 9630, 9635.1 ,9800 ,9810, 9921, 9940.

Timing

The entire picture set was presented to the subjects randomly and continuously without any perceivable interstimulus interval (ISI) for $t = 333\,\text{ms}$ each using E-PRIME® software. This procedure was repeated a total of 10 runs, resulting in 3000 displayed pictures. Hence, a set of 1000 trials for each of the three classes (positive, neutral, and negative) was generated. In total, the presentation lasted about 40 minutes, with a short break between each run.

The timing parameters are displayed in Figure 9 to demonstrate the experiment.

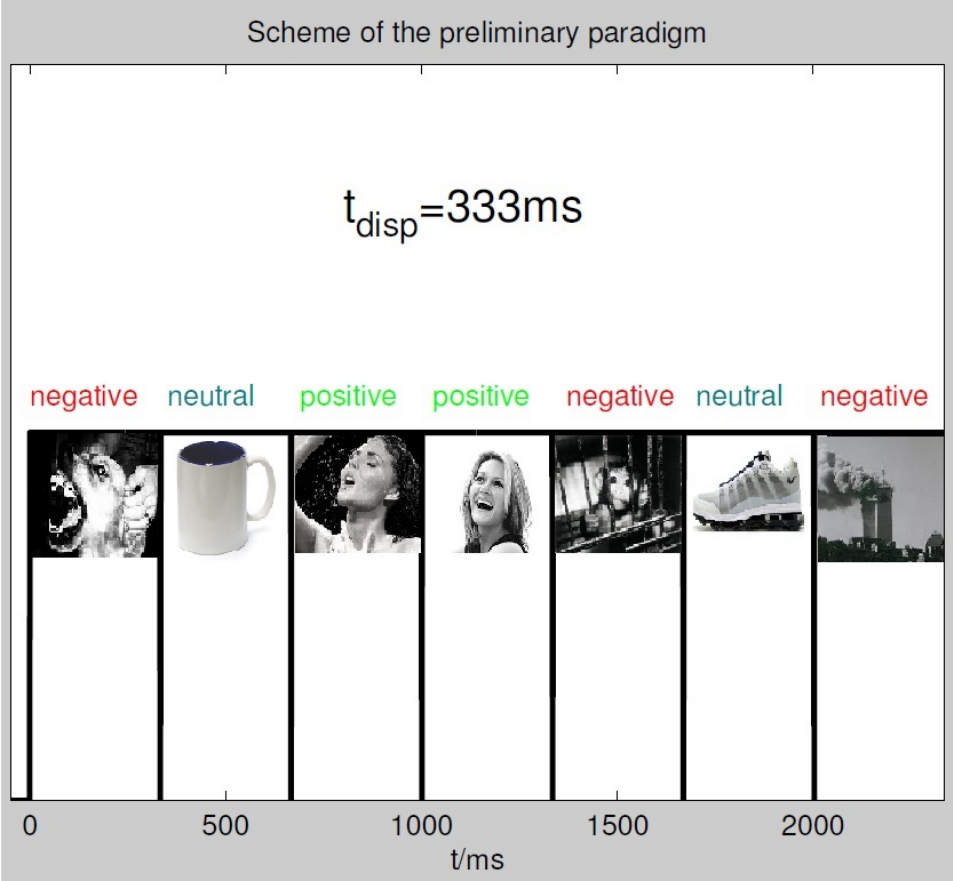

Figure 9: Timing scheme as it is done in the preliminary study. The images are displayed randomly for $t_{disp} = 333\,\text{ms}$ without any perceivable interstimulus interval (ISI).

Participants
Five subjects (2 female and 3 male) were asked to participate in this preliminary study. All of them had normal or corrected to normal vision, reported no history of epilepsy, and were aged between 25 and 28 ($mean = 26.20 \pm 1.30$). All subjects signed an informed consent letter prior to the experiments. The only instruction for the subjects was to relax, keep their eyes centered in the middle of the screen, and view the pictures.

2.4.2. Main Study

Paradigm
The parameters which were used in the preliminary study were changed after a review of the results. To enlarge the number of trials, $n = 80$ pictures are presented to the subjects. These consist of 40 pictures of automobiles and 40 pictures of chairs, all of them taken from free available sources in the Internet. All pictures were resized to 1024x786 pixels and converted to grayscale images. For the set of pictures, a color overlay in 4 different colors (red, blue, cyan and green) was created and 10 images of chairs and 10 images of cars, respectively were overlayed with one color.
Exemplary images used in the main study are depicted in Figure 11 and Figure 12.
One measurement consisted of 4 runs: During run 1 and 2, the subjects were asked to sit still and relaxed and just watch the pictures displayed on the screen. Afterwards, a paper and pencil test was used to get the information of each subject, whether a picture seems attractive, comfortable or innovative to them. These three items were examined with a seven-point Likert scale. Also, they were asked to select one picture as their personal favorite. This selected image was used in the following runs: In run 3 and 4, subjects were asked to focus on their previously selected favorite picture and to count the number the picture appears. This paradigm was used to elicit a P300 wave, in order to verify the processing routine afterwards.

Timing
The pictures were displayed for $t_{disp} = 100\,\text{ms}$ with an interstimulus interval (ISI) of $t_{ISI} = 400\,\text{ms}$. Each picture was shown 25 times per run, resulting in a total of 2000 pictures per run and a total duration of $t_{duration} = 16.7\,\text{min}$. A paradigm for the later on described EOG correction was conducted before each measurement. In this paradigm, the subjects were asked to repeatedly blink and roll their eyes. In total, the measurement time (including the time needed for mounting the electrodes) was kept under 3 hours.

The timing parameters for the main study are depicted schematically in Figure 10

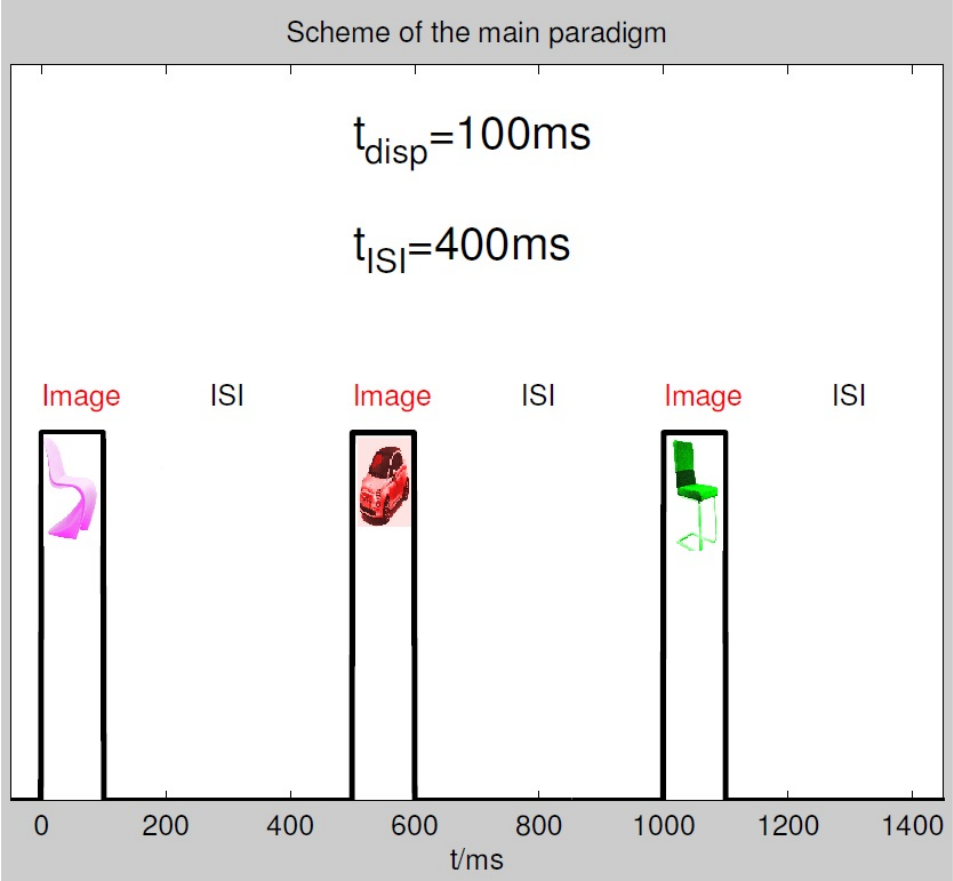

Figure 10: Timing scheme as it is done in the main study. The images are displayed randomly for $t_{disp} = 100\,\text{ms}$ without an interstimulus interval (ISI) of $t_{ISI} = 400\,\text{ms}$.

Participants

In the main study, a larger number of subjects ($n = 10$) were asked to participate. The subjects were aged from 23 to 32 ($mean = 26.40 \pm 2.46$). All of them had normal or corrected to normal vision and reported no history of epilepsy. All subjects were relaxed ($mean_{relaxation} = 8.33 \pm 1.12$) and motivated ($mean_{motivation} = 8 \pm 1$). This was assessed before the measurements on a scale form 1 to 10, with 10 being highly motivated or relaxed. All subjects signed an informed consent letter prior to the experiments.

(a)

(b)

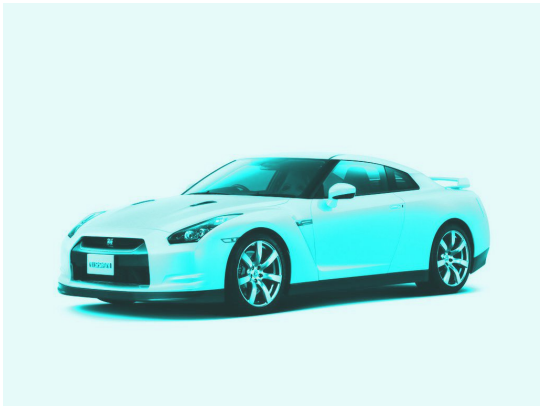

(c)

(d)

(e)

Figure 11: Five exemplary pictures showing cars as used in the main study.

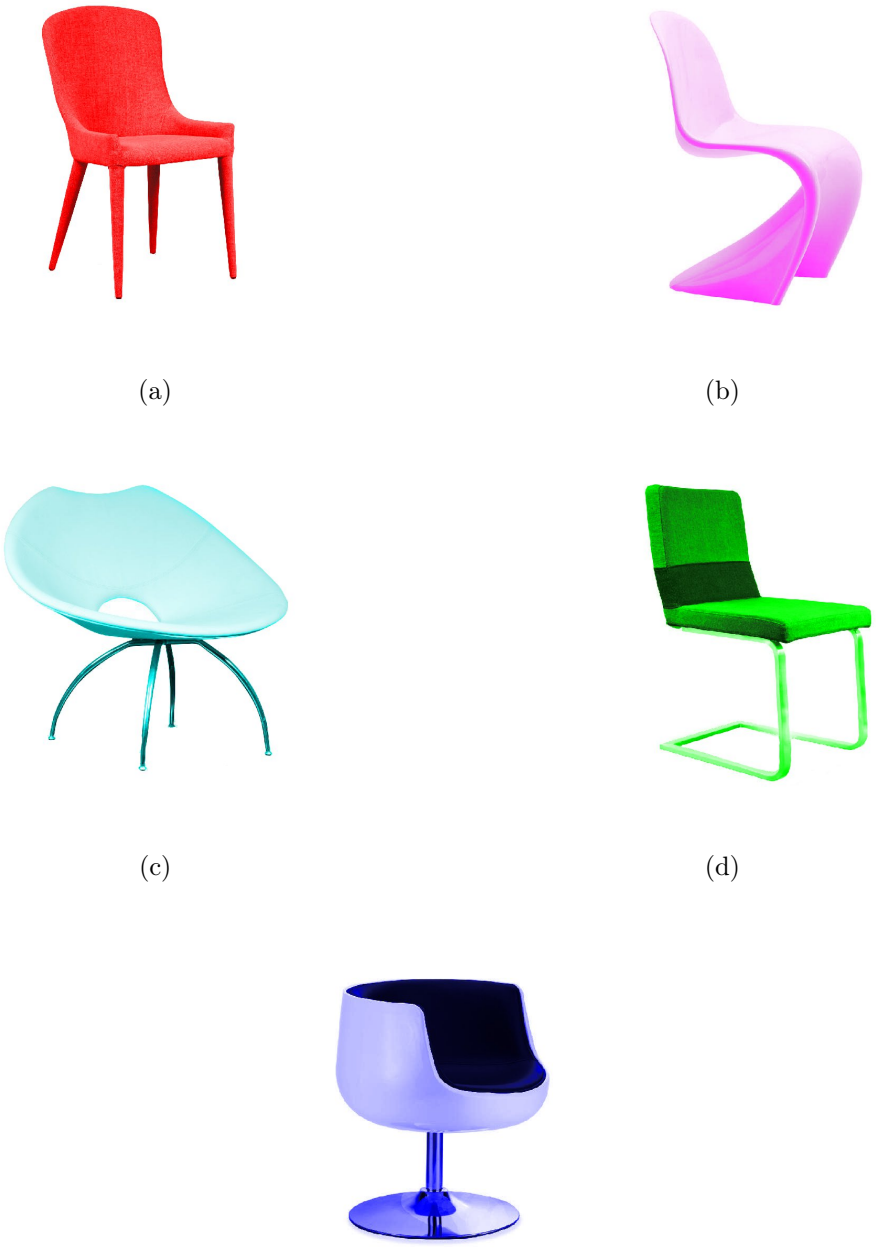

(a) (b)

(c) (d)

(e)

Figure 12: Five exemplary pictures showing chairs as used in the main study.

2.5. Preprocessing

In this following section, all of the computational preprocessing steps are described in the order they were applied. A flowchart of the processing steps can be seen in Figure 13.

System Setup
The raw EEG and EOG data was recorded via one PC (here: measurement PC) and the paradigms are shown through another (presentation PC). By connecting a trigger cable from the parallel port of the presentation PC to the Data Input/Output (I/O) port of the master amplifier, a trigger signal could be sent to this amplifier and from there on to the measurement PC.
The data was filtered with a low-pass filter (cut-off frequency $f_{c,low} = 0.5\,\text{Hz}$) and a high-pass filter (cut-off frequency $f_{c,high} = 100\,\text{Hz}$) using the built-in filters of the biosignal amplifier.

File Merging
Each measurement generated 2 datasets: one .gdf-File with the recorded raw EEG/EOG data and one E-Prime® file, with the timing points of each stimulus. These 2 sets of data had to be merged together into a single file. During the startup of the paradigm, the E-Prime® program sets the output of the parallel port from 0 V to 1 V and is thus generating a trigger signal, which is acquired by the measurement PC. In the E-Prime® paradigm, all starting and finishing points of each presented stimulus are saved into one file. Using both, the trigger signal from the measurement PC and the saved trigger points in E-Prime®, one file with all of the timepoints when a stimulus is presented and finishes are now connected to the EEG and EOG data file.

EOG Correction
Using the data from the previously recorded EOG correction paradigm, all datasets were EOG-corrected via regression in order to reduce artefacts from blinking and eye movements. This was accomplished by using a regression model based on Schlögl et al. [50].

Filtering
Although certain filters have already been applied by the measurement amplifiers, some additional filters are used in order to narrow the frequency bands to values, where event-related potentials most likely occur and can be measured. A IIR (infinite impulse response) bandpass filter with cut-off frequencies between $f_{c,low} = 0.5\,\text{Hz}$ and $f_{c,high} = 10\,\text{Hz}$ was applied on the input signal. The filter was implemented as a 4^{th} order Butterworth filter. Matlab's® *filtfilt* function, which corrects the phase of the data automatically, was used for the implementation of the filter. The filtering process before the downsampling of the data secured anti-aliasing.

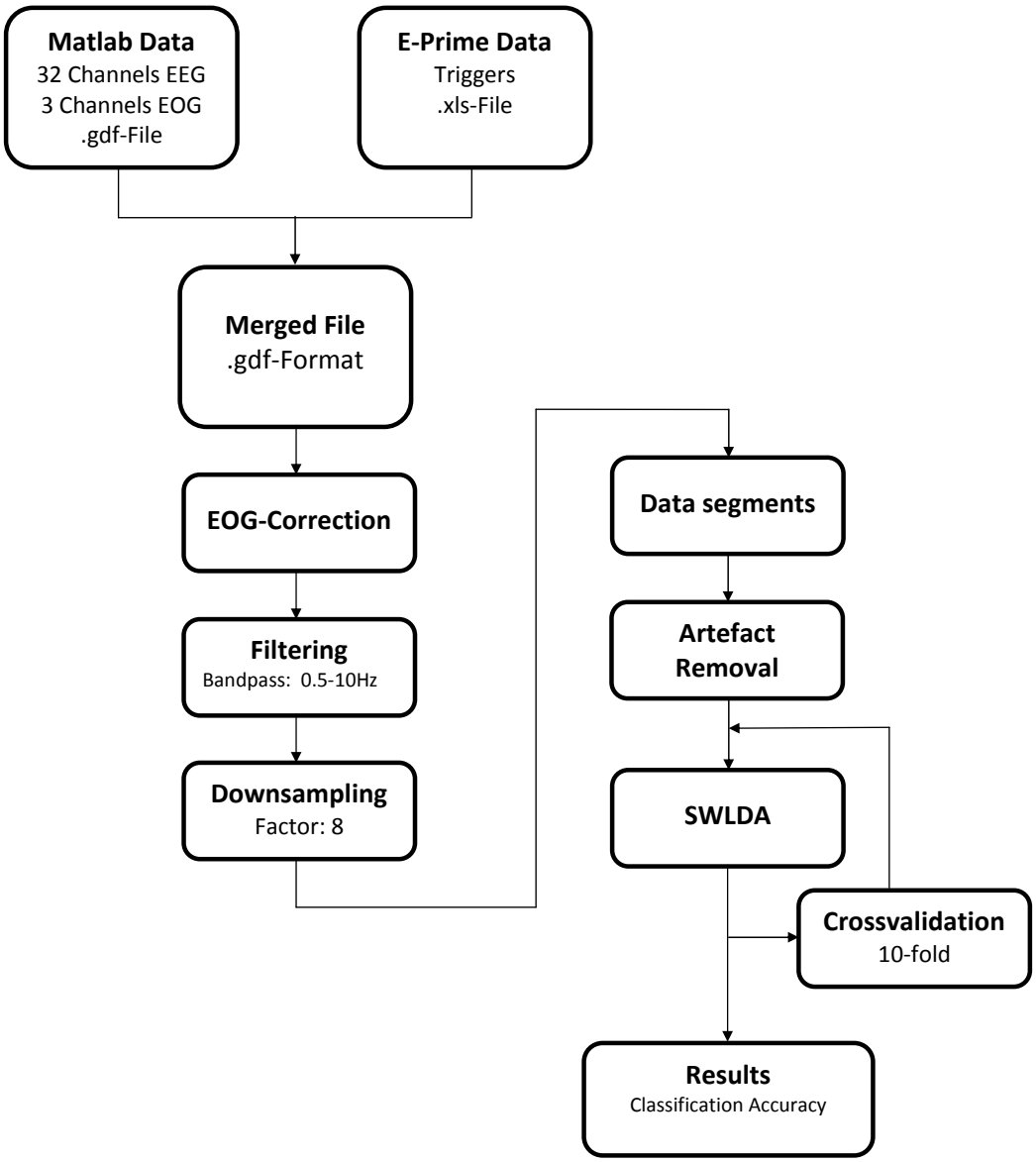

Figure 13: Flowchart of all the data processing steps.

Downsampling
To reduce the amount of data for classification and subsequently the time used for processing, the data was downsampled from 512 Hz to 64 Hz. Because the important information is located in a low frequency range and has been filtered between 0.5Hz and 10Hz, this does not affect the results.

Data Segmentation
Using the triggers from the E-Prime®-datafile, the corrected, filtered, and downsampled EEG signal can be split up into short data segments. These segments now correspond to each trial or condition individually and can be varied in their length.

Artefact Removal
As one run of the main study lasts for more than 15 minutes and although the subjects are advised to just relax and sit as still as possible, some artefacts during the measurement are inevitable. These artefacts are automatically removed with an algorithm, that discards a certain trial for all channels, if an amplitude value of more than 45 μV in magnitude was found. This value served as a valid maximum magnitude after visual inspection of the data.

2.6. Classification

LDA

Linear discriminant analysis (LDA) has been described originally by Fisher in 1936 [16]. A more detailed description can be found in Hastie et al. [23]. In general, this method searches for a linear hyperplane in between two datasets (classes), which both have Gaussian distributions. The datasets are split into a training and a test dataset. The parameters of this distribution are estimated using the training data. Suppose we have each class density as multivariate Gaussian, the LDA rule classifies to class 2, if

$$x^T\hat{\Sigma}^{-1}(\hat{\mu}_2 - \hat{\mu}_1) > \frac{1}{2}\hat{\mu}_2^T\hat{\Sigma}^{-1}\hat{\mu}_2 - \frac{1}{2}\hat{\mu}_1^T\hat{\Sigma}^{-1}\hat{\mu}_1 + \log(N_1/N) - \log(N_2/N) \tag{2}$$

and to class 1 otherwise. In Equation(2) $\hat{\mu}_1$ and $\hat{\mu}_2$ denote the estimation of the mean value of class 1 and class 2, respectively, $\hat{\Sigma}$ denotes estimation of the covariance, N_k is the number of class-k observations and N the total number of observations. A simplified version of the LDA would be:

$$w = (\mu_1 - \mu_2)^T \cdot \Sigma_{12}^{-1} \tag{3}$$

$$y = w^T x + w_0 \tag{4}$$

where μ_1 and μ_2 denote the mean values of each class, Σ_{12} the covariance, w the weighting vector, w_0 the bias and y the output function. The classes are selected based on the algebraic sign of the output function y.

SWLDA

A version of LDA is the stepwise linear discriminant analysis (SWLDA) algorithm. This method upgrades linear discriminant analysis by using only statistically significant predictor variables. These variables are chosen using stepwise regression and taken as features to project the weights the discriminant function [13].

1. A variable that has been entered into the linear discriminant analysis model may turn out to be nonsignificant once other variables have been entered into this model. So first, the stepwise procedure performs a F-test using partial sum of squares for each entered variable and sorts the features according to their p-Value.
2. If a variable is no longer significant, it is removed from the model.
3. An entry criteria (p_{enter}) and an exit criteria (p_{remove}) are chosen and the model acts according to these parameters: If the calculated p-Value is smaller than p_{enter},

this variable is added to the model. If the p-Value of the feature is larger than p_{remove}, it is discarded.

4. The procedure terminates when no further variables can be entered or removed [33].

The parameters for the SWLDA were:

- $p_{enter} = 0.1$
- $p_{remove} = 0.15$
- Iterations: 40

These parameters have been evaluated in [51], although only 10 Iterations were used. Krusienski et al. used a larger number of iterations in his studies (60 iterations) [30]. After some prelimiary tests, 40 iterations were found to be the the most effective setting, when it comes to classification performance and processing time.

MATLAB'S® "stepwisefit"-function from the built-in Statistics Toolbox was used to select the desired features.

As in some of the tested paradigms, a total number of 80 classes are to be compared against each other, the method of One-vs-All (more precisely: One-vs-Rest) classification is applied. Here, each class is individually compared to the rest of the classes, and the one class, that performs best in the classification routine is considered the "winner".

For an unequal number of trials per class, classification accuracy does not serve as a measure for the performance of a classifier. With Cohen's kappa coefficient (κ) this problem can be excluded. Equation 5 shows the κ-coefficient as stated in [7]:

$$\kappa = \frac{p_0 - p_c}{1 - p_c} \tag{5}$$

In Equation 5, p_o denotes the relative observed agreement among raters and p_c the proportion of units which is expected hypothetically.

2.6.1. Cross Validation

To evaluate the accuracy and therefore the performance of the classifier, cross validation is used [29]. In the here used 10x10 cross validation, the dataset is randomly split into 10 mutually exclusive subsets (folds). Each subset is now used to train and to test the classifier's performance. The results of each validation are averaged which serves consequently as a more reliable value for the overall performance of the classifier.

2.7. Statistics

As high classification accuracies (or high κ-Values) are only accomplished if the different datasets are well separable from each other, this accuracy measure serves as a value for the differences between each dataset. Now, as each subject performs an online paper and pencil test, where they are asked to rate each picture according to it's attractiveness, comfortability, and innovativeness, another dataset of values is obtained. Subsequently, these two datasets are to be compared against each other. In order to accomplish this, the Spearman's rank correlation coefficient is used. This coefficient denotes the relationship between two variables according to their ranks [60].
Spearman's rank correlation coefficient r_s is given by Equation 6, where N is the number of subjects, or in this particular case the number of different pictures, d_i^2 is the quadratic difference between the ranks of picture i between the two variables (classification accuracy and picture rating).

$$r_s = 1 - \frac{6 \cdot \sum_{i-1}^{N} d_i^2}{N \cdot (N^2 - 1)} \tag{6}$$

The null hypothesis H_0 in this case would be, that $r_s = 0$, meaning that there is no correlation between the ranks of the two tested variables and therefore it is not possible to discriminate between the brain potentials related to one's personal favor and others. Of course, the correlation is only of statistical significant interest for a p-value smaller than 0.05.

Bootstrapping
In order to calculate confidence intervals, the method of bootstrapping based on MATLAB'S® "bootci"-function is used. Basically, it is a method of statistical resampling, where random sampling with replacement is used [14]. A huge advantage of bootstrapping is, that the theoretical distribution of the data has not to be known in order to calculate the confidence intervals, as it is the case here.

3. Results

This chapter illustrates all the obtained results from the predefined measurements, graphically as mean waveforms and topographic representations of the acquired data. The resulting classification performance are described as classification accuracy or using Cohen's κ.

3.1. Preliminary Study

Three different categories of pictures were to be observed: positive, neutral, and negative images of the IAPS. Each category serves as one condition.

3.1.1. Mean waveforms

Mean waveforms for each of these categories were calculated and compared against each other. Figure 14 shows the reaction to each category of images as mean values over $n = 1000$ trials for the channels Fz, Cz, and Pz. This was done for all of the subjects, Figure 14 and 15 serve as an example.

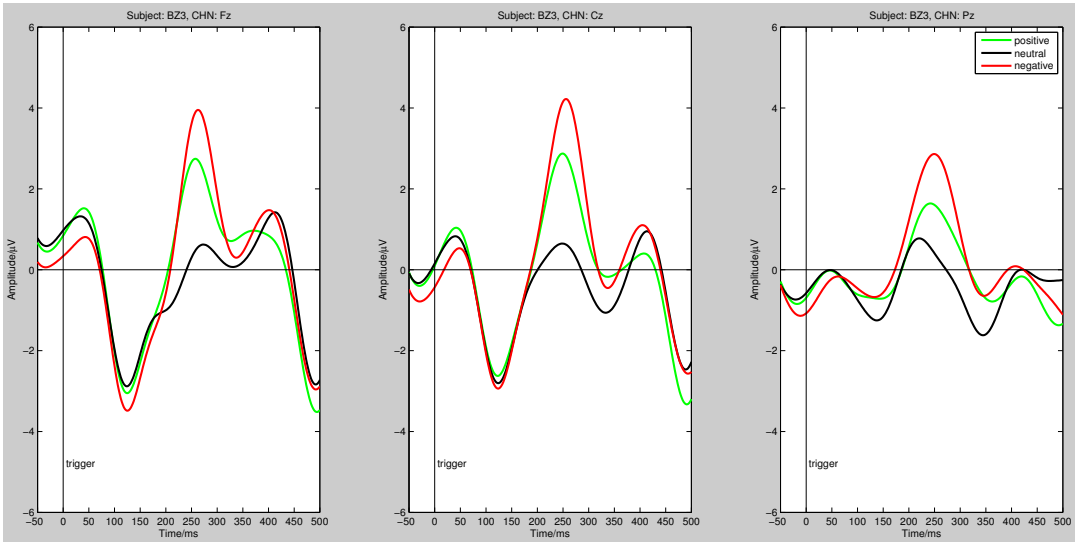

Figure 14: Subject BZ3: Mean waveforms elicited from positive, neutral and negative images in the prestudy. Black waveform: Response to neutral image; Green waveform: Response to positive image; Red waveform: Response to negative image. A clear difference in amplitude at $t = 250\,\text{ms}$ can be seen in all three channel locations.

Subject BZ3 shows a clear difference in mean in a time interval between $t_1 = 150\,\text{ms}$ and $t_2 = 300\,\text{ms}$ after the stimulus occurs. The negative images elicit a larger potential

in this time interval than the positive or neutral images. The neutral images show the lowest amplitude of all three mean waveforms.

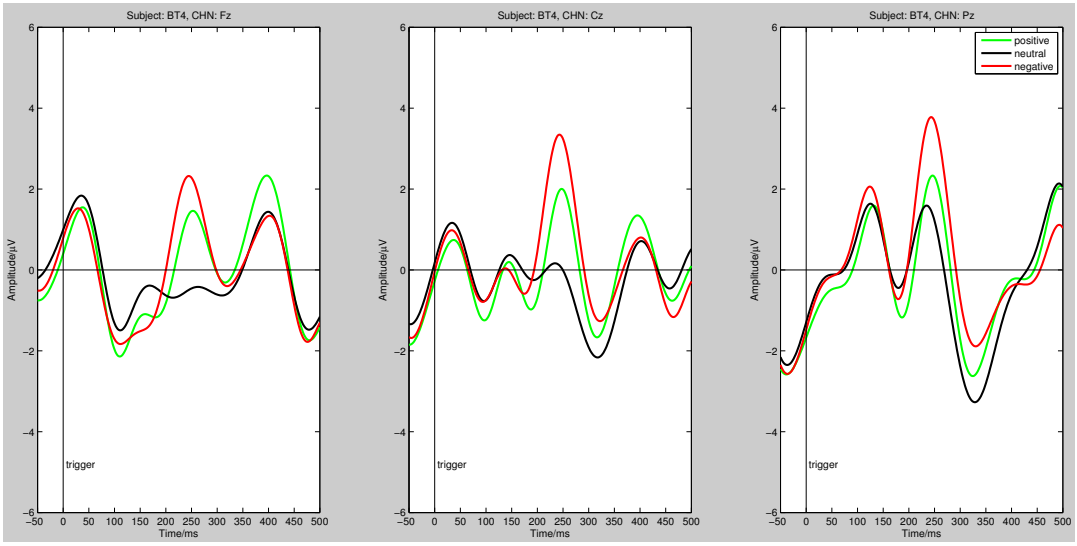

Figure 15: Subject BT4: Mean waveforms elicited from positive, neutral and negative images in the prestudy. Black waveform: Response to neutral image; Green waveform: Response to positive image; Red waveform: Response to negative image. A clear difference in amplitude at $t = 250\,\text{ms}$ can be seen in all three channel locations.

In subject BT4, the same effect as before can be observed: Positive and negative images seem to elicit a greater amplitude of a potential between $t_1 = 150\,\text{ms}$ and $t_2 = 300\,\text{ms}$ than neutral images. Again, the lowest amplitude in this interval can be seen in the response to neutral pictures. The negative condition is accountable for the highest amplitudes in mean in this time interval.
The effect, that the waveform of the response to positive and negative images differs in mean from the "neutral" waveform can also be observed with the subjects BL5, BX2, and CC1. The corresponding waveforms can be seen in the appendix (Figures 33, 34, and 35).

3.1.2. Variation in the data

The variation in the data was quite high, which can be seen, if the 95 % confidence intervals are added to Figure 14 and to Figure 15 as it is done in the Figures 16 and 17, respectively.

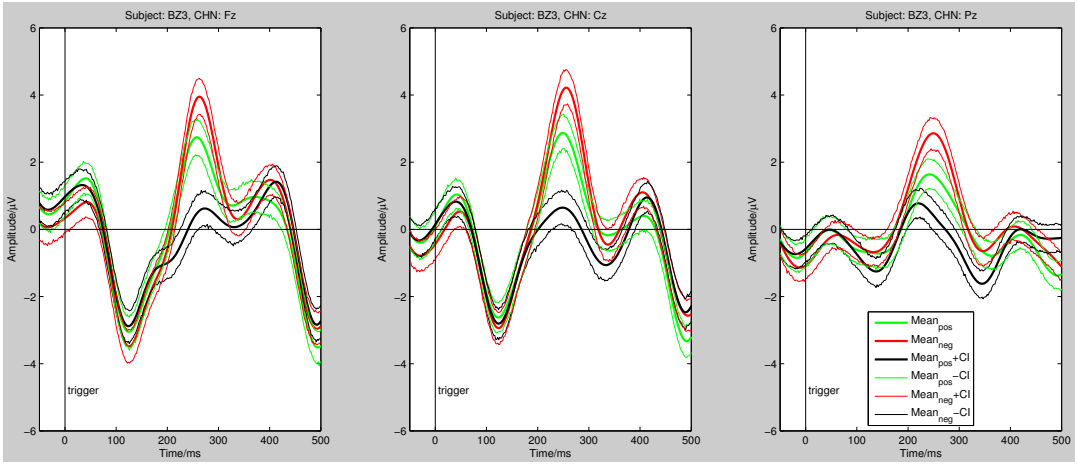

Figure 16: Subject BZ3: Mean waveforms and 95% confidence intervals elicited from positive, neutral and negative images in the prestudy. Black waveform: Response to neutral image; Green waveform: Response to positive image; Red Waveform: Response to negative image. All waveforms are the mean values over the number of trials ± the 95% confidence interval.

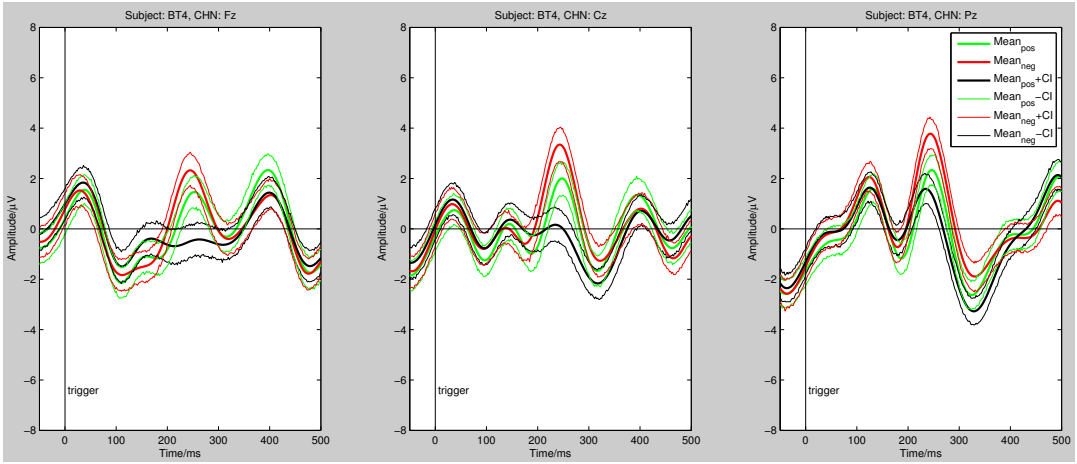

Figure 17: Subject BT4: Mean waveforms and 95% confidence intervals elicited from positive, neutral and negative images in the prestudy. Black waveform: Response to neutral image; Green waveform: Response to positive image; Red Waveform: Response to negative image. All waveforms are the mean values over the number of trials ± the 95% confidence interval.

In all of the subjects, the mean waveforms for positive and negative images differed from the mean waveform of neutral images. The mean waveforms for positive and negative images are not as distinct from each other. By looking at the confidence intervals of the waveforms, a slight significant difference between the image categories can be observed, especially between the emotional arousing conditions (positive and negative images) and the neutral condition.

3.1.3. Classification

After looking at the mean waveforms and their corresponding 95 % confidence intervals, the reactions to each positive, negative, and neutral image were classified against each other using SWLDA. Table 2 shows the classification accuracy after a 10x10 cross-validation for the following three data subsets: positive vs. negative images; positive vs. neutral images; negative vs. neutral images. The better than random accuracy, which was calculated as in [37] in this case was at about $ACC_{BTR} = 52\,\%$.

Table 2: Single trial classification results of the prestudy after a 10x10 cross-validation using SWLDA. All three conditions (positive, neutral, and negative) were classified against each other for the 5 subjects of the prestudy. Classification of the conditions negative vs. neutral resulted in the highest accuracies in 4 of the subjects, subject CC1 scored the higher classification accuracy while comparing the conditions positive and neutral to each other.

	Classification Accuracy/%		
Subject	positive vs. negative	positive vs. neutral	negative vs. neutral
BX2	62.20	68.27	69.07
CC1	62.36	70.91	69.64
BL5	60.13	66.03	68.17
BZ3	57.89	63.13	64.05
BT4	55.62	60.29	62.20

In 4 of the subjects, the condition negative vs. neutral is considered the "winner", as the classification is carried out binary, classifying each class against the rest seperately. The results for the condition positive vs. negative are the lowest in all of the subjects.

3.2. Main study

The main study consists of a test or "oddball"-paradigm and the actual paradigm.

3.2.1. Oddball paradigm

For the main study, the performance of the postprocessing routine had to be tested using an oddball paradigm, as described in the previous chapter, in order to elicit a P300 wave. As there were 80 different conditions (pictures) to be classified against each other, a one-vs-rest classification routine is used. Table 3 shows the results of this classification routine for the target condition versus the rest of all the conditions. In total, $80 \cdot 50 = 4000$ trials were recorded (50 conditions, 80 trials per condition). Considering a one-vs-rest classification, a maximum of 50 vs 3950 trials can be discriminated from each other. As in some trials artefacts appear, these trials were eliminated using the before described artefact correction.
Of course, this one-vs-rest routine was computed for all of the conditions, and the winner (highest classification accuracy after a 10x10 cross-validation) was chosen. The whole table with all the classification results for each condition can be found in the appendix (B). It was possible to classify the condition, where the P300 wave was expected in all of the subjects with classification accuracies between 82.48 % and 98.55 % (Mean accuracy of the target condition over all subjects 88.38 % $\pm$ 0.053 %). The resulting values for the classification accuracy are obtained through averaging the two generated accuracies for class 1 and class 2 after a 10x10 cross-validation, as it has been done in every classification in this study.

Table 3: Classification results of the oddball paradigm after a 10x10 cross-validation using SWLDA. In each case, the response to each images is being classified against all the rest of the images. This results in a classification of all trials of a target condition (maximum of 50 trials) vs. all trials of the other conditions (maximum of 3950 trials) in each case. The mean accuracy is a mean over all the resulting classification accuracies for each subject (see Table 7).

Subject	Selected Picture	Classification accuracy/%	Mean accuracy/%
CD2	30	90.62	67.65
CD3	49	82.93	65.55
CD4	7	82.48	70.47
CD5	27	90.04	68.59
CD6	16	82.62	62.33
CD7	18	89.31	55.85
CD8	41	83.96	70.02
CD9	30	98.55	74.23
CE1	16	91.66	67.07
CE3	41	91.60	68.16

In Figure 18, all mean waveforms for the 80 conditions can be seen with the corresponding Grand Average (black curve). The red curve denotes the mean waveforms of all trials for the target condition, the green curves are the remaining conditions. Channels Cz, Pz, and Oz serve as an example.

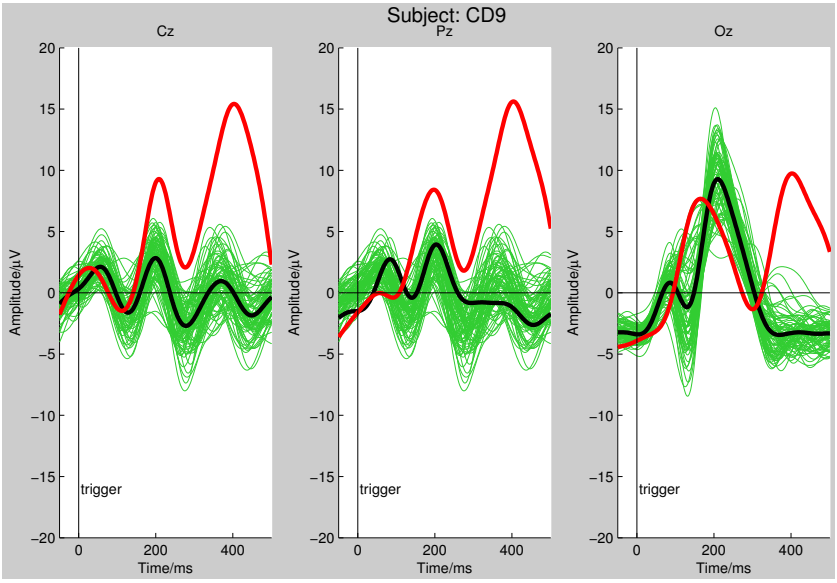

Figure 18: Subject CD9: Mean waveforms of the oddball paradigm. black curve: Grand Average; red curve: target condition; green curves: Remaining conditions. All conditions are mean waveforms over the number of trials per condition. The image is presented at $t = 0\,\text{ms}$ (trigger).

The mean target waveform of Subject CD9 showed the greatest detectability of all subjects. This can be seen primarily in the high classification accuracy (98.55 % for the target condition) and also in the mean waveform of the target condition (red curve) in Figure 18.

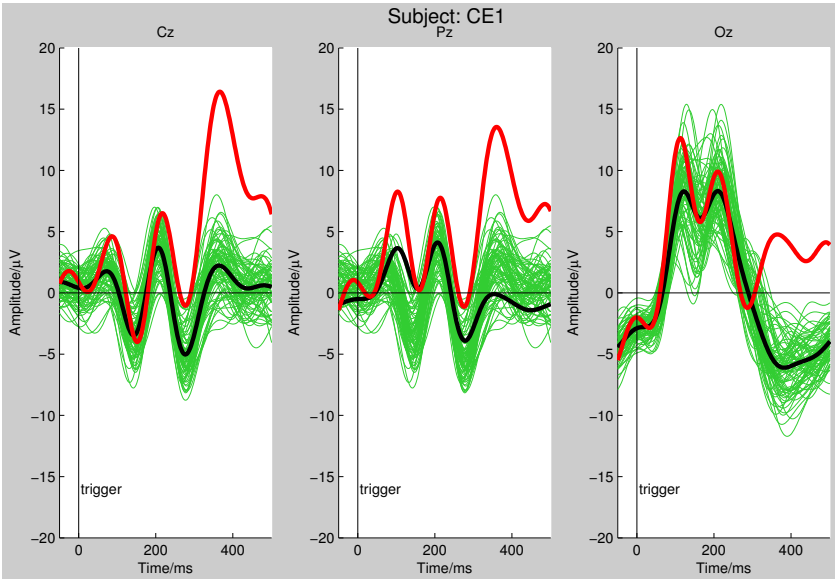

Figure 19: Subject CE1: Mean waveforms of the oddball paradigm. black curve: Grand Average; red curve: target condition; green curves: Remaining conditions. All conditions are mean waveforms over the number of trials per condition. The image is presented at $t = 0\,\text{ms}$ (trigger).

Subject CE1 also showed a good discriminability between the target conditions and all others, as seen in Figure 19. In a time interval starting at about $t = 300\,\text{ms}$, a P300 wave is observable in all three channels displayed in the figure.

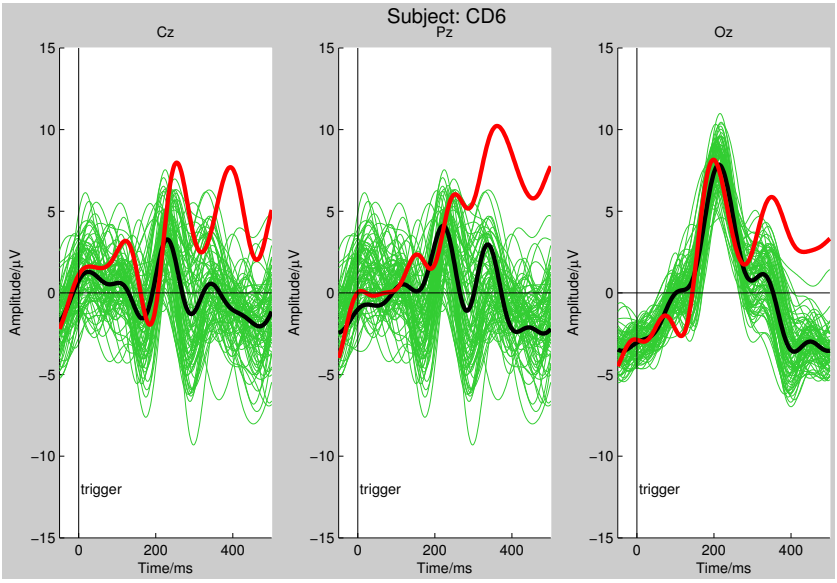

Figure 20: Subject CD6: Mean waveforms of the oddball paradigm. black curve: Grand Average; red curve: target condition; green curves: Remaining conditions. All conditions are mean waveforms over the number of trials per condition. The image is presented at $t = 0\,\text{ms}$ (trigger).

Subject CD6 had a rather low classification accurcy of 82.62 % compared to the other subjects. But still, the mean waveform of the target condition is clearly different in mean in a time interval starting at about $t = 300\,\text{ms}$ after the onset stimulus (see Figure 20).

In all subjects, the mean waveform of the target condition differed clearly from the waveforms of the other conditions, if averaged over the number of trials, mostly in the central, the parietal, and the occipital region of the scalp. The other subjects' waveforms can be seen in the appendix (see A). This is consistent with the previous results considering the classification between the conditions.

3.2.2. Actual paradigm

The actual paradigm consists of runs 1 and 2 for each subject. First, images with a strongly positive and also images with a strongly negative rating in the 7-point Likert scale, are classified against each other. Figures 21, 22, and 23 show the mean waveforms of highly attractive and unattractive images as an example for three of the subject, for the channels Fz, Cz, and Pz.

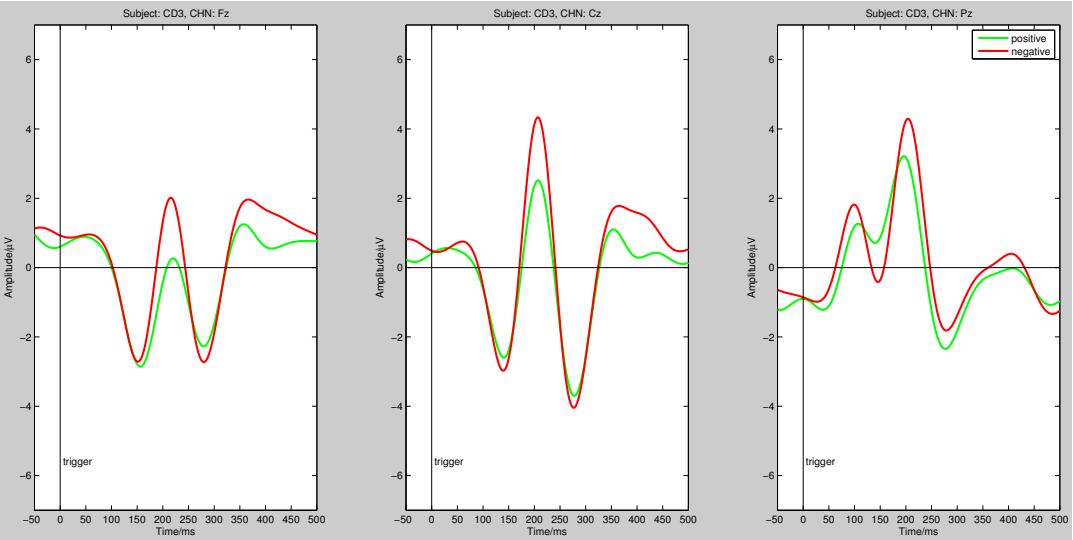

Figure 21: Subject CD3: Mean waveforms of the actual paradigm. Red curve: positive/attractive conditions; green curve: negative/unattractive condition. All conditions are mean waveforms over the number of trials per condition. A difference in amplitude at about $t = 200\,\text{ms}$ can be seen in all three channel locations.

The difference between negative and positive pictures, as observed in the preliminary study, is not as clear when comparing attractive and unattractive images from the main study with each other. In subject CD3, this difference though is still observable.

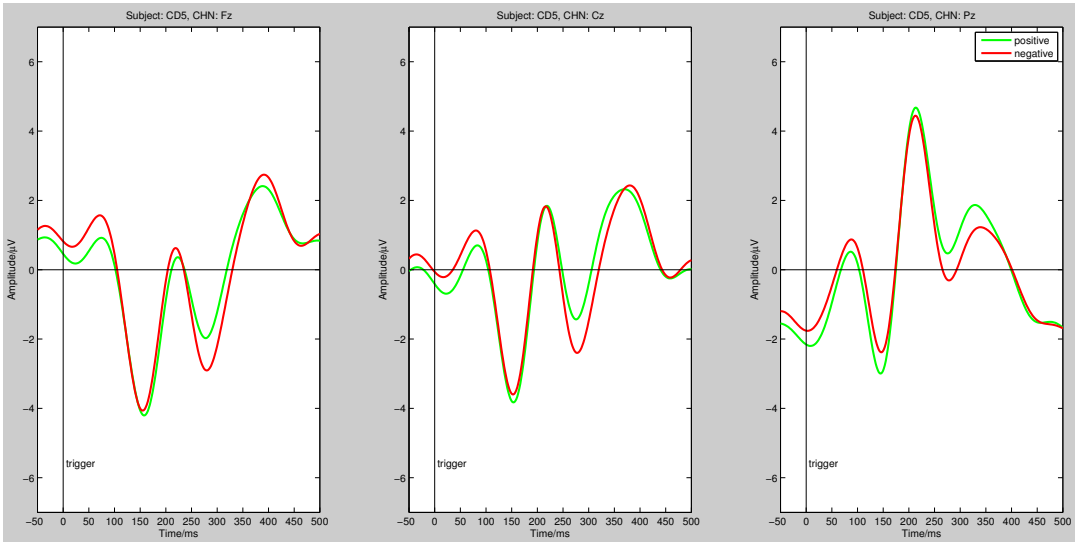

Figure 22: Subject CD5: Mean waveforms of the actual paradigm. Red curve: positive/attractive conditions; green curve: negative/unattractive condition. All conditions are mean waveforms over the number of trials per condition. The image is presented at $t = 0\,\text{ms}$ (trigger).

The mean waveforms of attractive and unattractive images for subject CD5 do not show a major difference. In a time interval between $t_1 = 250\,\text{ms}$ and $t_2 = 350\,\text{ms}$, the amplitude of the attractive pictures is slightly higher than the amplitude of the mean waveform of unattractive images (Channel Pz).

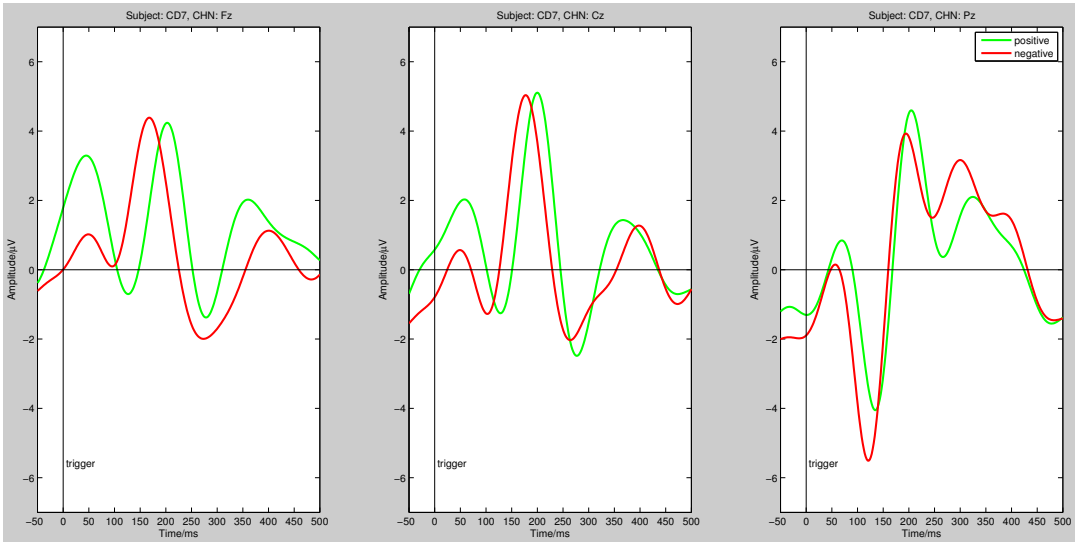

Figure 23: Subject CD7: Mean waveforms of the actual paradigm. Red curve: positive/attractive conditions; green curve: negative/unattractive condition. All conditions are mean waveforms over the number of trials per condition. The image is presented at $t = 0\,\text{ms}$ (trigger).

As subject CD3 shows a difference in amplitude and subject CD5 shows almost no difference while comparing the mean waveforms of selected attractive and unattractive images, the waveforms for subject CD7 seem to differ rather in latency than in amplitude. There is a higher amplitude in channel Pz for unattractive images.

The variance in the data for these three subjects are shown in the Figures 24, 25, and 26. All figures are the mean waveforms of selected attractive and unattractive images with the corresponding 95 % confidence interval.

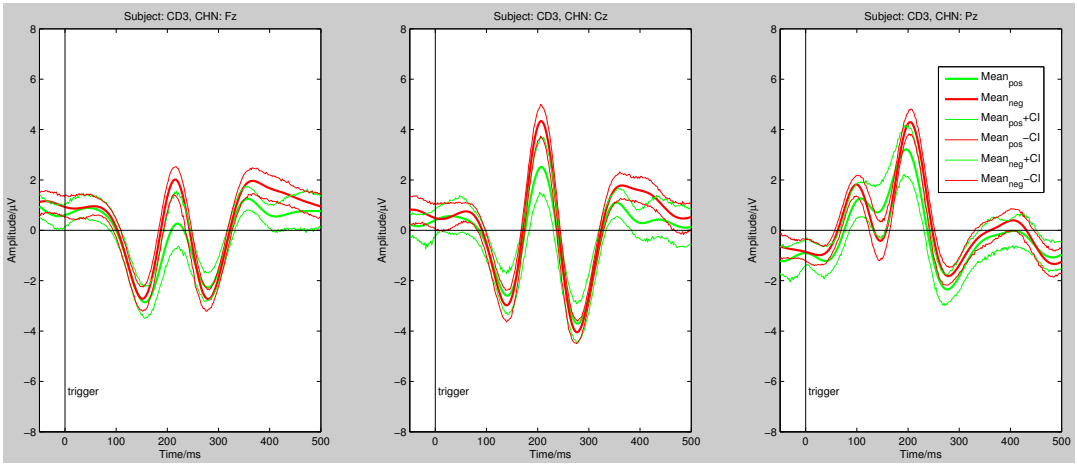

Figure 24: Subject CD3: Mean waveforms and 95% confidence intervals of the actual paradigm. Red curve: positive/attractive conditions; green curve: negative/unattractive condition. All conditions are mean waveforms ± confidence interval over the number of trials per condition. The image is presented at $t = 0\,\text{ms}$ (trigger).

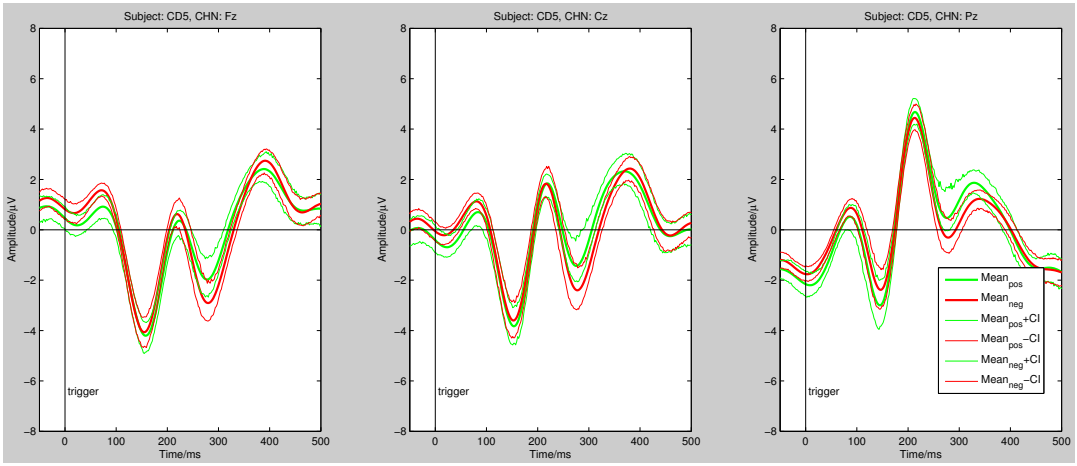

Figure 25: Subject CD5: Mean waveforms and 95% confidence intervals of the actual paradigm. Red curve: positive/attractive conditions; green curve: negative/unattractive condition. All conditions are mean waveforms ± confidence interval over the number of trials per condition. The image is presented at $t = 0\,\text{ms}$ (trigger).

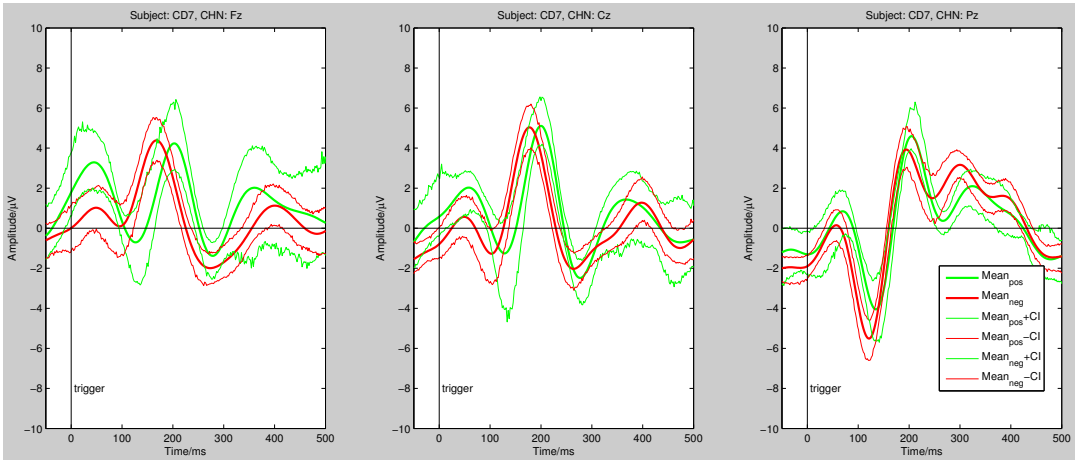

Figure 26: Subject CD7: Mean waveforms and 95% confidence intervals of the actual paradigm. Red curve: positive/attractive conditions; green curve: negative/unattractive condition. All conditions are mean waveforms ± confidence interval over the number of trials per condition. The image is presented at $t = 0\,\text{ms}$ (trigger).

In none of the subjects a clear significant difference between attractive and unattractive images can be seen, as the mean waveforms with their corresponding 95% confidence intervals are not clearly separable from each other. In some of the subjects, a slight difference between the waveforms can be observed, but this difference is inly significant in a small time interval of about $t = 20 - 30\,\text{ms}$ as in Figure 24 in channel Cz for a time period starting at about 380 ms. But this small difference in one subject can not be seen in all of the other subjects for these 3 channels (see appendix A).

The Grand Average over all trials for subject CD3 is shown in Figure 27 as a topographic plot over the scalp. Also, the difference between the attractive and the unattractive images is show again as a topographic plot over the scalp.

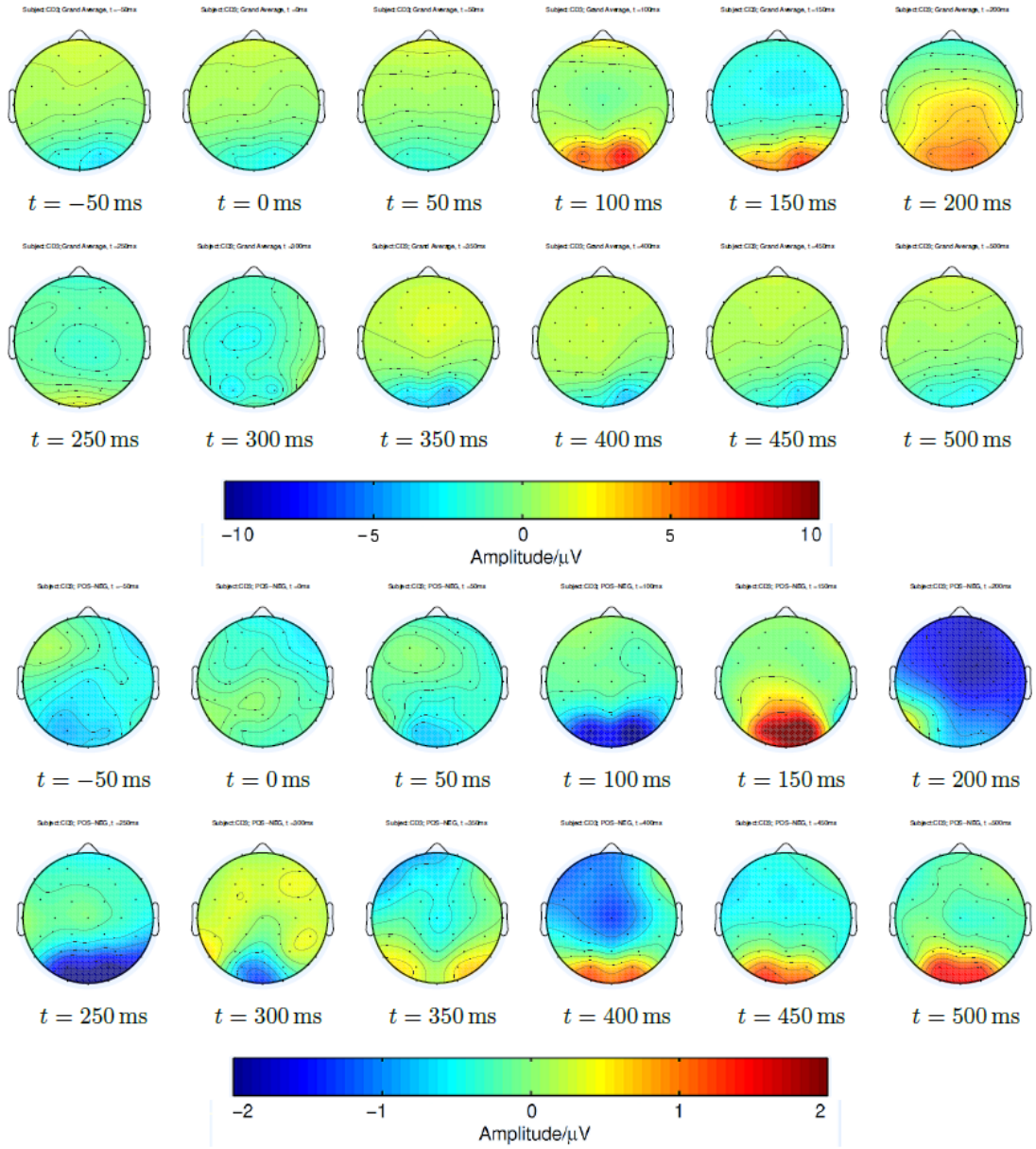

Figure 27: Subject CD3: Topographic plot of the Grand Average over the scalp (top) and the difference between attractive and unattractive images as a distribution over the scalp (bottom) for the time interval between $t_1 = 50\,\text{ms}$ and $t_2 = 500\,\text{ms}$ in $50\,\text{ms}$ steps.

The topographic distribution of the Grand Average shows, that the occipital and parietal electrodes record a high amplitude in the time interval between $t = 100\,\text{ms}$ and $t = 200\,\text{ms}$, as the visual cortex then is activated by the stimulus. At the time $t = 400\,\text{ms}$, the stimulus seems to be fully processed as there are no more relevant changes in amplitude.

Figure 27 shows, that through subtraction of attractive and unattractive images, a slight difference between these two conditions can be observed. Note that the amplitudes in the scalp are between $-2\,\mu\text{V}$ and $+2\,\mu\text{V}$. At the time point $t = 200\,\text{ms}$, there is a overall negativation in amplitude and at a time point $t = 150\,\text{ms}$ there are more positive amplitudes to be observed, which means that at these timepoints, the difference between the conditions is the highest, but still only in a range from about $-1.5\,\mu\text{V}$ and $+1\,\mu\text{V}$.

Figure 28 shows the Grand Average and the difference between attractive and unattractive images for subject CD5 over all trials as a topographic distribution over the scalp.

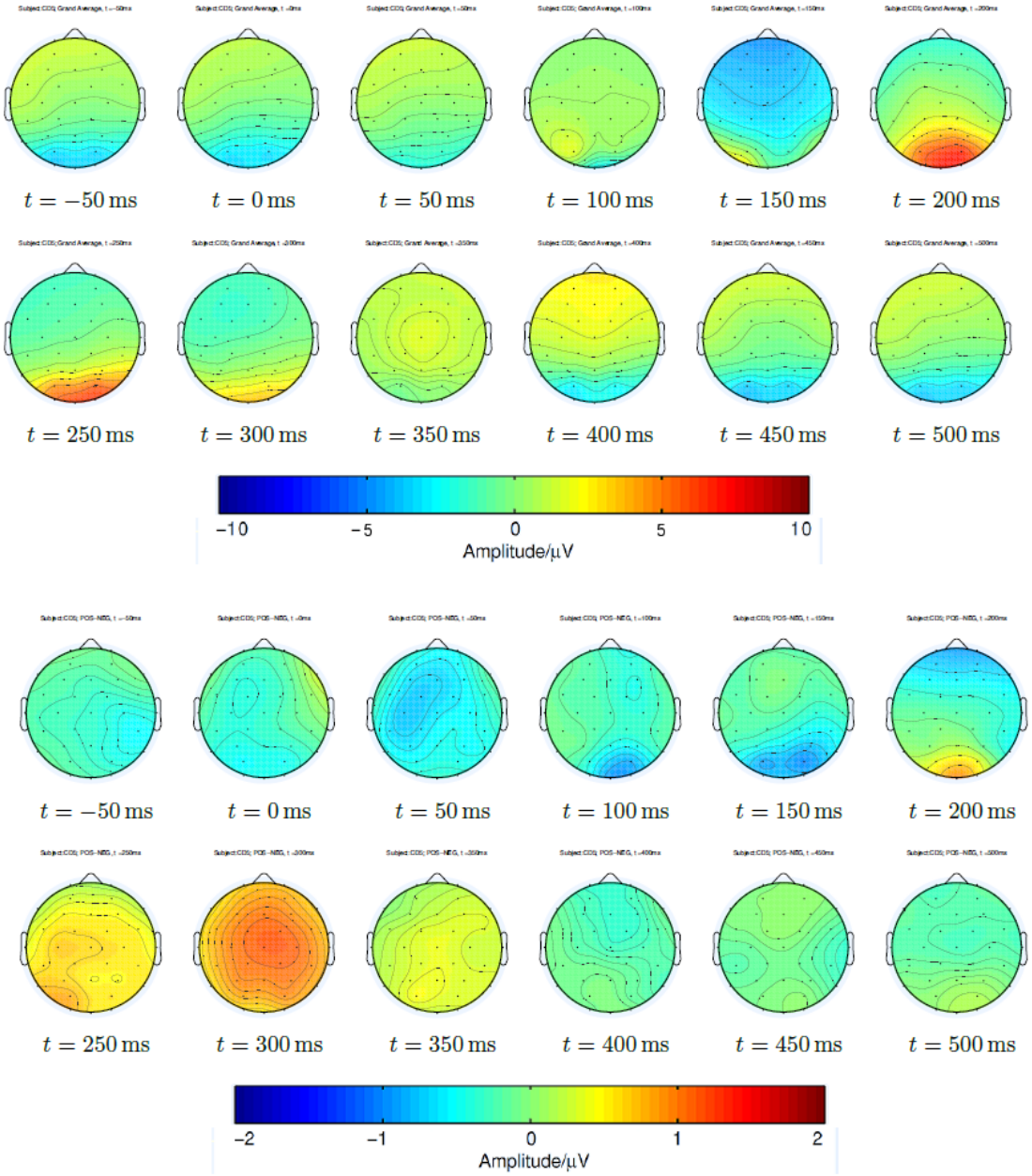

Figure 28: Subject CD5: Topographic plot of the Grand Average over the scalp (top) and the difference between attractive and unattractive images as a distribution over the scalp (bottom) for the time interval between $t_1 = 50\,\text{ms}$ and $t_2 = 500\,\text{ms}$ in 50 ms steps.

Here, in a time interval between $t = 200\,\text{ms}$ and $t = 250\,\text{ms}$, the amplitudes in the occitpital and pariatal region of the brain are the highest. The visual cortex is activated during this interval.

Subject CD5 (Figure 28) shows minor differences in amplitude than thoses examined with subject CD3. Between the timepoints $t = 200\,\text{ms}$ and $t = 350\,\text{ms}$, the difference between attractive and unattractive images is the greatest.

The topographic distribution of the Grand Average of subject CD7 can be seen in Figure 29. Also, the difference between attractive and unattractive images is observable.

Again, an activation of the visual cortex can be seen with subject CD7 (Figure 29), although there is a negativation of the primary visual cortex at a time of $t = 150\,\text{ms}$.

The overall differential amplitudes over the scalp show the largest variation in subject CD7 (see Figure 29). The difference in amplitudes is greater than the scale in the bottom, as values over $|2\,\mu\text{V}|$ occur. This scale is set to an amplitude range between $-2\,\mu\text{V}$ and $+2\,\mu\text{V}$ intentionally, as the other figures for the differential amplitudes refer to the same scale. What it exposes is, that in subject CD7 the difference between the conditions was quite high, especially between $t = 100\,\text{ms}$ and $t = 350\,\text{ms}$. Also, subject CD7 chose less images to be attractive and unattractive, so that the mean value over the trials is has less data points to average from and this results in a higher noise for the mean values (see Eq. 1).

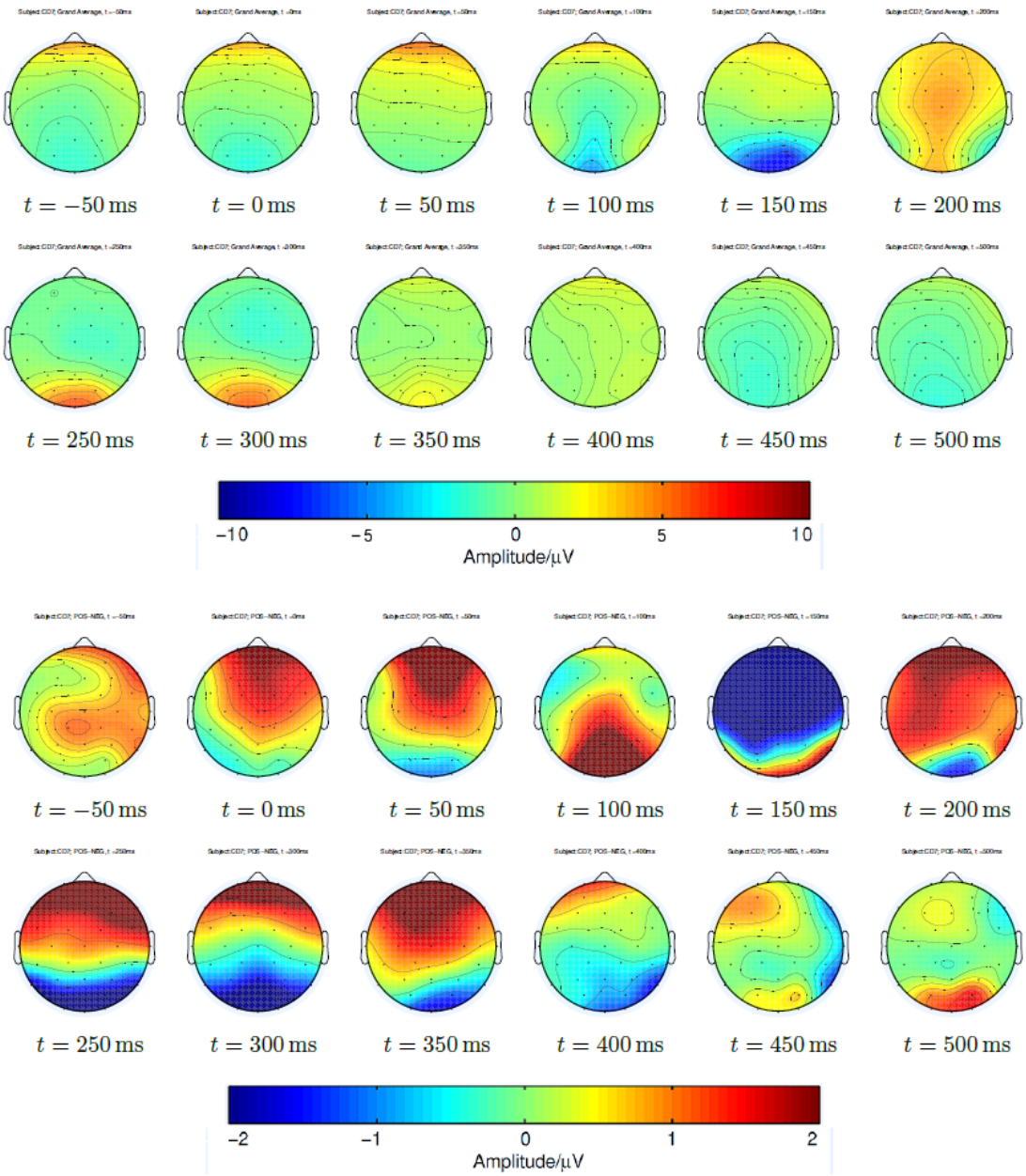

Figure 29: Subject CD7: Topographic plot of the Grand Average over the scalp (top) and the difference between attractive and unattractive images as a distribution over the scalp (bottom) for the time interval between $t_1 = 50\,\text{ms}$ and $t_2 = 500\,\text{ms}$ in 50 ms steps.

Now, attractive and unattractive images/conditions were chosen from each subject by evaluating the data obtained with the paper- and pencil test. Only images that were rated 7 or 6 in the Likert scale were taken as attractive images. An image was considered unattractive to the subject, if a score of 1 or 2 was chosen. A total list of the subjects' answers can be found in the appendix (B).

Table 4 shows a summary of the classification results, when comparing selected attractive and unattractive images with each other. As an equal number of trails in this procedure can not be obtained, the values for the classification accuracy can not be used as a valid measure and κ is used instead.

Table 4: Attractive vs. unattractive classification: κ-Values and values for the classification accuracy with the corresponding selected trials for each condition (attractive vs. unattractive).

Subject	κ	Classification accuracy/%	# trials attractive	# trials unattractive
CD2	**0.23**	62.66	747	1693
CD3	**0.43**	72.18	858	1432
CD4	**0.16**	60.52	243	831
CD5	**0.21**	60.45	784	1020
CD6	**0.04**	52.94	541	1962
CD7	**0.30**	68.25	137	415
CD8	**0.14**	60.93	422	1945
CD9	**0.18**	59.02	1239	1249
CE1	**0.15**	72.46	138	2407
CE3	**0.11**	61.59	319	2589

The mean kappa value over all subjects is $mean_\kappa \pm std = 0.195 \pm 0.109$, the mean accuracy over all subjects is calculated at $mean_{ClassificationAccuracy} \pm std = 62.616 \pm 6.217$. As each subject chose an unequal number of images to be attractive and unattractive to them, the number of trials differ in every subject and in both of the two conditions. Therefore, the κ-Value seems to be the more accurate measure compared to just the simple classification accuracy.

Table 5 denotes the correlation coefficient r_p obtained from comparing the classification accuracies from each condition (image) with the self-assessment ratings of each subject individually. Usually, the result can be considered statistically significant for $p \leq 0.05$, but as the 10 rank correlation for each of the 10 subjects are calculated, the significance level has to be divided by the number of observations ($n = 10$), which leads to a significance level of $p_{corrected} \leq 0.005$.

Table 5: Correlation (r_p) of the classification results with the personal ratings and the corresponding p-values.

	Attractive		**Comfortable**		**Innovative**	
Subject	r_s	p	r_s	p	r_s	p
CD2	0.0972	0.3909	0.2474	0.0269	0.1655	0.1422
CD3	0.1417	0.2100	0.0926	0.4139	0.2573	0.0212
CD4	0.1669	0.1389	0.1679	0.1365	0.1464	0.1949
CD5	-0.2309	0.0393	0.0716	0.5276	-0.1257	0.2664
CD6	0.0616	0.5873	0.0431	0.7045	-0.0944	0.4051
CD7	-0.1486	0.1882	0.0121	0.9149	-0.0083	0.9415
CD8	-0.0520	0.6472	0.0284	0.8023	0.1121	0.3223
CD9	0.1047	0.3554	0.0958	0.3981	0.0558	0.6227
CE1	-0.011	0.9230	0.1581	0.1612	0.221	0.0488
CE3	0.0363	0.7493	0.3207	0.1137	-0.0374	0.7422

The classification accuracies and the self-assessment rankings of each subject did not correlate statistically significant in any of the subjects. Even if not considering the Bonferroni correction for the p-Values and thus taking a p-Value of $p = 0.05$ as the border for statistical significance, only 3 of the subjects showed a slight correlation of $r_p = 0.2474$ for subject CD2 (comfortability and classification accuracies), $r_p = 0.2573$ for subject CD3 (innovativeness and classification accuracies), and a slight negative correlation ($r_p = -0.2309$) in subject CD5 (attractiveness and classification accuracies).

Graphically, the classification accuracies and their corresponding personal ratings can be seen in Figure 30 (ratings for attractiveness), Figure 31 (ratings for comfortability), and Figure 32 (ratings for innovativeness). These figures are graphical representations of the mean classification accuracies (and their standard deviations) according to each value of the 7-point Likert scale of the personal ratings for each subject.

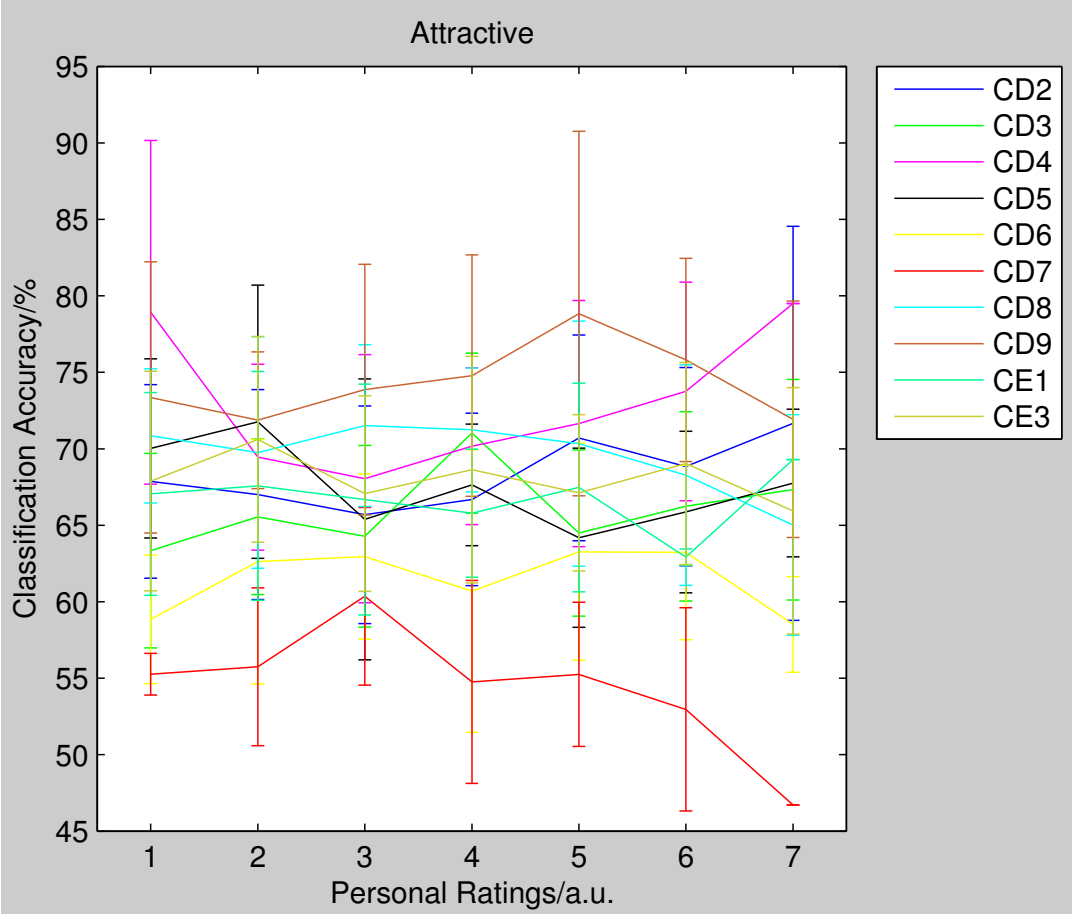

Figure 30: Graphical representation of personal ratings and the corresponding classification accuracies (attractive). All values are mean ± std over each value of the 7-point Likert scale.

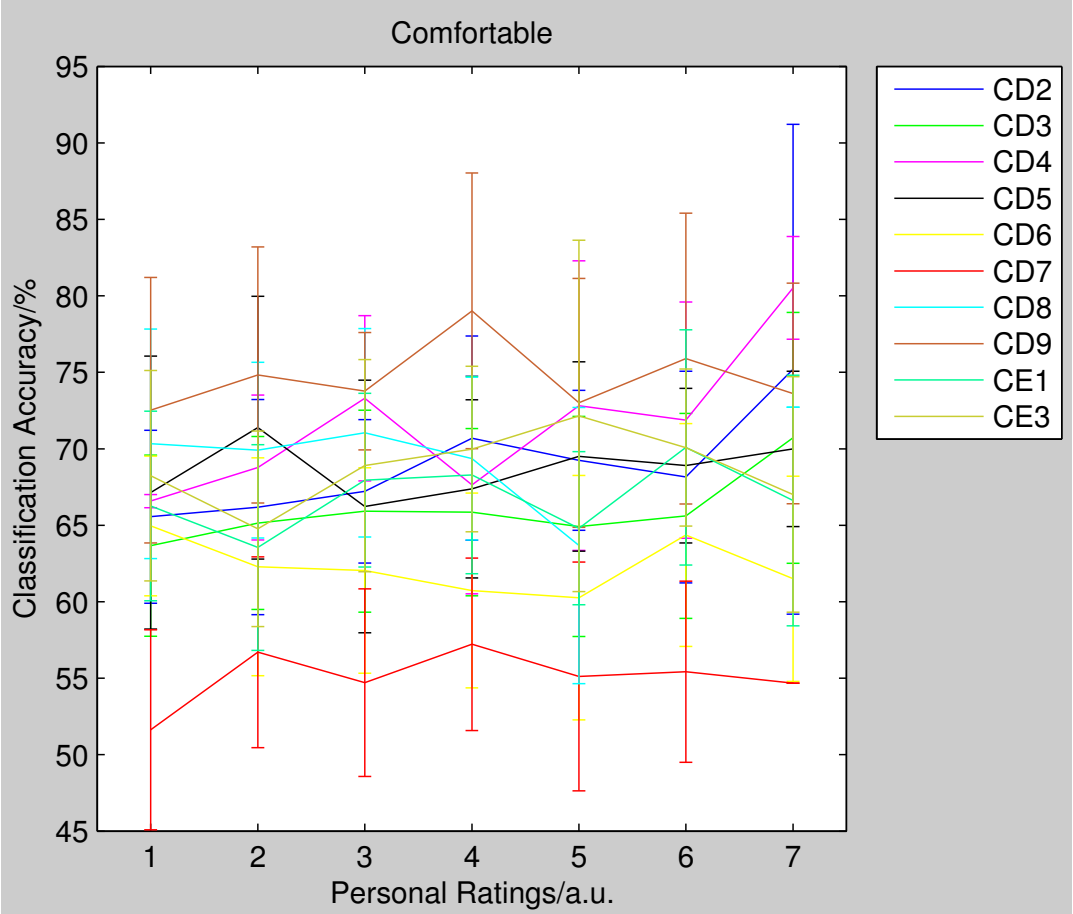

Figure 31: Graphical representation of personal ratings and the corresponding classification accuracies (comfortable). All values are mean ± std over each value of the 7-point Likert scale.

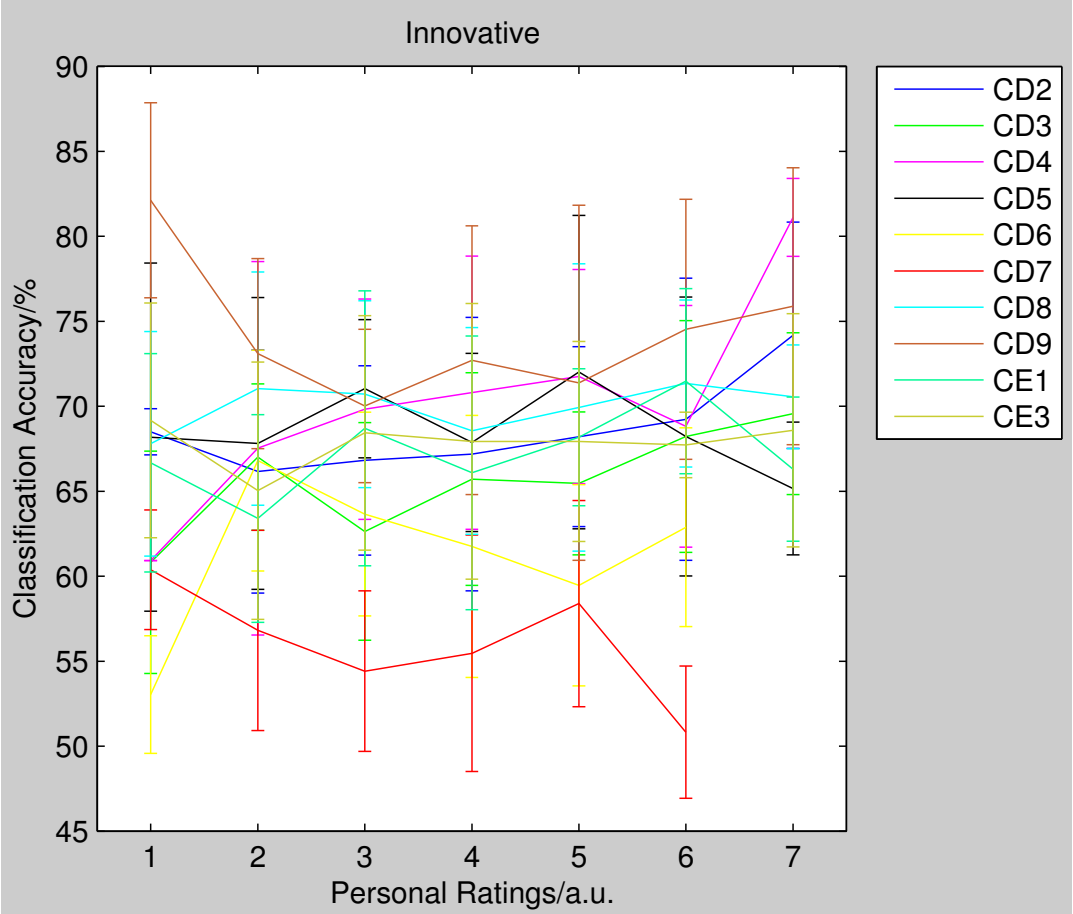

Figure 32: Graphical representation of personal ratings and the corresponding classification accuracies (innovative). All values are mean ± std over each value of the 7-point Likert scale.

An ideal curve, where classification accuracy correlates positive and/or negative with the individual personal ratings, would have its maximum at one of the ends of the curve, or at both of them. This would declare a true correlation between the classification accuracies and the personal ratings for each scale. In Figures 30, 31, and 32, no statistical significanttendencies to one of the outer values of the Likert scale (1 and 7) can be observed. This is congruent with the results obtained by calculating the correlation between the classification accuracies and the personal ratings.

4. Discussion

This chapter summarizes and gives an interpretation of the obtained results. It also states, whether the results fit into recent findings of the literature and gives an overview of the general issues of the work done.
In the preliminary study, the mean waveforms of the response to positive, neutral, and negative images have been recorded and a classification attempt between these three conditions has been made. For the main study, another set of images has been chosen and the subjects were asked to rate these images according to their personal favor. These ratings have been taken as a measure of how likable the objects on the images are to each subject. After classifying the EEG response to each image against all of the other images, the correlation between the personal ratings and the classification accuracies has been calculated. Also, as the subjects were asked to focus on one of the images in the last 2 of the 4 runs in the main study, this one target images has been successfully classified against the other images for each subject.

4.1. Preliminary Study

The mean waveforms elicited by neutral images differed in amplitude in a range between $t_1 = 150\,\text{ms}$ and $t_2 = 350\,\text{ms}$ from the mean waveforms of positive and negative images. This is consistent with the results of Flaisch et al. [17], where images with highly emotional content show a larger posterior negativity compared with neutral pictures and consequently, emotional target pictures showed a better detectability. The classification between images of different emotional content should therefore be possible.
This has not been achieved very satisfactory as the classification results were not as high as expected. The winner of the binary classification performed with the data of the preliminary study has been the condition "negative vs. neutral" in 4 of the subjects and the condition "positive vs. neutral" in subject CC1. The classification accuracies varied between 62.20% and 70.91% for the winning condition. This actually means that the conditions with images containing emotional content show a higher difference in the data to the neutral condition than comparing the positive and the negative condition with each other. As it has been stated in Flaisch et al. [17], images with a higher hedonic valence are discriminant from neutral pictures, but the difference between pleasant and unpleasant pictures is lower. This can also be reported here. Now, if even images with a strong positive and negative hedonic valence can not be discriminated from each other, the classification of images with a lower emotional content might be even harder to accomplish.
What might have also raised the variance in the data and consequently lower the classification accuracies, is the fact, that the IAPS images, although a broad selection has been made, still varied in their content. As 100 different images per class were taken for the preliminary study, of course, these pictures do not only consist of one category,

as for example positive images contained images displaying erotica, scenes of sports and adventure, landscapes, and food. All of them were rated with high valence and arousal values (see IAPS [32]), but might have a different meaning for each subject individually. This is one factor, that might raise the variance in the data.

4.2. Main Study

Oddball Paradigm
The results form the oddball paradigm are quite promising, as the classification of the individual target condition was accomplished to full satisfaction in all of the subjects (Classification accuracies between 82.48 % and 98.55 % for the individual subjects). The mean waveforms show a clear difference between the target condition and all others. There was though no statistical test (for example t-test) applied, if the waveforms differ statistical significant from each other, as afterwards a classification routine is implemented instead. The results indicate, that there were no major errors in the paradigm and the recording and preprocessing of the data was done satisfactory. This proven pre- and postprocessing routine can therefore be applied on the actual paradigm.

Actual Study
Considering the runs 1 and 2 of the main paradigm, the results do not look quite promising. The mean waveforms of selected attractive and unattractive pictures differ slightly in mean in every subject, but the confidence interval is still at a high level. Considering the classification of attractive vs unattractive images, the resulting accuracies are in a range between 52.94 % and 72.46 %. But for an unequal number of trials, classification accuracy does not serve as a valid measure for the performance of a classifier. Because of that, Cohen's kappa coefficient (κ) is taken into account: This parameter is in a range between $\kappa_{CD6} = 0.04$ and $\kappa_{CD3} = 0.43$ ($mean_\kappa \pm std = 0.195 \pm 0.109$). Landis and Koch proposed the following labels (Table 6) for the ranges of κ, to describe the relative strength of agreement [31]:

Table 6: Value ranges for Cohen's kappa coefficient and the corresponding strength of agreement as in [31].

Kappa Statistic	**Strength of Agreement**
<0.00	Poor
0.00-0.20	Slight
0.21-0.40	Fair
0.41-0.60	Moderate
0.61-0.80	Substantial
0.81-1.00	Almost Perfect

Taking these arbitrary divisions into account, one of the subjects (CD3) shows a moderate agreement in the classification performance, 3 subjects showed a fair agreement, and the rest of the subjects' performance was only slight. The meaning of this is, that the classifier in this case can not provide a valid performance over all of the subjects, so that the classification between attractive and unattractive images can not be accomplished to satisfaction.

Another attempt to classify between each dataset is to use a one-vs-rest classification of each image (or condition) individually for all of the conditions. As a high classification performance can only be accomplished if there is a observable difference within the conditions, classification accuracy after the 10x10 cross-validation here is taken as one value for the difference between each condition and the rest and therefore between each single condition. Classification accuracy increases with the difference in each dataset. Now, the hypothesis, that a high classification performance correlates with an image which is from importance to each subject is to be reviewed: As seen in Table 5, the classification accuracy does not correlate in any of the subjects with either the subjective attractiveness, the comfortability, or the innovativeness of an image or of the object on the specific image. There is no statistically significant correlation at all to be observed. If the Bonferroni correlation is not to be taken in account, there would have been a negative statistically significant correlation ($r_p = -0.2309$) between attractiveness and the performance in subject CD5, and a slight positive correlation ($r_p = 0.2474$) between comfortability and performance in subject CD2, and also a positive correlation ($r_p = 0.2573$) between innovativeness and performance in subject CD3. But with a p-Value as low as $p_{corrected} = 0.005$, no statistically significant and hence relevant correlation between the datasets can be found. The figures 21, 22, and 23 show the diversity of the results: In subject CD3, the mean waveforms differed in amplitude to a certain extend, subject CD5 showed almost no difference in the mean waveforms, and the waveforms of subject CD7 differed in latency.

4.3. General Aspects

Measurement Setup
In general, the measurement setup served as a good way of displaying the stimuli at a high rate. This has been proven through the oddball paradigm, where, as expected, the target condition was correctly classified in all of the subjects. E-PRIME® served as a valid software for a rapid presentation of the different images. Canto et al. reported an onset asynchrony for an ERP experiment with E-PRIME® of less than 1 ms using a parallel port [4]. Although this software could be used in a sufficient way in this offline experiment, the applications for an online BCI are quite limited, as there are some processing steps in between for merging the .gdf-file generated from MATLAB® and the E-PRIME®-file. An online paradigm could be made possible using OpenGL[8] or Python[9] Interfaces. The speed and the accuracy of displaying the stimuli is crucial for the success of such an experiment. Another issue for an online implementation of the system is the built-in filter function *filtfilt*. Because it corrects the phaseshift of the delay of the signal automatically through filtering primarily in the forward and afterwards in the backward direction, which raises the effective filter order. This is something that can not by applied to a online system in this special way.

The reason for reducing the stimulus duration from $t_{disp} = 333\,\text{ms}$ in the preliminary study to $t_{disp} = 100\,\text{ms}$ in the main study and introducing an ISI of $t_{ISI} = 400\,\text{ms}$ is, that effects like the attentional blink as in [45, 52] can occur if a stimulus is presented right after another. Also, the number of runs was reduced to 4 while increasing the duration of the runs to keep the subjects focused and concentrated.

Subjects
All of the subjects stated, that they were relaxed and motivated for the study. But a relatively long measurement time and long runs did in fact lower their motivation. As for being relaxed, some subjects reported fatigue in between some of the runs, and this might also have contributed to the quality of the results. Some subjects did also find it hard, to keep their eyes open without a constriction of their facial muscles. This enhances the noise on the frontal channels and is also a sign of increasing fatigue. A factor for reducing the fatigue, would be to reduce the measurement time, which was set to about $t_{duration} = 16.7\,\text{min}$, but the reported fatigue commenced already in the beginning or the mid of one run.
Overall, the subjects were though still focused and motivated and none of them had to be excluded from the study.

[8] Open Graphics Library; http://www.opengl.org/
[9] Python Programming Language; http://www.python.org/

Stimulus Intervariability
The variance in the data for the preliminary study is also due to the fact, that the emotional pictures can all be summarized into three categories, but still are different from each other in a way, that might have an outcome on the results. The cancellation of this effect was one of the reasons, why only two different categories of images (cars and chairs) were displayed in the main study.

Possible Improvements
One possible improvement could be the implementation of a paradigm that focuses on attention and/or concentration of the subjects. As the image search and the resulting image triage has been proven to work properly in other studies, this might be a crucial factor to success. But if a subject is instructed to focus on a likeable object, the effect of objectivity might be lost.
What can also be improved is, as said before, the software. In order to construct a online BCI, E-Prime® is not the right software to chose. The implementation of a online BCI has to be postponed though, until further measurements are conducted on this topic and a valid and proven way of discriminating between the conditions is found.
Other methods of discriminating between different conditions are also to be evaluated, such as principal component analysis (PCA) or a discrimination between the mean waveforms. This might though lower the speed of data processing and also diminish the chances of online applications.

What can be examined in further studies are the timing parameters. Are 100 ms stimulus time enough for a thorough processing of a high-level object? The attentional blink might be one factor for the disagreement of the subjective evaluation of the images and the classification performance. If a stimulus if followed by another immediately, the visual processing for the brain is harder to accomplish. As seen in figure 4, high-level object discrimination occurs at a time between 80 and 100 ms after the stimulus and the findings of Thrope et al. indicate, that for a highly demanding task, information processing can be accomplished in under 150 ms [54]. But this study was also based on the detection of one target image inside a series of non-target images in a go/no-go categorization, and not for the rating of images. As the emotional content of images displaying cars/chairs or other objects of advertisement or as seen on everyday life is of course lower than the hedonic valence of the emotional pictures of the IAPS [32], another workaround has to be found than the ideas of previous studies using pictures with an emotional content [17, 27, 5].

If a combination of the search for a target image in a series of non-target images and a subliminal rating of the (a priori not known) target images could be done, such a system might work in the future.
Another option is the inclusion of emotional design [9]. Here, different appraisal patterns of emotions such as contentment/satisfaction, happiness/joy, anger/irritation, and disappointment/dissatisfaction are used to seperate emotional groups of product design from each other. A way of creating a "product-design BCI" could be the a priori evaluation of these factors and how they could be applied on a certain product. This could be a reverse way of design and as objects with emotional content are examined, a difference in the subjective reactions can be expected.

The ideal way of implementation of such a "product-design BCI" would be, that a subject is placed in front of a monitor and at first, various forms of objects are displayed on the screen. The subject than "choses" his or her favorite form using a BCI. After finding a individually "perfect" form, different sets of color are evaluated. This procedure continues steadily, until the best (or most perfectly designed) object is chosen by the subject and therefore a "perfect" product in this case can be created. This has not only possible applications for the creation of the design of a product, but may also be adaptable for the evaluation of existing products.

5. Conclusion

In conclusion, the aims of the thesis were partially fulfilled. The chances of a creating passive BCI system in the way it was proposed, meaning that it uses ERPs for product design are presently quite low, as there was no statistically significant correlation between the rated attractiveness/comfortability/innovativeness and the classification performance.
There are several issues that should be evaluated before the design of such a BCI system can begin. Also, other measures than classification accuracy should be taken into account. Overall, the proposed system works well for the classification of a target image in a series of non-target images and would therefore also work for the image triage in a large set of target and non-target images. As in such a paradigm, focus and concentration are the main effects that provide good results, the paradigm for a "Product design-BCI" should also be implemented in a way, where visual attention is a factor to success.

Bibliography

References

[1] N. Bigdely-Shamlo, A. Vankov, R.R. Ramirez, and S. Makeig. Brain activity-based image classification from rapid serial visual presentation. *IEEE Trans Neural Syst Rehabil Eng*, 16(5):432–41, 2008.

[2] N. Birbaumer, N. Ghanayim, T. Hinterberger, I. Iversen, B. Kotchoubey, A. Kübler, J. Perelmouter, E. Taub, and H. Flor. A spelling device for the paralysed. *Nature*, 398(6725):297–298, 1999.

[3] C. Brunner. *Informationsverarbeitung im Menschen.* Lecture notes, Graz University of Technology, 2010.

[4] R. Canto, I. Bufalari, and A. D'Ausilio. A convenient and accurate parallel Input/Output USB device for E-Prime. *Behavior Research Methods*, pages 1–5, December 2010.

[5] L. Carretié, M. Martín-Loeches, J.A. Hinojosa, and F. Mercado. Emotion and attention interaction studied through event-related potentials. *J Cogn Neurosci*, 13(8):1109–1128, 2001.

[6] M.M. Chun and M.C. Potter. A two-stage model for multiple target detection in rapid serial visual presentation. *Journal of experimental psychology. Human perception and performance*, 21(1):109–127, February 1995.

[7] J. Cohen. A Coefficient of Agreement for Nominal Scales. *Educational and Psychological Measurement*, 20(1):37–46, April 1960.

[8] A.R. Damasio. *Descartes' Error: Emotion, Reason and the Human Brain.* Grosset/Putnam, 1994.

[9] E. Demir, P.M.A. Desmet, and P. Hekkert. Appraisal patterns of emotions in human-product interaction. *International Journal of Design*, 3(2):41–51, 2009.

[10] M.W. Donald and W.R. Goff. Attention-related increases in cortical responsivity dissociated from the contingent negative variation. *Science*, 172(3988):1163–6, 1971.

[11] E. Donchin, K.M. Spencer, and R. Wijesinghe. The mental prosthesis: assessing the speed of a P300-based brain-computer interface. *Rehabilitation Engineering, IEEE Transactions on [see also IEEE Trans. on Neural Systems and Rehabilitation]*, 8(2):174–179, 2000.

[12] J.P. Donoghue. Connecting cortex to machines: recent advances in brain interfaces. *Nature Neuroscience*, 5:1085–1088, 2002.

[13] N. Draper and H. Smith. *Applied Regression Analysis (Wiley Series in Probability and Statistics)*. John Wiley & Sons Inc, 2 sub edition, 1998.

[14] B. Efron and R.J. Tibshirani. *An Introduction to the Bootstrap*. Chapman & Hall, New York, 1993.

[15] T. Elbert, B. Rockstroh, W. Lutzenberger, and N. Birbaumer. Biofeedback of slow cortical potentials. *Electroencephalography and Clinical Neurophysiology*, 48(3):293–301, March 1980.

[16] R.A. Fisher. The use of multiple measurements in taxonomic problems. *Annals Eugen.*, 7:179–188, 1936.

[17] T. Flaisch, M. Junghöfer, M.M. Bradley, H.T. Schupp, and P.J. Lang. Rapid picture processing: Affective primes and targets. *Psychophysiology*, 45(1):1–10, 2008.

[18] K. Forster. Visual perception of rapidly presented word sequences of varying complexity. *Attention, Perception, & Psychophysics*, 8(4):215–221, July 1970.

[19] A.D. Gerson, L.C. Parra, and P. Sajda. Cortically coupled computer vision for rapid image search. *IEEE Transactions on Neural and Rehabilitation Systems Engineering*, 14(2):174–179, 2006.

[20] E.B. Goldstein. *Wahrnehmungspsychologie: Der Grundkurs, 7. Aufl.* Spektrum Akademischer Verlag, Heidelberg, 2007.

[21] B. Graimann. *Movement-related patterns in ECoG and EEG: visualization and detection*. PhD thesis, Graz University of Technology, 2002.

[22] K. Grill-Spector, N. Knouf N., and Kanwisher. The fusiform face area subserves face perception, not generic within-category identification. *Nature Neuroscience*, 7:555–562, 2004.

[23] T. Hastie, R. Tibshirani, and J.H. Friedman. *The Elements of Statistical Learning*. Springer, corrected edition, 2003.

[24] K.E. Hild II, S. Mathan, Y. Huang, D. Erdogmus, and M. Pavel. Optimal set of eeg electrodes for rapid serial visual presentation. *Conf Proc IEEE Eng Med Biol Soc*, 1:4335–8, 2010.

[25] H. Intraub. Presentation rate and the representation of briefly glimpsed pictures in memory. *Journal of Experimental Psychology: Human Learning and Memory*, 6:604–610, 1980.

[26] H. Intraub. Rapid conceptual identification of sequentially presented pictures. *Journal of Experimental Psychology: Human Perception and Performance*, 7:604–610, 1981.

[27] M. Junghöfer, M.M. Bradley, T.R. Elbert, and P.J. Lang. Fleeting images: A new look at early emotion discrimination. *Psychophysiology*, 38(02):175–178, 2001.

[28] E.R. Kandel, J.H. Schwartz, and T.M. Jessell. *Principles of Neural Science*. McGraw-Hill Medical, 4th edition, 2000.

[29] R. Kohavi. A study of cross-validation and bootstrap for accuracy estimation and model selection. In *Proceedings of the Fourteenth International Joint Conference on Artificial Intelligence*, volume 2, pages 1137–1143, 1995.

[30] D.J. Krusienski, E.W. Sellers, F Cabestaing, S. Bayoudh, D.J. McFarland, T.M. Vaughan, and J.R. Wolpaw. A comparison of classification techniques for the p300 speller. *Journal of Neural Engineering*, 3(4):299, 2006.

[31] J.R. Landis and G.G. Koch. The Measurement of Observer Agreement for Categorical Data. *Biometrics*, 33(1):159–174, March 1977.

[32] P.J. Lang, M.M. Bradley, and B.N. Cuthbert. *International affective picture system (IAPS : Affective ratings of pictures and instruction manual. Technical Report A-8.* University of Florida, Gainesville,FL., 2008.

[33] D.T. Larose. *Data Mining Methods and Models*. Wiley-IEEE Press, January 2006.

[34] M. Middendorf, G. McMillan, G. Calhoun, and K.S. Jones, 2000.

[35] J.d.R. Millán, R. Rupp, G.R. Müller-Putz, R. Murray-Smith, C. Giugliemma, M. Tangermann, C. Vidaurre, F. Cincotti, A. Kubler, R. Leeb, C. Neuper, K.R. Mueller, and D Mattia. Combining brain-computer interfaces and assistive technologies: State-of-the-art and challenges. *Frontiers in Neuroscience*, 4(00161), 2010.

[36] G.R. Müller-Putz, R. Scherer, C. Brauneis, and G. Pfurtscheller. Steady-state visual evoked potential (SSVEP)-based communication: impact of harmonic frequency components. *Journal of Neural Engineering*, 2(4):123, 2005.

[37] G.R. Müller-Putz, R. Scherer, C. Brunner, R. Leeb, and G. Pfurtscheller. Better than random? A closer look on BCI results. *International Journal of Bioelectromagnetism*, 10:52–55, 2008.

[38] G.R. Müller-Putz, R. Scherer, C. Neuper, and G. Pfurtscheller. Steady-state somatosensory evoked potentials: suitable brain signals for brain-computer interfaces? *IEEE Transactions on Neural Systems and Rehabilitation Engineering*, 14:30–37, 2006.

[39] E. Niedermeyer and F.H.L. Silva. *Electroencephalography: basic principles, clinical applications, and related fields*. Doody's all reviewed collection. Lippincott Williams & Wilkins, 2005.

[40] J.K. Olofsson, S. Nordin, H. Sequeira, and J. Polich. Affective picture processing: an integrative review of ERP findings. *Biol Psychol*, 77(3):247–65, 2008.

[41] G. Pfurtscheller and F. H. Lopes da Silva. Event-related EEG/MEG synchronization and desynchronization: basic principles. *Clinical Neurophysiology*, 110:1842–1857, 1999.

[42] G. Pfurtscheller, G.R. Müller-Putz, A. Schlögl, B. Graimann, R. Scherer, R. Leeb, C. Brunner, C. Keinrath, F. Lee, G. Townsend, C. Vidaurre, and C. Neuper. 15 years of BCI research at Graz University of Technology: current projects. *IEEE Transactions on Neural Systems and Rehabilitation Engineering*, 14(2):205–210, 2006.

[43] E. Pohlmeyer, D. Jangraw, J. Wang, S.F. Chang, and P. Sajda. Combining computer and human vision into a bci: Can the whole be greater than the sum of its parts? In *The 32nd Annual International Conference of the IEEE Engineering in Medicine and Biology Society (EMBC)*, Buenos Aires, Argentina, August 2010.

[44] M.C. Potter and E.I. Levy. Recognition memory for a rapid sequence of pictures. *Journal of Experimental Psychology*, 81(1):10–15, 1969.

[45] J.E. Raymond, K.L. Shapiro, and K.M. Arnell. Temporary suppression of visual processing in an RSVP task: an attentional blink? *Journal of experimental psychology. Human perception and performance*, 18(3):849–860, August 1992.

[46] C. Scheier and D. Held. *Wie Werbung wirkt: Erkenntnisse des Neuromarketing*. Haufe Sachbuch Wirtschaft. Haufe, 2006.

[47] A. Schlögl and C. Brunner. BioSig: a free and open source software library for BCI research. *IEEE Computer Magazine*, 41:44–50, 2008.

[48] A. Schlögl, C. Brunner, R. Scherer, and A. Glatz. BioSig: an open-source software library for BCI research. In G. Dornhege, J. del R. Millán, T. Hinterberger, D. J. McFarland, and K.-R. Müller, editors, *Toward brain-computer interfacing*, chapter 20, pages 347–358. MIT Press, 2007.

[49] A. Schlögl. Gdf - a general dataformat for biosignals. *CoRR*, abs/cs/0608052, 2006.

[50] A. Schlögl, C. Keinrath, D. Zimmermann, R. Scherer, R. Leeb, and G. Pfurtscheller. A fully automated correction method of EOG artifacts in EEG recordings. *Clinical Neurophysiology*, 118(1):98–104, January 2007.

[51] E. W. Sellers and E. Donchin. A P300-based brain-computer interface: initial tests by ALS patients. *Clin Neurophysiol*, 117(3):538–548, Mar 2006.

[52] K.L. Shapiro, J.E. Raymond, and K.M. Arnell. Attention to visual pattern information produces the attentional blink in rapid serial visual presentation. *Journal of experimental psychology. Human perception and performance*, 20(2):357–371, April 1994.

[53] D.L. Sheinberg and N.K. Logothetis. The role of temporal cortical areas in perceptual organization. *Proc Natl Acad Sci U S A*, 94(7):3408–3413, 1997.

[54] S. Thorpe, D. Fize, and C. Marlot. Speed of processing in the human visual system. *Nature*, 381:520 – 522, 1996.

[55] J.J. Vidal. Toward direct brain-computer communication. *Annual review of biophysics and bioengineering*, 2(1):157–180, 1973.

[56] J.J. Vidal. Real-time detection of brain events in EEG. *Proceedings of the IEEE*, 65(5):633–641, 1977.

[57] J.R. Wolpaw, N. Birbaumer, D.J. McFarland, G. Pfurtscheller, and T.M. Vaughan. Brain-computer interfaces for communication and control. *Clinical Neurophysiology*, 113:767–791, 2002.

[58] G. Zaltman. *How customers think*. Harvard Business School Press, Boston, Mass., 2003.

[59] T.O. Zander and C. Kothe. Towards passive brain-computer interfaces: applying brain-computer interface technology to human-machine systems in general. *Journal of Neural Engineering*, 8(2):025005, 2011.

[60] M. Ziegler and M. Bühner. *Statistik für Psychologen und Sozialwissenschaftler*. Pearson Studium. Pearson, 2009.

A. Remaining figures

Preliminary study

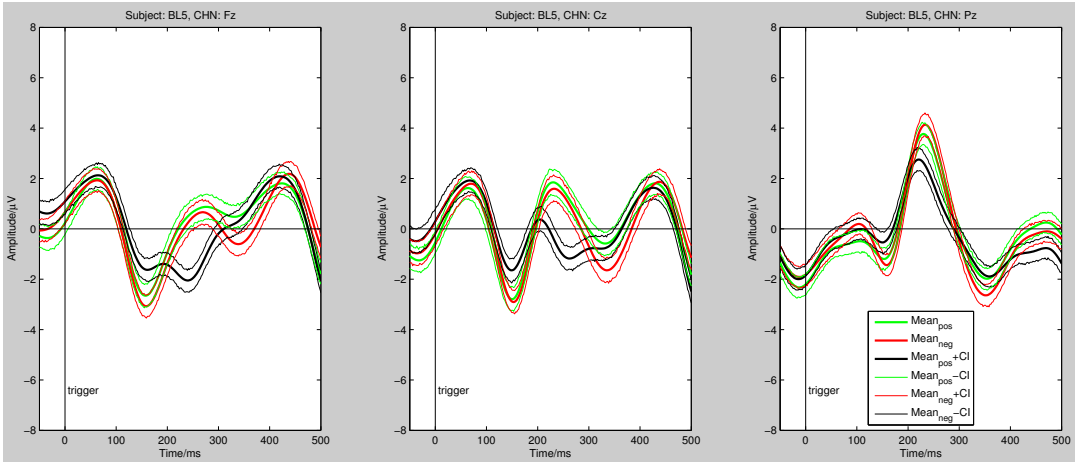

Figure 33: Subject BL5: Mean waveforms and 95% confidence intervals elicited from positive, neutral and negative images in the prestudy. Black waveform: Response to neutral image; Green waveform: Response to positive image; Red Waveform: Response to negative image. All waveforms are the mean values over the number of trials ± the 95% confidence interval.

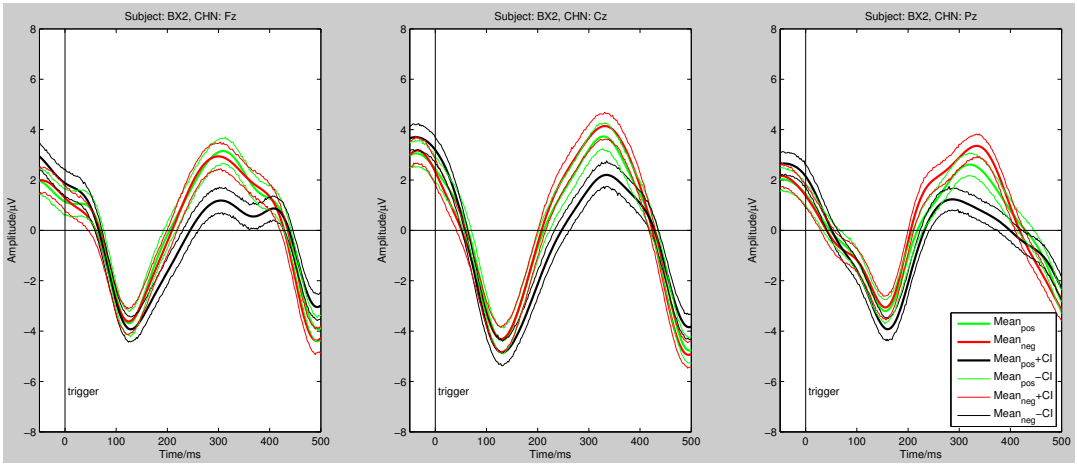

Figure 34: Subject BX2: Mean waveforms and 95% confidence intervals elicited from positive, neutral and negative images in the prestudy. Black waveform: Response to neutral image; Green waveform: Response to positive image; Red Waveform: Response to negative image. All waveforms are the mean values over the number of trials ± the 95% confidence interval.

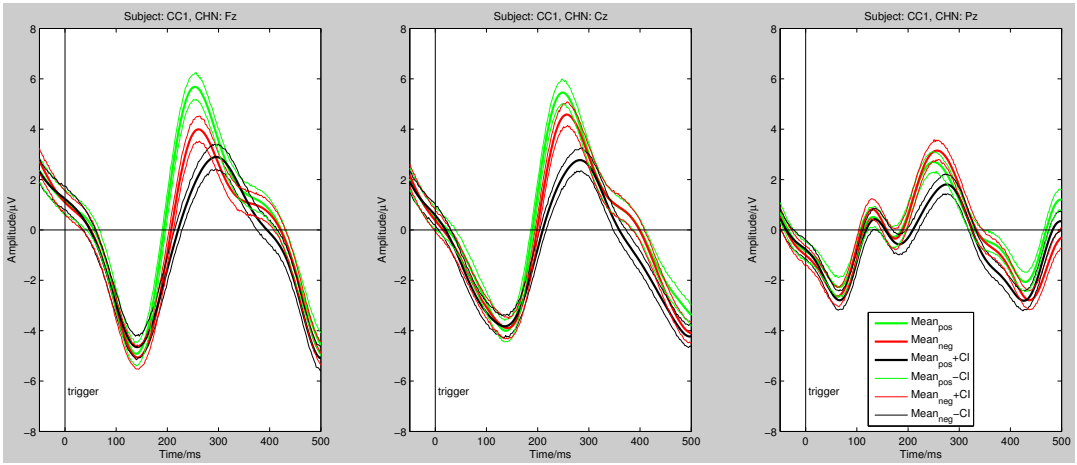

Figure 35: Subject CC1: Mean waveforms and 95% confidence intervals elicited from positive, neutral and negative images in the prestudy. Black waveform: Response to neutral image; Green waveform: Response to positive image; Red Waveform: Response to negative image. All waveforms are the mean values over the number of trials ± the 95% confidence interval.

Mainstudy, P300-Paradigm

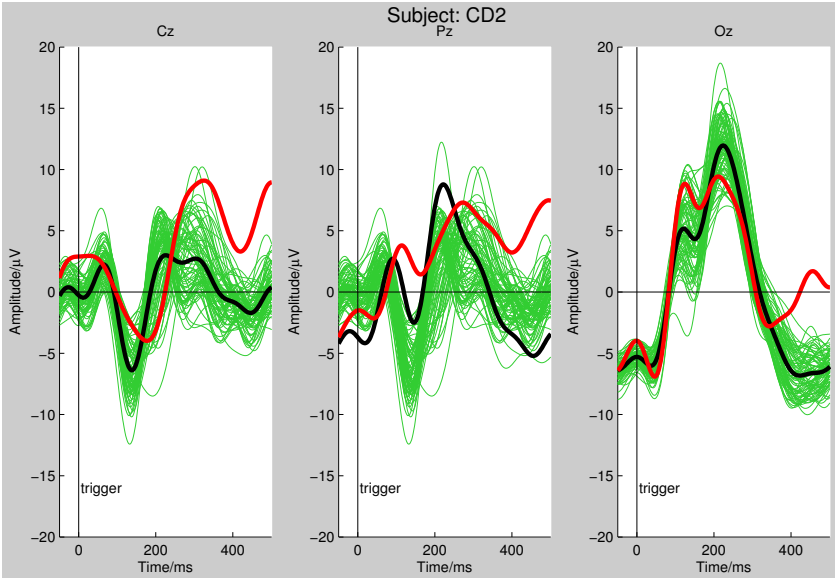

Figure 36: Subject CD2: Mean waveforms of the oddball paradigm. black curve: Grand Average; red curve: target condition; green curves: Remaining conditions. All conditions are mean waveforms over the number of trials per condition. The image is presented at $t = 0\,\text{ms}$ (trigger).

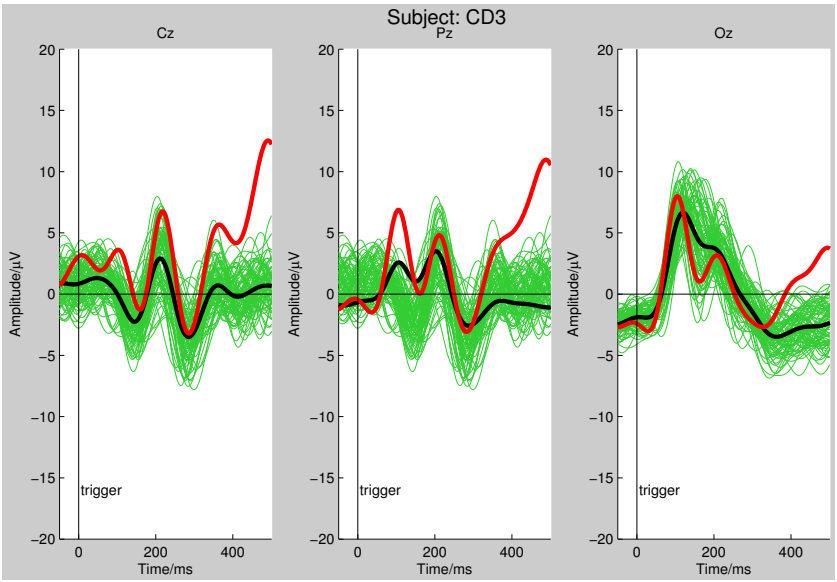

Figure 37: Subject CD3: Mean waveforms of the oddball paradigm. black curve: Grand Average; red curve: target condition; green curves: Remaining conditions. All conditions are mean waveforms over the number of trials per condition. The image is presented at $t = 0\,\text{ms}$ (trigger).

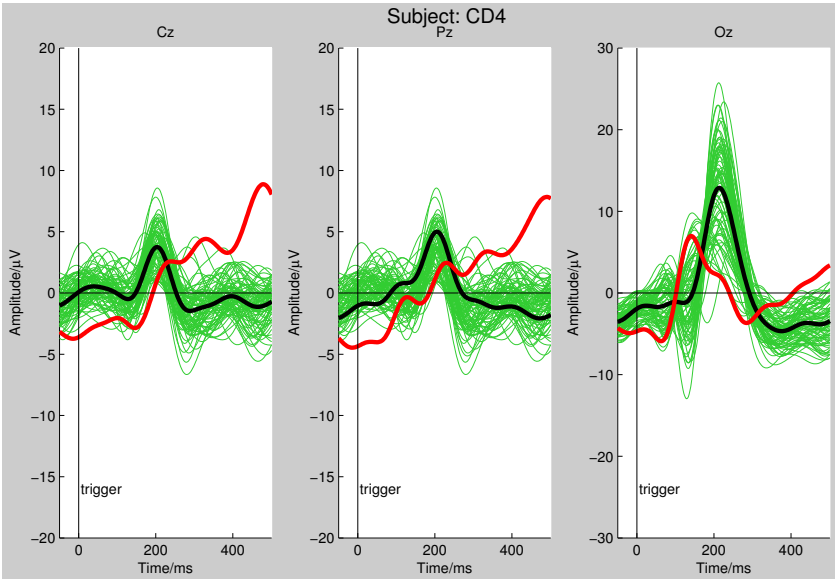

Figure 38: Subject CD4: Mean waveforms of the oddball paradigm. black curve: Grand Average; red curve: target condition; green curves: Remaining conditions. All conditions are mean waveforms over the number of trials per condition. The image is presented at $t = 0\,\text{ms}$ (trigger).

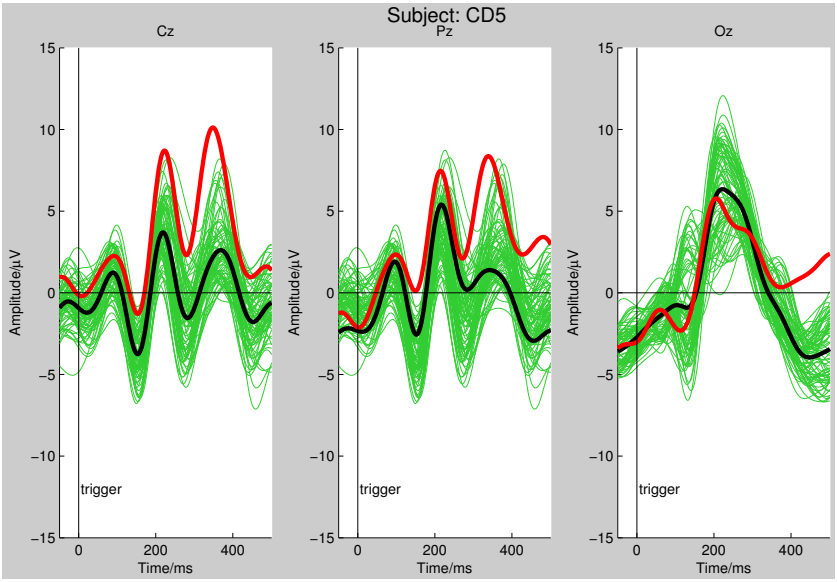

Figure 39: Subject CD5: Mean waveforms of the oddball paradigm. black curve: Grand Average; red curve: target condition; green curves: Remaining conditions. All conditions are mean waveforms over the number of trials per condition. The image is presented at $t = 0\,\text{ms}$ (trigger).

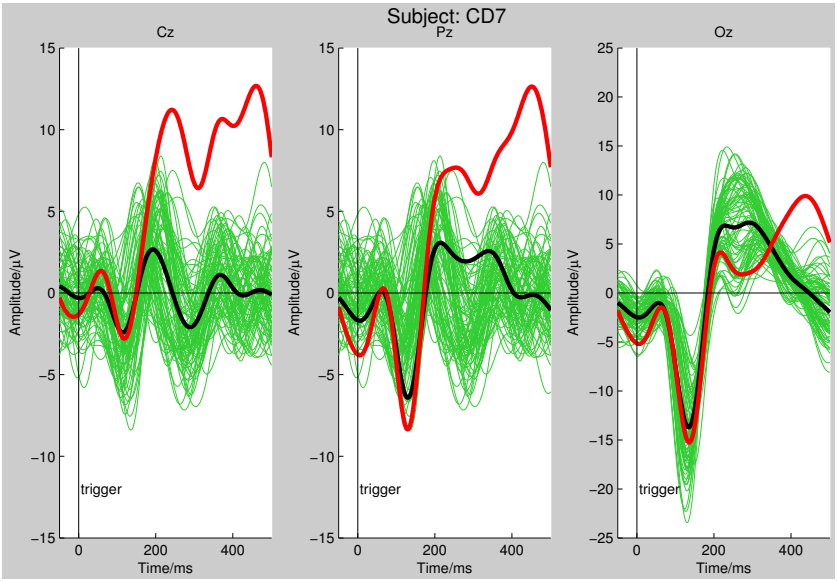

Figure 40: Subject CD7: Mean waveforms of the oddball paradigm. black curve: Grand Average; red curve: target condition; green curves: Remaining conditions. All conditions are mean waveforms over the number of trials per condition. The image is presented at $t = 0\,\text{ms}$ (trigger).

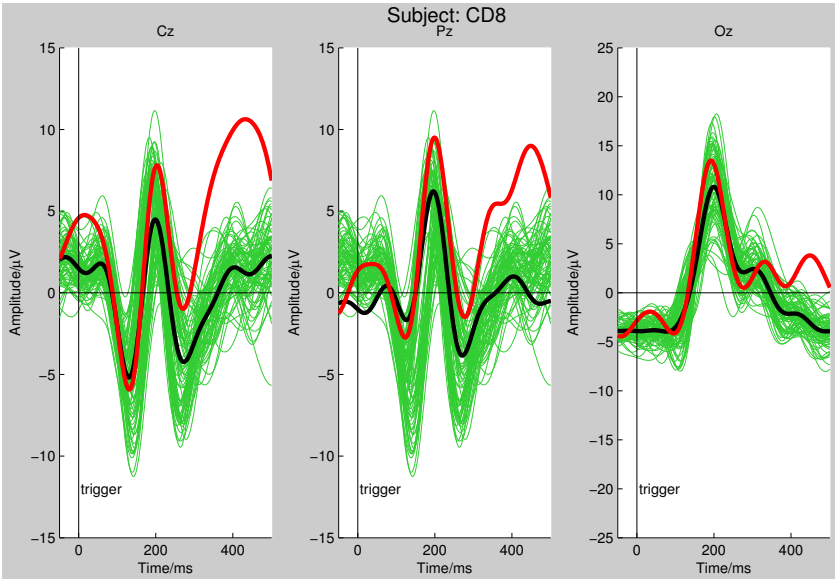

Figure 41: Subject CD8: Mean waveforms of the oddball paradigm. black curve: Grand Average; red curve: target condition; green curves: Remaining conditions. All conditions are mean waveforms over the number of trials per condition. The image is presented at $t = 0\,\text{ms}$ (trigger).

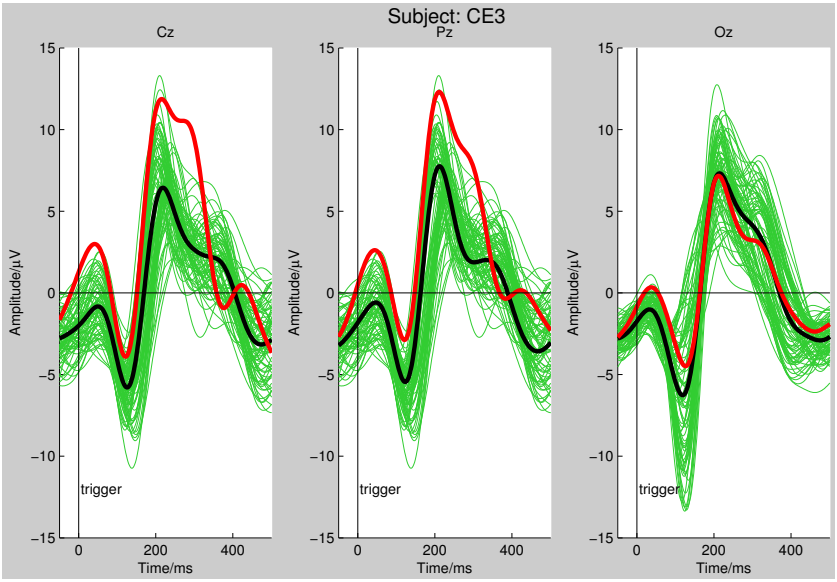

Figure 42: Subject CE3: Mean waveforms of the oddball paradigm. black curve: Grand Average; red curve: target condition; green curves: Remaining conditions. All conditions are mean waveforms over the number of trials per condition. The image is presented at $t = 0\,\text{ms}$ (trigger).

Main study; Actual paradigm

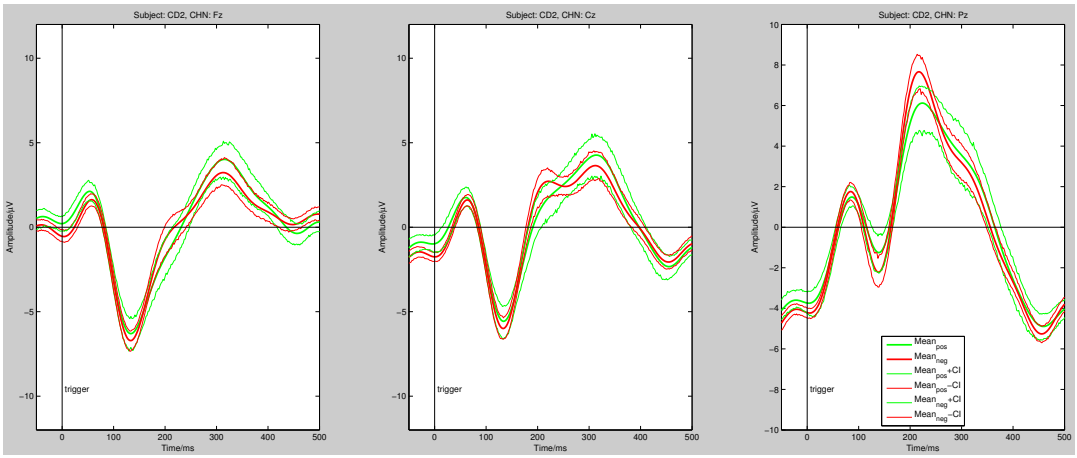

Figure 43: Subject CD2: Mean waveforms and 95% confidence intervals of the actual paradigm. Red curve: positive/attractive conditions; green curve: negative/unattractive condition. All conditions are mean waveforms ± confidence interval over the number of trials per condition. The image is presented at $t = 0\,\text{ms}$ (trigger).

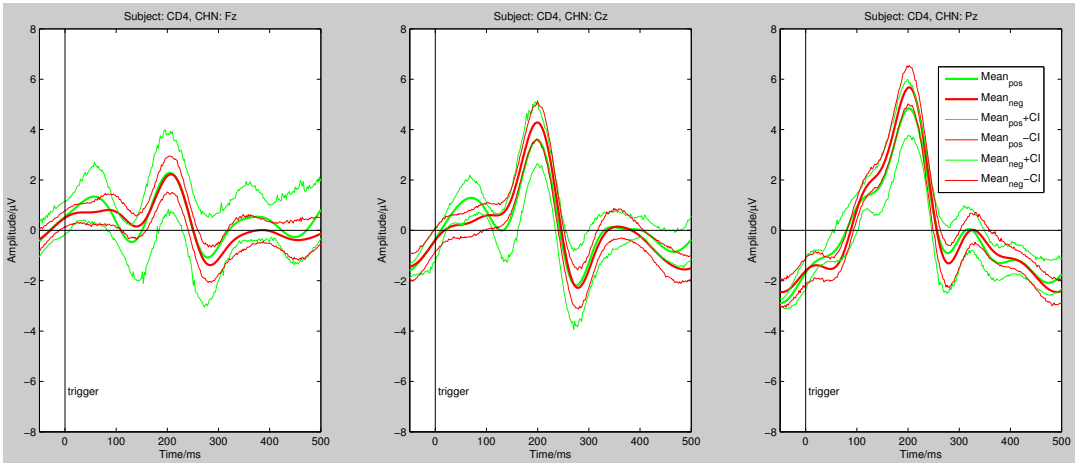

Figure 44: Subject CD4: Mean waveforms and 95% confidence intervals of the actual paradigm. Red curve: positive/attractive conditions; green curve: negative/unattractive condition. All conditions are mean waveforms ± confidence interval over the number of trials per condition. The image is presented at $t = 0\,\text{ms}$ (trigger).

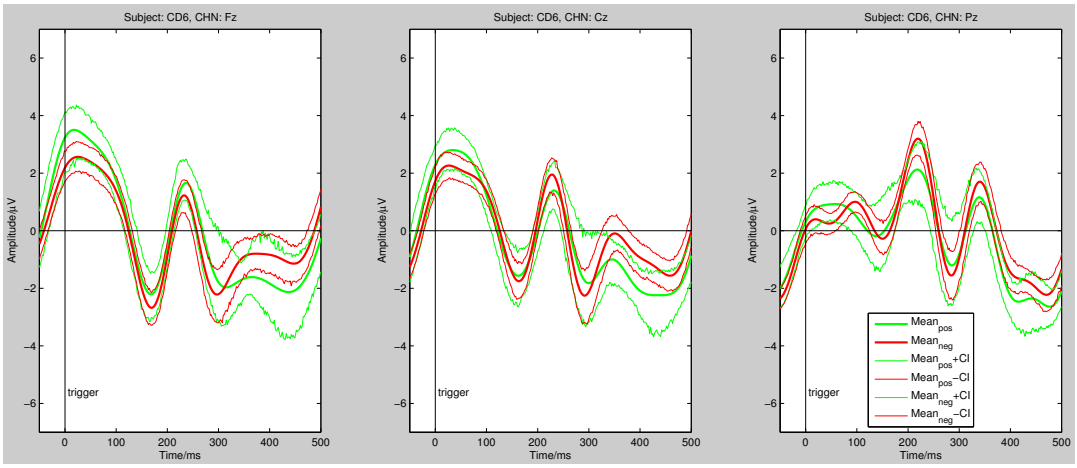

Figure 45: Subject CD6: Mean waveforms and 95% confidence intervals of the actual paradigm. Red curve: positive/attractive conditions; green curve: negative/unattractive condition. All conditions are mean waveforms ± confidence interval over the number of trials per condition. The image is presented at $t = 0\,\text{ms}$ (trigger).

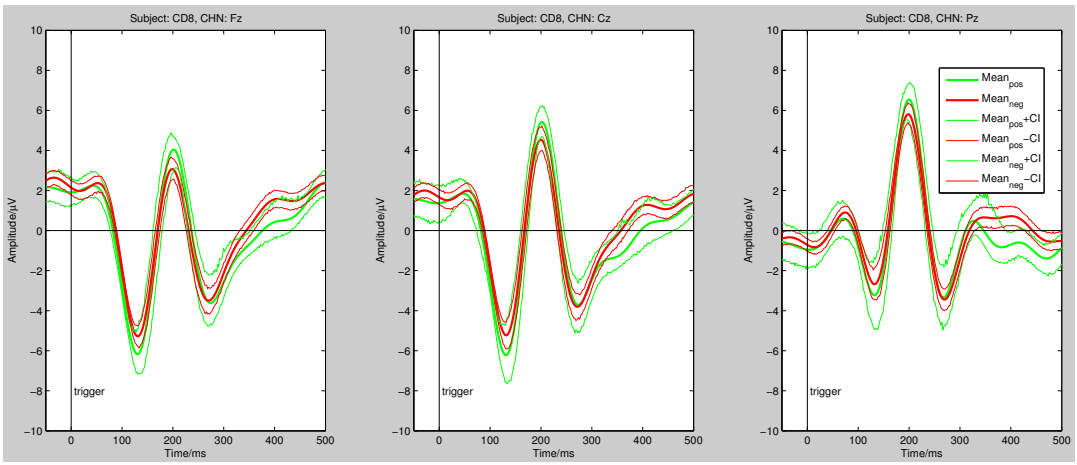

Figure 46: Subject CD8: Mean waveforms and 95% confidence intervals of the actual paradigm. Red curve: positive/attractive conditions; green curve: negative/unattractive condition. All conditions are mean waveforms ± confidence interval over the number of trials per condition. The image is presented at $t = 0\,\text{ms}$ (trigger).

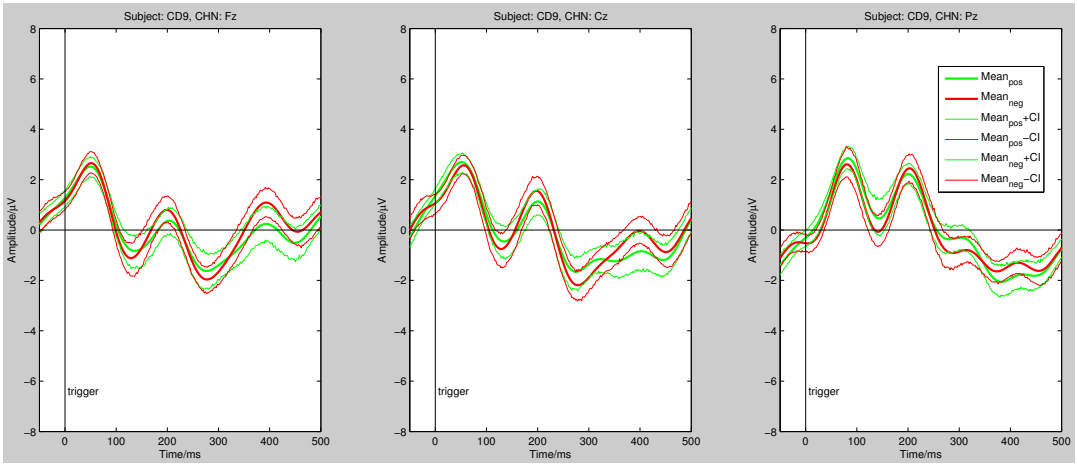

Figure 47: Subject CD9: Mean waveforms and 95% confidence intervals of the actual paradigm. Red curve: positive/attractive conditions; green curve: negative/unattractive condition. All conditions are mean waveforms ± confidence interval over the number of trials per condition. The image is presented at $t = 0\,\text{ms}$ (trigger).

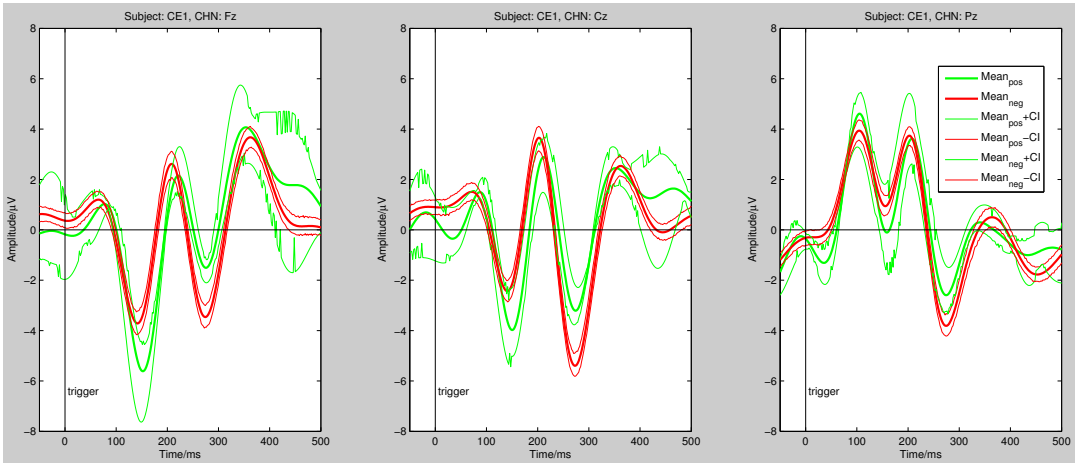

Figure 48: Subject CE1: Mean waveforms and 95% confidence intervals of the actual paradigm. Red curve: positive/attractive conditions; green curve: negative/unattractive condition. All conditions are mean waveforms ± confidence interval over the number of trials per condition. The image is presented at $t = 0\,\text{ms}$ (trigger).

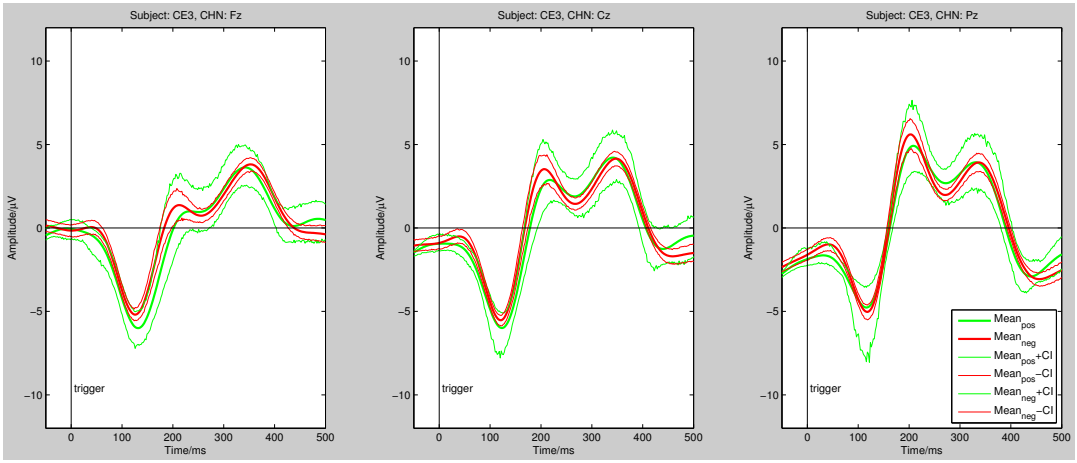

Figure 49: Subject CE3: Mean waveforms and 95% confidence intervals of the actual paradigm. Red curve: positive/attractive conditions; green curve: negative/unattractive condition. All conditions are mean waveforms ± confidence interval over the number of trials per condition. The image is presented at $t = 0\,\text{ms}$ (trigger).

Topography

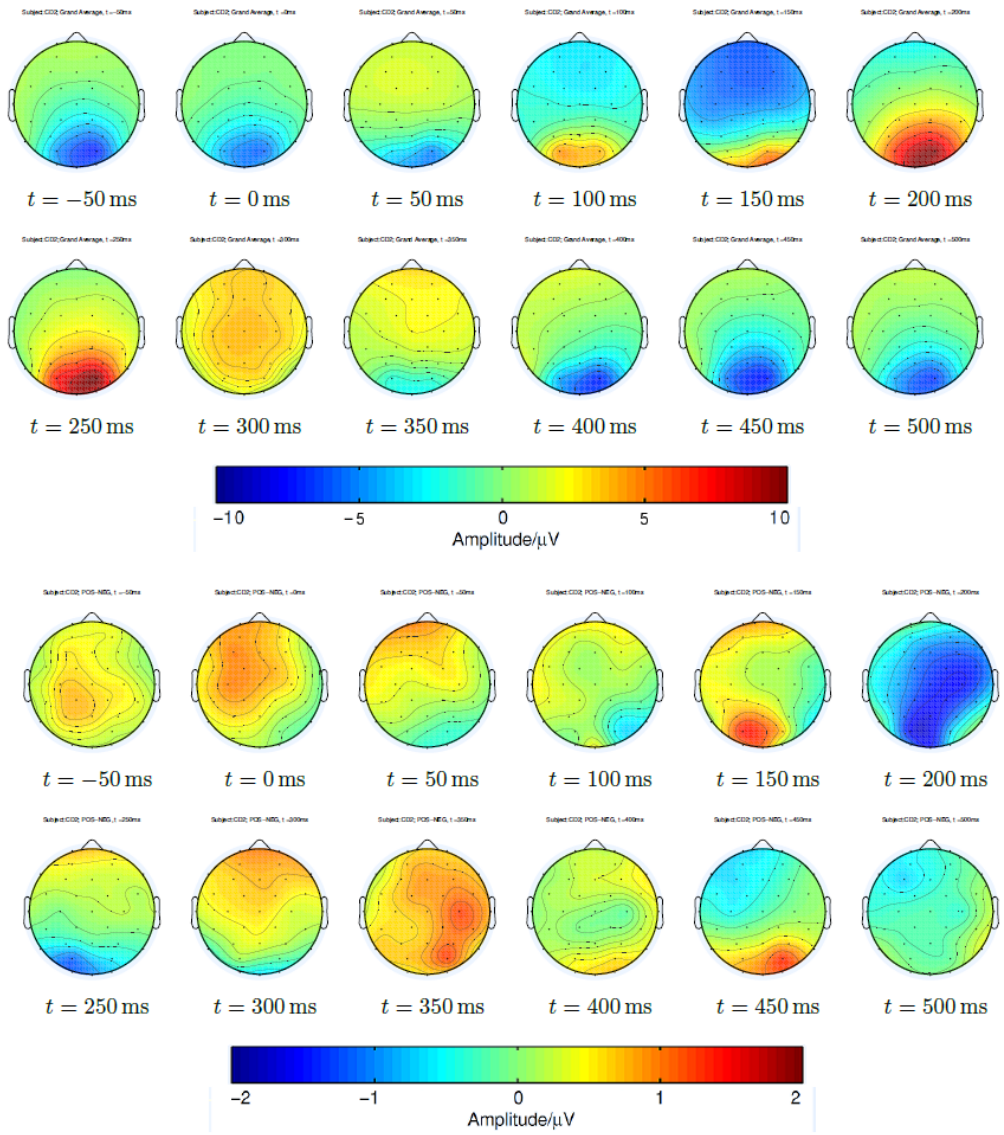

Figure 50: Subject CD2: Topographic plot of the Grand Average over the scalp (top) and the difference between attractive and unattractive images as a distribution over the scalp (bottom) for the time interval between $t_1 = 50\,\text{ms}$ and $t_2 = 500\,\text{ms}$ in $50\,\text{ms}$ steps.

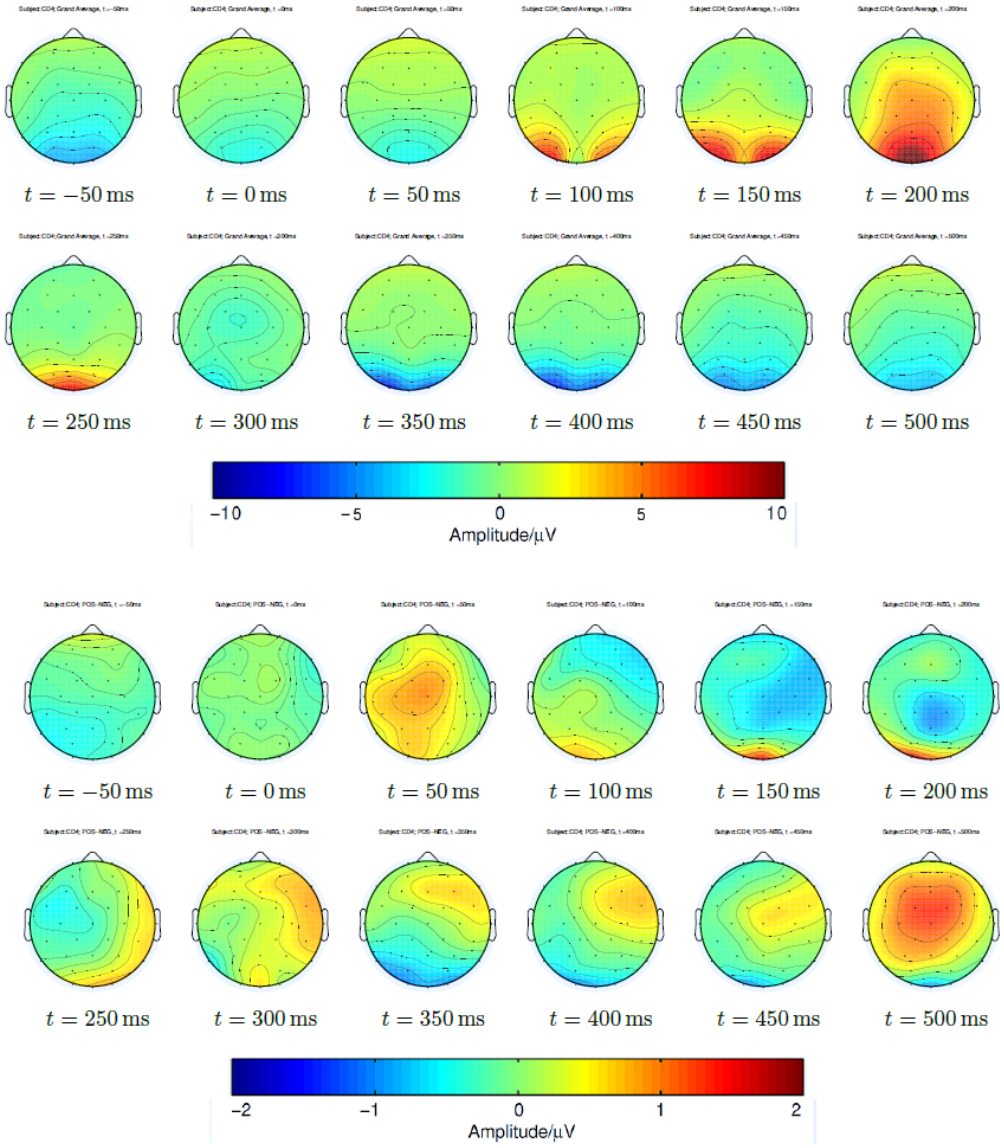

Figure 51: Subject CD4: Topographic plot of the Grand Average over the scalp (top) and the difference between attractive and unattractive images as a distribution over the scalp (bottom) for the time interval between $t_1 = 50\,\text{ms}$ and $t_2 = 500\,\text{ms}$ in 50 ms steps.

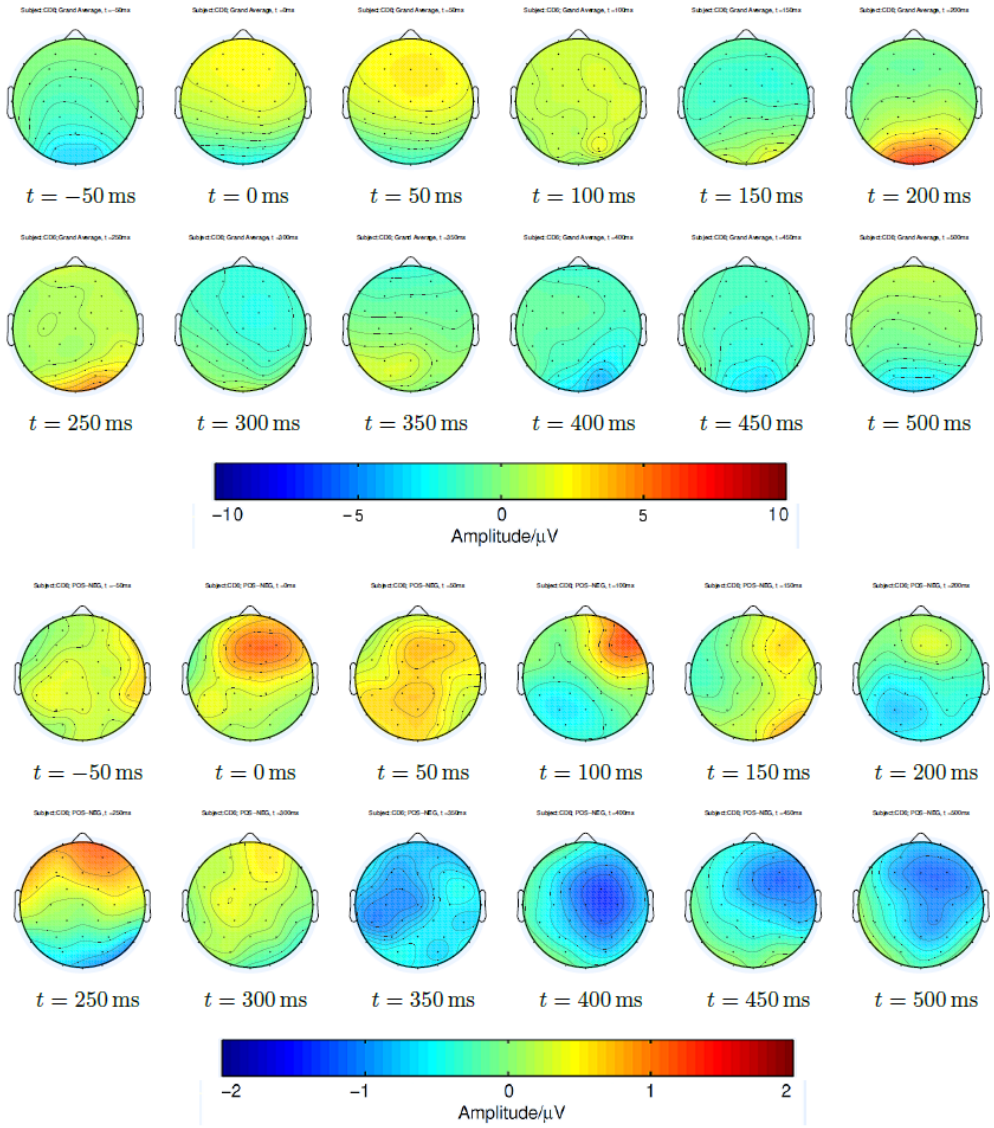

Figure 52: Subject CD6: Topographic plot of the Grand Average over the scalp (top) and the difference between attractive and unattractive images as a distribution over the scalp (bottom) for the time interval between $t_1 = 50\,\text{ms}$ and $t_2 = 500\,\text{ms}$ in $50\,\text{ms}$ steps.

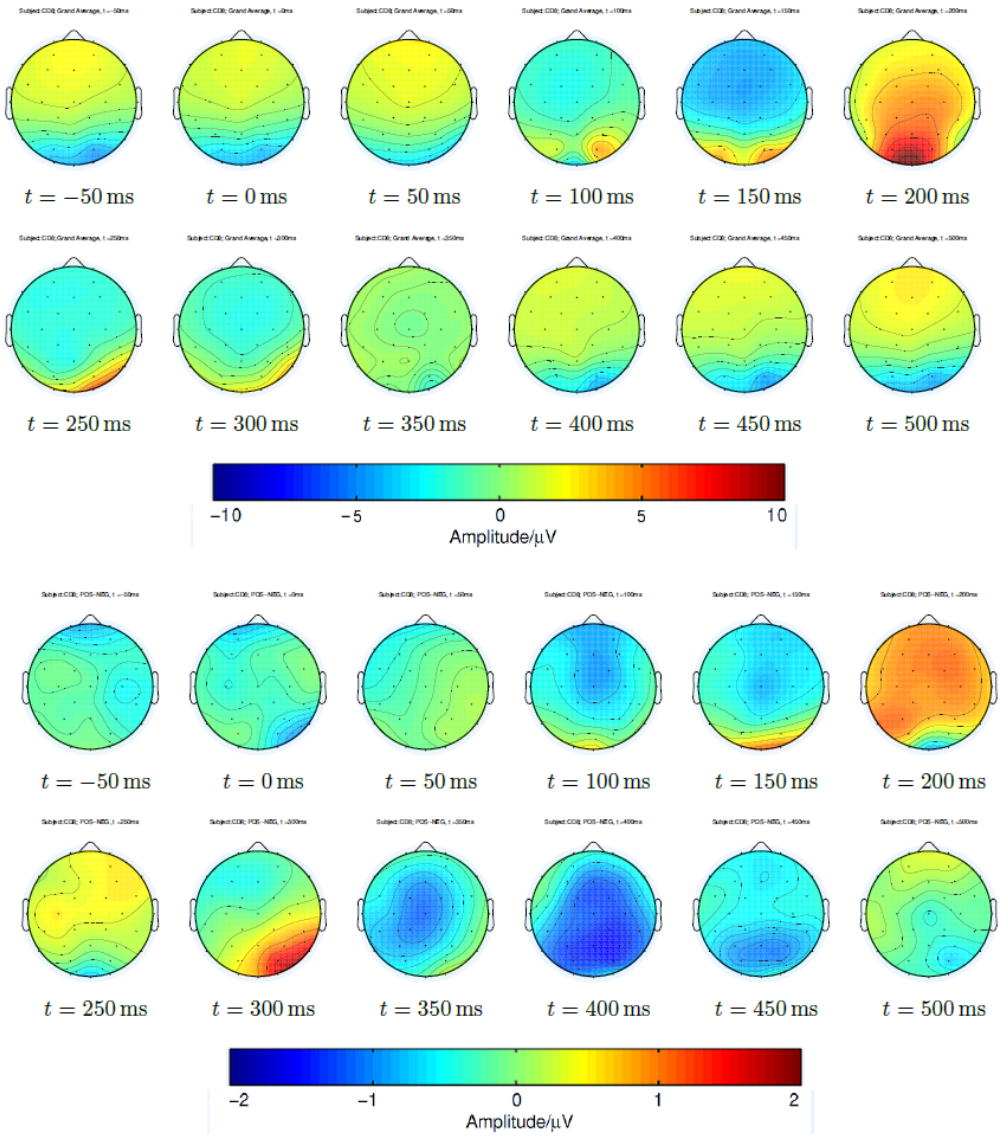

Figure 53: Subject CD8: Topographic plot of the Grand Average over the scalp (top) and the difference between attractive and unattractive images as a distribution over the scalp (bottom) for the time interval between $t_1 = 50\,\text{ms}$ and $t_2 = 500\,\text{ms}$ in 50 ms steps.

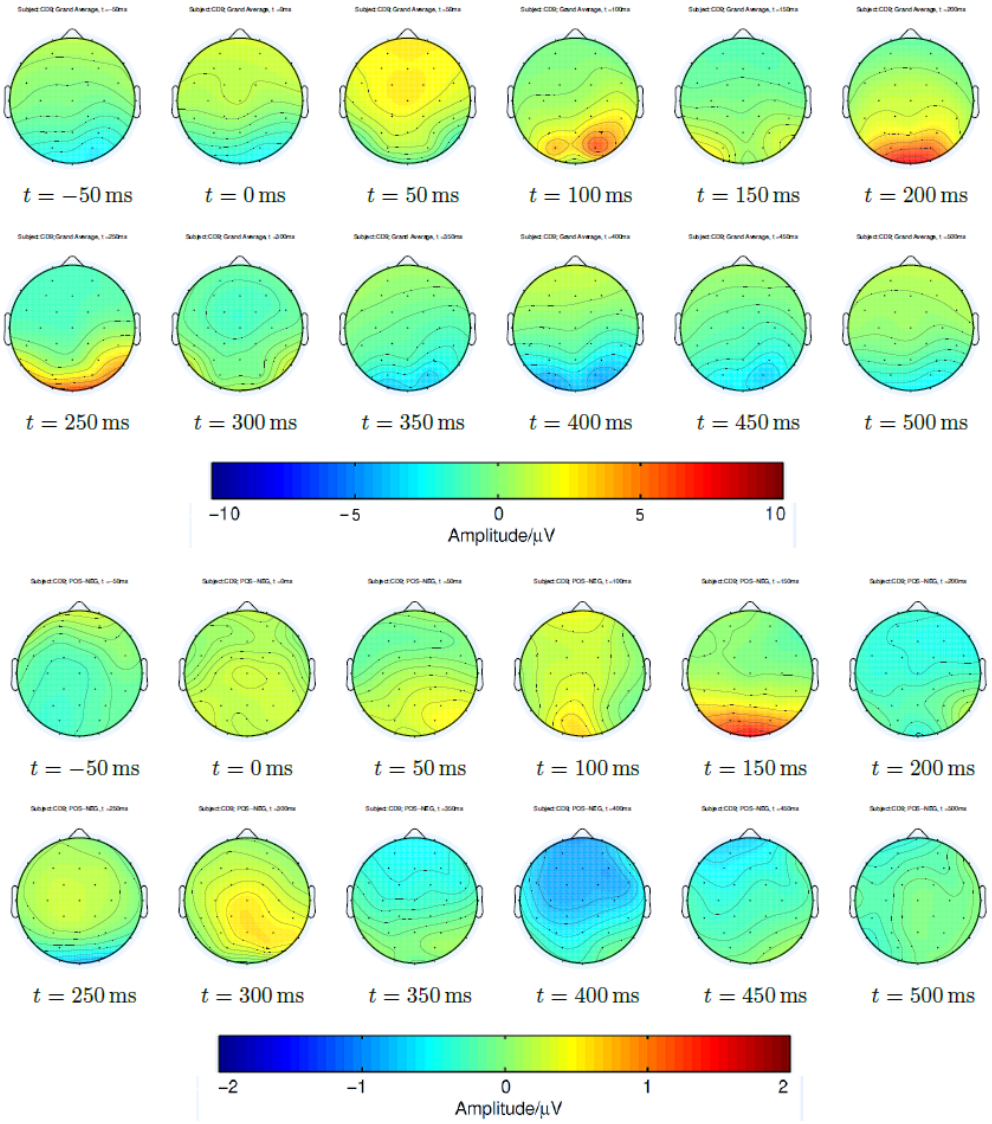

Figure 54: Subject CD9: Topographic plot of the Grand Average over the scalp (top) and the difference between attractive and unattractive images as a distribution over the scalp (bottom) for the time interval between $t_1 = 50\,\text{ms}$ and $t_2 = 500\,\text{ms}$ in 50 ms steps.

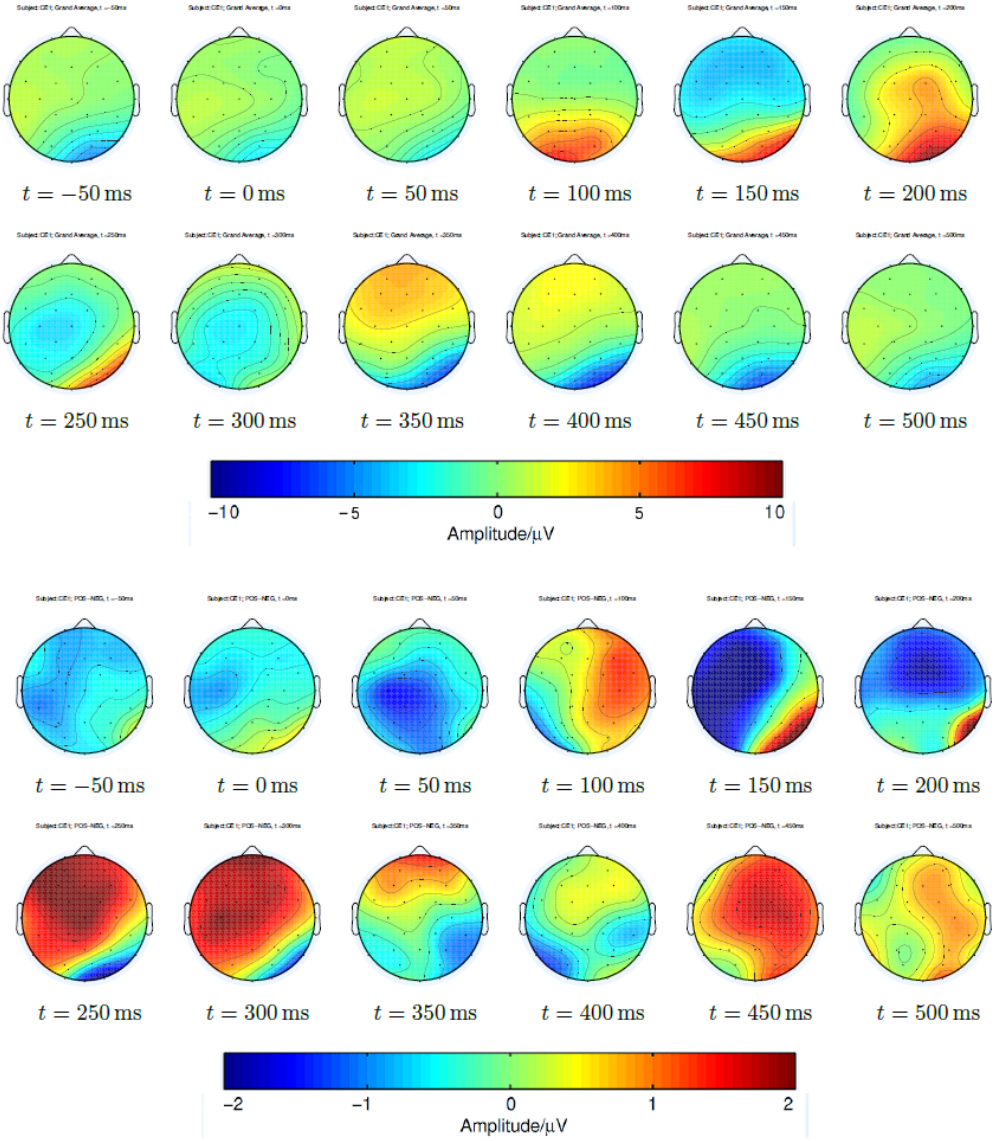

Figure 55: Subject CE1: Topographic plot of the Grand Average over the scalp (top) and the difference between attractive and unattractive images as a distribution over the scalp (bottom) for the time interval between $t_1 = 50\,\text{ms}$ and $t_2 = 500\,\text{ms}$ in 50 ms steps.

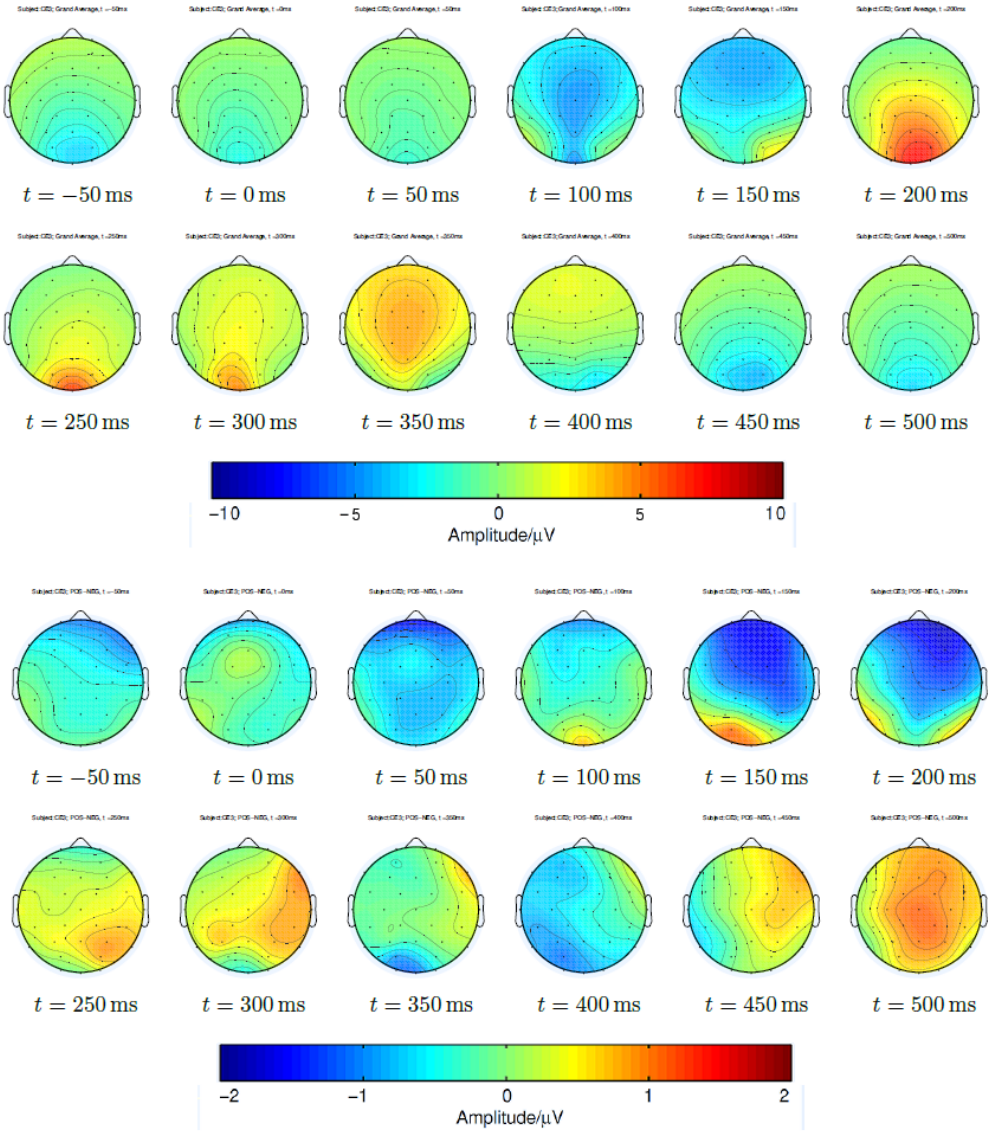

Figure 56: Subject CE3: Topographic plot of the Grand Average over the scalp (top) and the difference between attractive and unattractive images as a distribution over the scalp (bottom) for the time interval between $t_1 = 50\,\text{ms}$ and $t_2 = 500\,\text{ms}$ in $50\,\text{ms}$ steps.

B. Remaining tables

Table 7: Main study: Classification accuracies (Oddball-Paradigm, One-vs-rest classification)

Pic	CD2	CD3	CD5	CD6	CD4	CD7	CD8	CD9	CE1	CE3
1	79.94	57.06	60.76	79.64	59.61	65.69	67.40	86.18	65.60	63.25
2	72.59	51.64	61.67	65.58	57.95	60.35	65.01	75.75	60.18	60.35
3	73.89	62.18	63.41	82.93	59.34	69.07	55.65	91.25	64.56	51.83
4	71.61	65.29	62.38	65.57	70.38	63.84	66.31	73.78	76.78	55.36
5	82.75	71.64	80.05	66.18	73.33	70.60	78.08	88.67	81.67	68.39
6	71.49	49.44	68.52	76.65	51.62	57.10	74.12	80.43	69.40	57.94
7	77.52	72.43	82.48	76.69	59.68	54.44	68.80	85.76	67.47	58.88
8	85.11	68.29	66.50	83.00	62.39	60.37	79.21	86.58	76.01	60.85
9	78.48	61.08	59.72	75.51	54.68	59.33	58.78	69.66	70.86	62.32
10	60.44	63.97	48.81	67.51	73.99	47.81	49.04	46.89	70.21	61.36
11	62.65	56.77	64.45	77.42	65.27	46.72	55.87	61.15	76.43	54.23
12	61.52	63.62	59.50	71.62	69.74	58.69	58.69	69.40	61.35	62.70
13	87.58	62.35	68.46	65.82	64.54	52.48	46.65	85.12	81.75	56.67
14	66.39	54.82	70.50	71.42	68.05	60.52	65.23	55.95	74.92	60.45
15	79.64	66.07	61.78	81.64	59.51	60.97	56.05	78.11	73.83	57.66
16	63.57	61.89	64.59	68.16	82.62	56.51	60.35	63.14	91.66	61.66
17	63.16	64.21	52.45	74.54	58.41	51.65	56.66	65.83	56.26	52.82
18	71.14	59.92	69.47	72.50	63.85	89.31	70.24	72.33	65.19	55.62
19	75.42	64.66	72.89	73.27	64.08	71.43	50.73	80.41	58.84	57.09
20	74.08	60.87	70.78	68.87	64.52	56.40	72.16	76.59	64.65	60.09
21	61.90	60.43	72.92	63.39	75.74	72.25	60.66	77.76	81.33	53.06
22	80.32	52.76	65.51	73.56	53.39	71.12	63.66	72.02	58.68	53.39
23	82.51	62.65	72.11	79.29	61.97	75.86	79.72	82.22	68.22	62.33
24	65.85	55.33	57.36	76.78	60.60	77.52	66.12	63.05	61.27	51.96
25	65.74	63.82	58.71	75.63	61.82	66.81	64.57	73.71	65.15	52.68
26	75.68	59.20	60.26	65.42	72.26	53.65	48.83	74.64	63.79	63.85
27	67.20	62.65	62.93	90.04	70.81	65.43	56.88	68.77	64.79	58.11
28	73.98	75.65	68.77	77.43	75.52	70.95	50.68	70.60	68.04	61.26
29	67.40	49.83	67.44	75.84	58.16	54.60	71.57	68.42	69.96	51.97
30	90.62	65.25	65.27	84.60	66.05	62.67	78.21	98.55	71.46	56.28
31	70.08	59.23	67.91	74.23	54.39	46.97	55.76	82.87	65.38	56.04
32	72.00	67.50	59.82	80.79	57.79	60.26	53.53	74.00	66.98	62.42
33	79.80	72.93	58.71	69.15	52.20	50.24	69.67	87.97	69.65	60.62
34	67.32	49.05	66.94	67.18	58.60	47.59	62.46	78.67	66.33	53.40
35	80.42	57.91	73.85	70.06	64.47	67.40	64.01	83.08	59.03	55.52

Continued on next page

Table 7 – continued from previous page										
Pic	**CD2**	**CD3**	**CD5**	**CD6**	**CD4**	**CD7**	**CD8**	**CD9**	**CE1**	**CE3**
36	82.18	62.87	58.69	73.12	65.07	50.54	67.15	79.21	71.59	62.90
37	71.80	52.36	62.27	66.26	51.02	50.27	70.51	74.86	59.89	57.37
38	80.32	57.12	60.06	71.63	58.13	70.67	61.70	72.10	68.77	56.22
39	80.21	77.36	74.57	71.06	63.80	48.70	70.30	92.12	76.36	59.39
40	76.41	70.03	74.29	61.88	60.67	68.19	67.04	90.55	66.54	58.58
41	79.84	69.84	55.16	62.27	60.63	56.55	83.96	66.89	71.96	91.60
42	68.71	46.16	56.78	66.99	52.77	64.31	62.24	64.82	66.77	51.76
43	81.75	69.64	58.87	70.25	63.06	71.58	49.63	70.67	57.11	59.42
44	69.55	57.35	59.67	72.27	62.78	49.37	60.01	60.81	63.53	52.63
45	69.32	65.94	68.40	69.24	55.67	57.16	55.82	67.23	68.28	64.32
46	61.76	62.36	65.04	65.36	57.30	61.17	58.55	65.29	76.99	57.73
47	68.65	57.79	59.46	62.45	59.28	56.07	60.73	76.04	56.53	61.56
48	64.66	62.77	49.92	62.28	55.77	56.07	72.23	65.94	71.43	64.41
49	68.64	82.93	65.92	61.83	52.09	53.31	64.34	73.16	83.05	66.31
50	57.35	73.24	66.95	72.05	57.04	65.20	50.71	77.87	67.80	50.94
51	61.08	60.20	59.95	65.30	58.56	60.68	71.51	65.74	63.20	63.33
52	62.89	68.68	67.92	64.48	62.85	62.62	65.45	84.83	65.62	67.75
53	79.25	62.25	74.08	74.21	60.46	68.14	49.66	80.53	76.35	54.19
54	64.85	56.40	68.04	67.95	58.95	58.29	54.84	60.34	52.83	53.23
55	69.80	67.68	66.61	66.65	61.32	60.35	68.97	73.30	69.18	59.04
56	67.14	51.02	61.12	60.80	49.72	55.61	59.04	77.68	75.50	52.24
57	67.83	50.09	53.76	64.21	68.36	53.82	73.85	49.51	63.19	57.02
58	61.64	60.30	63.21	64.91	62.30	53.55	49.74	61.05	62.09	61.11
59	70.45	69.61	55.97	71.12	61.86	57.73	54.46	75.77	65.93	65.36
60	61.94	50.84	61.59	71.36	57.52	71.98	67.17	73.33	63.65	49.19
61	63.55	54.25	47.51	68.78	54.01	60.67	53.68	70.26	58.59	58.24
62	70.93	47.97	61.04	68.84	52.83	61.76	58.18	64.34	60.69	55.16
63	63.50	59.86	64.89	69.63	59.76	54.73	63.17	55.30	58.24	59.30
64	65.18	62.66	61.16	71.03	55.65	58.50	46.87	81.37	58.80	58.41
65	63.53	56.82	59.83	56.58	54.91	60.40	77.40	67.00	52.84	62.46
66	70.69	55.76	64.48	57.18	56.24	56.74	49.47	71.62	50.14	47.61
67	63.70	52.97	55.96	68.66	62.10	63.61	62.53	79.96	60.18	48.61
68	76.52	62.08	64.24	63.60	63.49	52.00	49.80	65.44	63.80	62.41
69	54.91	57.48	65.93	66.52	55.72	67.84	49.87	57.53	49.66	66.67
70	76.48	61.97	60.34	64.78	59.80	55.05	58.67	60.15	68.89	53.82
71	72.77	49.14	75.47	65.34	63.61	57.95	62.62	67.00	72.74	63.64
72	69.97	66.92	65.36	66.51	67.23	75.00	54.57	71.09	50.40	51.63
73	74.67	58.57	65.19	75.20	67.33	56.98	67.14	84.69	78.76	57.31
74	70.08	64.97	54.63	61.44	65.45	63.42	59.58	79.05	67.80	72.95

Continued on next page

Table 7 – continued from previous page										
Pic	**CD2**	**CD3**	**CD5**	**CD6**	**CD4**	**CD7**	**CD8**	**CD9**	**CE1**	**CE3**
75	65.60	70.67	54.48	66.56	61.91	61.15	64.09	65.05	78.18	53.54
76	72.62	67.14	67.79	70.63	60.25	66.19	62.77	85.84	77.82	68.25
77	62.50	56.64	64.99	65.45	53.40	63.17	63.09	61.20	72.43	62.66
78	74.64	60.74	54.84	66.55	61.63	53.73	63.78	80.21	68.91	53.83
79	63.87	62.41	62.92	67.54	67.25	60.22	49.51	82.76	53.41	61.95
80	71.63	54.26	60.60	72.62	69.19	55.56	53.96	76.20	73.44	58.30

Table 8: Main study: Classification accuracies (Actual Paradigm, One-vs-Rest classification)

Pic	CD2	CD3	CD5	CD6	CD4	CD7	CD8	CD9	CE1	CE3
1	73.96	65.26	81.00	76.16	70.72	60.67	75.88	83.78	83.78	67.72
2	70.13	61.00	61.05	73.43	50.59	49.01	72.58	72.58	72.58	71.20
3	72.15	53.52	75.67	83.12	62.10	64.15	73.04	90.19	90.19	70.82
4	61.88	75.32	74.22	63.87	66.63	58.26	68.31	78.92	78.92	73.48
5	81.01	73.05	85.65	81.98	76.17	71.99	83.95	88.12	88.12	82.92
6	69.75	71.08	77.78	69.33	63.23	53.40	74.79	75.31	75.31	73.98
7	75.08	70.01	79.50	87.27	64.38	75.62	76.14	89.80	89.80	76.71
8	84.94	70.54	82.74	82.74	70.86	61.30	78.17	89.09	89.09	83.77
9	69.92	60.44	74.26	71.99	64.95	51.57	67.39	79.01	79.01	67.00
10	70.67	62.31	63.79	62.41	53.88	60.71	76.40	61.87	61.87	64.04
11	64.01	65.20	66.08	72.92	54.75	54.81	73.49	71.69	71.69	59.36
12	56.08	66.69	60.92	70.82	50.25	55.24	61.15	77.98	77.98	76.04
13	69.85	66.17	69.47	58.23	66.16	61.23	67.34	76.59	76.59	55.40
14	64.40	62.69	71.18	67.34	61.42	59.45	70.10	60.62	60.62	65.29
15	67.54	65.79	66.89	73.17	71.11	54.86	69.58	77.71	77.71	61.82
16	54.52	59.33	64.21	73.54	55.07	56.95	62.57	70.69	70.69	65.17
17	65.90	71.03	68.54	54.47	66.23	47.37	75.38	70.73	70.73	64.35
18	69.47	71.85	72.98	72.50	74.28	54.16	73.65	68.06	68.06	66.39
19	74.04	60.69	73.29	70.90	68.43	61.32	64.92	73.22	73.22	53.51
20	76.27	67.68	77.88	76.72	68.18	53.32	71.36	79.10	79.10	73.86
21	67.61	71.25	75.27	67.24	70.72	58.81	71.89	78.40	78.40	71.73
22	72.69	63.86	70.89	71.75	57.53	49.34	70.31	72.10	72.10	71.64
23	78.89	72.91	79.83	81.70	75.28	64.81	79.36	82.18	82.18	83.49
24	71.67	65.84	73.09	70.55	48.90	51.03	69.22	68.63	68.63	73.34
25	62.43	71.44	60.96	61.74	66.31	59.57	70.37	69.33	69.33	67.06
26	68.37	63.46	64.66	69.64	55.48	48.37	69.83	70.60	70.60	67.94
27	65.17	64.86	70.74	70.36	64.56	56.08	61.87	58.66	58.66	55.52
28	59.99	69.93	66.28	61.06	66.50	55.84	71.04	72.12	72.12	64.36
29	57.58	63.46	66.38	68.35	64.91	47.00	69.02	69.59	69.59	59.35
30	86.52	77.46	82.90	75.17	70.44	61.80	75.69	86.23	86.23	73.71
31	63.88	60.02	61.15	75.28	61.43	56.41	54.43	86.08	86.08	66.51
32	65.58	61.66	65.73	67.75	66.74	59.74	74.36	69.49	69.49	64.08
33	68.07	61.29	77.43	60.39	76.93	45.77	65.91	85.87	85.87	66.45
34	75.00	76.05	72.23	62.27	57.38	45.29	68.52	77.11	77.11	61.96
35	77.62	73.50	76.21	71.32	65.88	46.72	68.41	84.29	84.29	69.06
36	78.37	73.20	75.53	71.22	61.17	49.19	77.68	84.57	84.57	59.79
37	74.54	66.72	76.17	68.51	67.24	46.01	66.02	74.17	74.17	61.74

Continued on next page

Table 8 – continued from previous page

Pic	CD2	CD3	CD5	CD6	CD4	CD7	CD8	CD9	CE1	CE3
38	75.66	70.81	56.75	68.50	66.64	50.96	71.63	74.29	74.29	66.01
39	76.58	77.79	86.87	69.76	65.77	48.84	72.43	88.89	88.89	63.42
40	80.12	72.85	78.91	77.37	59.09	64.15	78.07	84.93	84.93	68.83
41	67.21	64.52	69.16	61.19	61.55	46.62	58.41	63.58	63.58	76.87
42	64.34	64.16	60.77	63.49	59.47	50.81	58.88	60.67	60.67	52.55
43	68.99	54.85	57.68	67.09	61.32	53.17	59.64	68.73	68.73	61.16
44	63.99	56.72	77.78	64.57	67.59	63.18	66.41	67.33	67.33	60.06
45	67.23	59.90	63.42	51.80	56.23	61.27	64.68	68.75	68.75	68.97
46	63.26	65.19	68.02	59.03	58.87	50.06	57.29	65.85	65.85	52.55
47	62.12	55.33	72.46	67.20	52.53	57.74	54.53	68.55	68.55	64.95
48	64.33	59.52	59.46	69.69	66.77	59.88	70.35	68.55	68.55	62.58
49	65.25	77.64	74.98	59.62	67.31	51.95	78.22	75.94	75.94	76.08
50	60.28	65.31	62.34	73.81	61.00	66.97	71.17	88.16	88.16	69.19
51	62.43	64.56	64.53	64.59	59.41	55.82	71.19	58.80	58.80	68.21
52	77.08	59.42	79.03	68.05	60.90	44.64	63.93	74.90	74.90	74.01
53	72.88	61.01	82.46	74.63	67.87	67.28	75.35	73.21	73.21	74.87
54	58.87	65.45	69.97	67.90	62.00	51.77	67.97	66.18	66.18	68.10
55	63.66	67.69	70.70	64.69	54.73	45.15	64.19	70.78	70.78	65.72
56	64.81	56.86	66.07	58.52	55.77	55.84	68.97	77.52	77.52	70.17
57	61.81	70.36	63.45	70.30	64.91	52.44	75.49	73.01	73.01	62.25
58	58.55	68.68	68.18	62.02	60.36	60.04	65.93	64.06	64.06	51.98
59	62.82	73.54	80.66	68.96	69.19	57.52	75.10	79.75	79.75	72.09
60	67.85	57.95	74.56	72.05	54.54	57.79	71.23	70.61	70.61	64.57
61	66.26	57.23	66.50	73.29	55.47	57.56	76.79	58.51	58.51	66.07
62	60.16	57.71	65.70	49.45	52.46	51.31	69.32	69.31	69.31	69.37
63	71.08	74.95	67.41	60.01	59.31	53.41	76.83	63.25	63.25	65.60
64	68.50	65.32	74.90	69.59	55.14	58.99	75.34	82.73	82.73	75.29
65	65.66	55.98	78.15	61.69	59.79	54.67	72.72	79.11	79.11	66.20
66	65.54	65.25	53.57	63.54	63.13	59.50	65.24	71.15	71.15	65.65
67	67.16	54.46	55.48	66.99	48.81	53.18	77.02	77.42	77.42	71.97
68	55.67	67.07	72.90	62.82	49.56	60.33	68.48	70.57	70.57	71.40
69	61.09	52.06	70.98	77.38	55.87	52.71	64.33	75.84	75.84	75.29
70	71.96	64.90	65.04	67.31	57.94	53.70	73.17	62.50	62.50	72.57
71	52.18	69.41	76.24	74.26	65.94	62.81	88.02	73.88	73.88	77.83
72	66.47	60.91	71.88	74.21	64.69	56.25	71.78	66.18	66.18	68.08
73	64.85	63.94	66.78	78.31	73.96	54.80	83.70	74.95	74.95	75.89
74	64.93	69.30	69.01	66.45	65.72	56.88	67.44	78.58	78.58	68.59
75	64.57	66.49	77.89	68.30	68.90	61.11	66.69	69.16	69.16	72.60
76	63.48	67.61	71.34	64.78	52.07	60.47	62.72	75.98	75.98	71.04

Continued on next page

Table 8 – continued from previous page										
Pic	**CD2**	**CD3**	**CD5**	**CD6**	**CD4**	**CD7**	**CD8**	**CD9**	**CE1**	**CE3**
77	58.57	64.11	61.68	69.84	53.50	59.59	61.55	73.89	73.89	67.85
78	69.46	65.74	65.43	68.46	66.68	51.89	65.23	75.56	75.56	76.71
79	64.31	64.62	61.92	61.23	61.37	53.90	62.81	86.26	86.26	73.45
80	67.22	70.36	73.98	66.99	65.62	54.15	71.10	76.34	76.34	75.29

Table 9: Main study: Image rating (attractiveness).

Pic	CD2	CD3	CD5	CD6	CD4	CD7	CD8	CD9	CE1	CE3
1	5	6	2	6	5	4	6	5	1	1
2	3	6	5	3	2	6	2	6	2	1
3	6	3	1	5	2	5	2	5	1	2
4	2	4	6	3	5	4	4	6	1	5
5	1	2	2	2	5	4	5	5	1	4
6	6	4	6	5	3	5	6	6	5	1
7	1	3	2	5	7	3	2	3	5	1
8	2	2	2	5	5	3	1	5	4	2
9	3	6	3	3	5	4	2	2	6	1
10	2	4	3	6	3	6	5	3	5	1
11	2	3	6	5	5	4	2	3	3	1
12	2	5	3	2	2	4	3	2	1	1
13	5	6	5	6	5	4	4	1	2	7
14	2	6	1	5	2	4	4	1	5	1
15	1	3	7	5	4	3	1	1	1	1
16	3	6	4	7	6	5	5	6	7	4
17	2	3	2	5	4	4	1	6	5	1
18	6	5	1	3	4	5	1	2	5	2
19	4	3	4	4	5	4	5	6	5	1
20	2	3	1	2	2	4	1	6	1	3
21	6	4	2	5	3	5	6	7	5	1
22	3	7	4	3	2	4	2	2	4	2
23	6	4	2	4	2	3	4	6	1	2
24	6	5	2	4	3	4	4	2	4	1
25	5	7	6	6	3	6	2	2	5	2
26	2	5	4	1	4	5	4	3	1	5
27	2	5	7	6	5	6	6	7	5	1
28	1	6	2	5	2	4	1	1	1	6
29	1	6	1	3	2	2	2	1	1	1
30	7	6	1	4	5	4	3	7	3	6
31	6	2	2	5	2	3	2	1	1	7
32	1	7	4	6	3	2	5	7	1	4
33	2	3	1	5	2	6	5	1	6	4
34	3	7	5	4	3	4	3	6	4	5
35	3	1	1	1	3	7	6	1	3	5
36	2	6	1	7	4	4	3	6	5	4
37	4	7	1	2	5	4	2	7	1	7
38	6	2	1	2	3	5	2	4	1	2

Continued on next page

Table 9 – continued from previous page

Pic	CD2	CD3	CD5	CD6	CD4	CD7	CD8	CD9	CE1	CE3
39	2	4	1	3	1	4	6	5	2	1
40	5	5	1	1	6	4	2	3	1	4
41	5	7	6	5	5	6	7	7	5	7
42	3	1	1	6	3	2	2	1	2	1
43	3	2	4	6	5	4	2	2	2	3
44	4	7	6	2	3	4	6	7	1	5
45	1	1	3	2	3	2	1	1	1	1
46	1	2	1	2	2	2	2	1	1	1
47	6	5	4	4	6	5	6	7	1	1
48	4	1	2	3	5	3	4	3	1	1
49	6	7	1	2	5	4	3	6	2	4
50	4	5	3	3	5	3	3	6	2	7
51	4	5	5	5	4	3	3	6	2	1
52	6	5	5	3	4	4	7	7	1	1
53	2	6	1	6	6	2	4	6	1	1
54	2	2	1	3	4	2	2	2	1	1
55	7	5	7	2	6	4	5	7	1	4
56	7	1	5	2	2	1	3	6	5	5
57	3	3	1	3	4	2	2	5	2	1
58	2	1	4	2	3	2	2	5	2	1
59	4	1	1	5	5	2	2	4	2	1
60	2	1	1	6	2	2	1	2	1	1
61	3	3	6	6	5	3	2	5	4	2
62	2	2	3	5	3	3	2	2	2	1
63	4	6	6	7	2	2	2	4	3	2
64	1	1	1	4	2	2	1	1	1	1
65	6	5	4	3	3	4	7	7	1	3
66	2	1	1	2	3	3	2	1	1	1
67	2	1	3	2	3	2	2	4	2	1
68	6	1	7	5	4	2	1	3	1	1
69	2	1	1	1	1	5	2	1	1	1
70	1	1	1	1	2	1	1	1	1	1
71	3	1	2	6	3	3	2	5	1	1
72	2	1	3	4	3	1	1	4	1	2
73	3	2	1	2	4	4	2	6	1	1
74	3	2	2	5	4	3	2	2	2	1
75	2	4	2	6	4	3	2	3	2	1
76	3	2	4	5	5	3	2	3	2	1
77	3	2	2	4	5	4	2	2	2	2

Continued on next page

Table 9 – continued from previous page										
Pic	**CD2**	**CD3**	**CD5**	**CD6**	**CD4**	**CD7**	**CD8**	**CD9**	**CE1**	**CE3**
78	1	2	1	2	2	2	1	3	1	1
79	2	2	2	3	5	4	1	4	2	1
80	1	2	3	5	5	2	3	4	2	1

Table 10: Main study: Image rating (comfortability).

Pic	CD2	CD3	CD5	CD6	CD4	CD7	CD8	CD9	CE1	CE3
1	6	6	5	4	6	2	2	5	6	1
2	3	6	6	6	6	5	5	6	5	1
3	4	2	2	6	4	6	3	6	1	1
4	2	3	3	3	6	4	3	6	6	5
5	2	2	4	6	5	4	3	6	6	5
6	6	3	2	3	3	3	2	3	6	1
7	1	2	1	3	6	2	2	2	2	1
8	2	2	2	4	3	3	1	2	6	1
9	2	4	2	6	3	4	2	3	6	3
10	2	2	2	6	2	5	3	5	6	1
11	3	2	3	2	2	4	2	3	5	1
12	2	2	4	4	4	5	2	3	5	1
13	2	4	1	1	2	2	2	2	5	7
14	2	3	4	2	2	4	2	1	2	3
15	1	2	1	1	1	2	1	1	1	1
16	2	4	2	3	4	3	2	5	7	2
17	1	3	2	3	2	2	1	6	4	1
18	6	4	7	6	6	6	3	1	6	4
19	5	3	4	6	4	3	2	6	5	1
20	4	4	1	6	4	3	2	6	3	4
21	5	3	5	5	4	4	3	6	4	1
22	2	4	4	4	3	3	2	1	5	3
23	6	2	5	3	3	3	2	5	3	3
24	5	5	5	2	5	3	3	3	4	2
25	4	5	4	2	4	4	3	5	4	1
26	3	6	7	7	6	6	3	7	4	7
27	3	4	5	6	2	5	4	6	3	1
28	1	4	1	1	1	3	1	2	1	4
29	1	5	5	2	3	1	1	1	1	1
30	7	5	7	7	7	5	4	7	6	6
31	7	1	2	2	2	2	1	1	1	3
32	1	7	7	6	2	2	2	7	1	1
33	3	4	4	2	3	3	2	1	5	6
34	4	6	6	3	3	2	2	5	3	1
35	2	3	1	6	4	5	3	1	5	2
36	4	4	1	3	3	2	2	5	3	1
37	2	6	4	6	2	3	2	5	1	2
38	6	3	7	7	6	4	4	7	7	7

Continued on next page

Table 10 – continued from previous page

Pic	CD2	CD3	CD5	CD6	CD4	CD7	CD8	CD9	CE1	CE3
39	4	4	1	6	5	2	2	4	4	3
40	4	7	7	7	6	5	2	7	6	7
41	6	5	4	1	6	3	3	7	1	7
42	2	3	2	1	4	2	2	1	5	2
43	2	3	4	2	4	4	3	2	5	2
44	6	5	6	5	6	5	4	7	7	5
45	1	1	1	3	4	2	1	1	1	1
46	2	2	1	3	4	2	2	1	1	1
47	6	5	7	4	6	6	5	7	6	3
48	4	1	3	3	4	2	3	1	1	1
49	4	7	1	4	4	3	2	5	6	1
50	3	4	4	4	4	3	2	6	4	1
51	3	5	5	5	5	2	4	6	6	1
52	3	6	7	4	6	5	5	7	6	1
53	2	4	2	4	5	2	3	6	6	1
54	2	3	1	4	3	2	2	2	5	1
55	5	6	7	3	5	5	3	7	6	2
56	6	4	5	6	4	2	2	6	5	1
57	2	4	1	5	5	2	2	5	2	1
58	2	2	4	4	3	3	2	5	2	1
59	2	1	5	3	5	2	2	2	3	1
60	2	1	4	4	4	2	1	2	1	1
61	2	2	5	3	5	3	1	5	4	1
62	2	2	3	5	3	3	1	2	3	2
63	4	6	1	4	3	2	2	2	1	1
64	2	1	1	2	2	2	1	1	1	1
65	4	6	7	6	7	7	7	7	7	1
66	2	3	4	4	4	4	2	1	2	1
67	3	2	6	5	4	2	1	4	3	1
68	6	2	4	3	4	2	1	3	1	1
69	4	3	7	7	4	6	2	1	6	4
70	2	2	6	5	4	4	1	1	2	1
71	2	1	3	2	4	2	1	5	3	1
72	2	2	2	2	4	1	2	4	3	1
73	2	4	6	6	6	4	3	6	3	1
74	2	2	3	3	4	2	1	2	5	1
75	2	3	4	3	3	2	2	3	4	1
76	2	2	5	4	4	2	1	3	5	1
77	2	3	6	6	5	5	1	2	5	1

Continued on next page

Table 10 – continued from previous page										
Pic	**CD2**	**CD3**	**CD5**	**CD6**	**CD4**	**CD7**	**CD8**	**CD9**	**CE1**	**CE3**
78	3	4	6	6	5	3	2	3	2	1
79	2	2	4	4	4	3	1	4	4	1
80	2	2	3	2	4	2	3	4	1	1

Table 11: Main study: Image rating (innovativeness).

Pic	CD2	CD3	CD5	CD6	CD4	CD7	CD8	CD9	CE1	CE3
1	5	6	3	2	5	3	4	6	5	4
2	5	6	5	1	3	4	3	3	3	1
3	6	6	5	2	4	5	5	1	1	3
4	3	6	6	4	4	2	5	6	1	2
5	2	6	6	2	4	5	5	7	6	3
6	6	7	7	6	4	6	6	7	6	1
7	4	6	6	6	7	4	6	7	6	1
8	4	7	5	6	7	3	5	6	5	4
9	2	1	3	2	5	3	2	4	5	3
10	3	2	4	5	4	5	3	4	3	3
11	2	2	4	5	5	6	3	5	2	1
12	2	1	4	4	1	3	2	1	1	1
13	5	3	4	3	4	2	3	2	2	2
14	2	3	3	3	3	3	2	6	5	1
15	1	2	4	4	4	2	2	1	1	1
16	2	3	5	5	5	5	3	6	7	3
17	2	3	2	3	3	2	1	4	3	1
18	7	4	3	2	2	5	2	2	1	1
19	4	3	4	2	3	5	4	6	4	1
20	2	1	1	2	3	5	3	6	1	2
21	6	2	3	4	3	5	3	7	6	1
22	4	4	5	4	4	4	2	5	6	1
23	7	2	5	6	5	4	3	6	5	1
24	6	4	5	6	3	4	2	2	4	1
25	5	5	4	5	4	5	2	3	4	1
26	2	5	6	1	2	6	4	5	5	3
27	2	3	4	3	3	5	2	5	2	1
28	3	4	4	4	3	3	2	5	5	7
29	4	7	6	6	6	5	5	6	6	4
30	6	3	4	3	3	1	2	4	3	1
31	6	2	2	4	3	2	1	1	1	1
32	3	5	4	3	3	1	1	5	1	1
33	4	5	7	4	5	4	6	6	7	5
34	5	7	7	2	4	3	6	6	5	5
35	5	4	7	5	5	6	7	6	5	5
36	4	5	6	6	4	4	3	6	5	5
37	4	7	7	3	6	4	5	7	2	7
38	4	3	5	3	3	3	3	3	1	3

Continued on next page

Table 11 – continued from previous page

Pic	CD2	CD3	CD5	CD6	CD4	CD7	CD8	CD9	CE1	CE3
39	3	4	6	6	4	3	5	5	3	4
40	3	4	1	2	2	1	2	1	1	1
41	5	4	6	6	5	3	4	5	4	7
42	5	3	4	4	6	3	2	6	4	4
43	5	3	7	4	4	4	3	6	4	4
44	3	4	6	3	3	4	3	3	1	2
45	3	3	6	6	6	4	1	6	2	3
46	3	4	1	5	6	4	1	6	2	2
47	4	3	4	3	3	4	5	3	1	1
48	4	4	4	6	6	4	3	6	2	4
49	5	6	1	5	6	4	2	4	4	3
50	5	4	5	3	5	2	3	5	4	3
51	5	5	6	6	5	3	4	4	5	6
52	4	4	6	4	5	4	5	4	5	3
53	5	5	4	6	6	4	3	6	5	5
54	4	4	6	6	6	4	2	6	5	4
55	3	2	4	3	4	4	3	4	2	2
56	6	3	2	5	3	1	1	6	5	2
57	4	4	4	6	6	4	2	7	4	3
58	4	2	4	4	5	3	2	6	4	3
59	4	2	3	4	4	2	2	6	4	4
60	3	3	5	5	4	3	1	6	4	3
61	2	1	2	4	4	3	2	5	5	3
62	4	4	5	4	4	4	1	6	4	6
63	6	6	4	6	4	4	2	7	3	6
64	3	6	4	6	3	4	1	6	1	5
65	3	3	7	3	4	4	7	2	2	2
66	3	6	5	5	2	4	2	6	4	1
67	2	4	3	5	4	3	1	6	4	1
68	6	6	7	4	5	4	1	7	4	7
69	2	1	2	3	3	4	1	1	2	1
70	3	4	2	5	3	3	1	3	2	1
71	4	4	4	4	5	4	2	6	4	3
72	4	5	4	5	6	4	2	7	3	5
73	3	2	3	3	4	3	2	4	3	1
74	4	5	4	6	5	4	2	6	4	3
75	5	5	6	4	5	5	2	7	3	4
76	4	5	6	4	5	4	1	7	6	4
77	3	3	3	4	4	4	2	4	5	2

Continued on next page

Table 11 – continued from previous page										
Pic	**CD2**	**CD3**	**CD5**	**CD6**	**CD4**	**CD7**	**CD8**	**CD9**	**CE1**	**CE3**
78	1	2	2	4	3	2	1	3	1	1
79	4	5	7	6	5	5	1	7	5	4
80	4	6	7	5	4	4	4	7	1	4